USE OF PRECAST, PRESTRESSED CONCRETE FOR BRIDGE DECKS

JULY 1969 — NUMBER 20

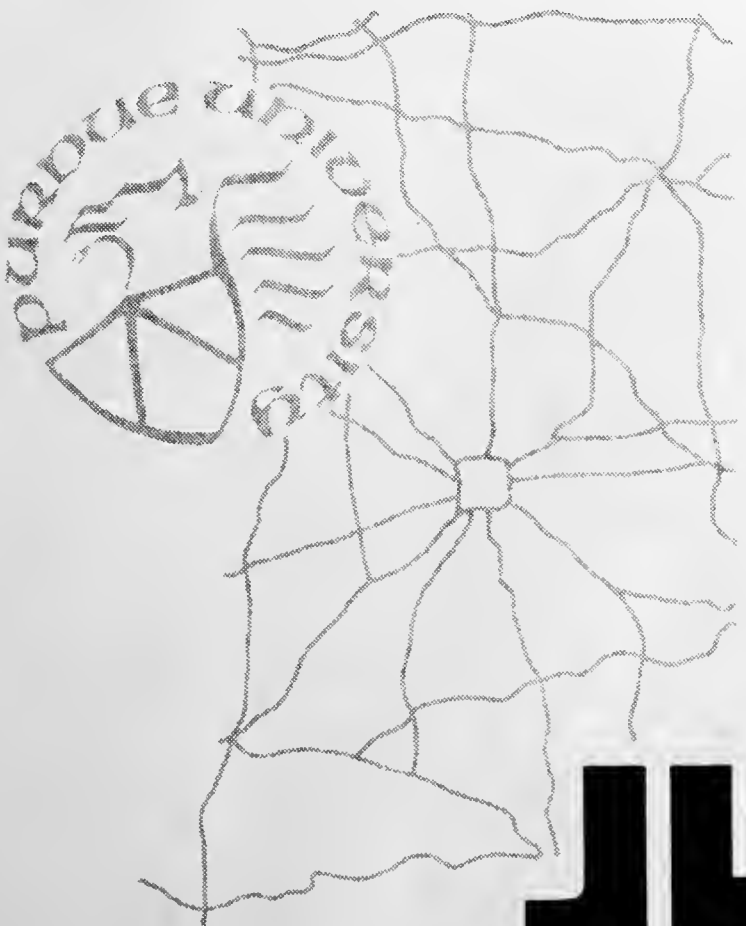

BY

JAMES H. FORD

JHRP

JOINT HIGHWAY RESEARCH PROJECT

PURDUE UNIVERSITY AND
INDIANA STATE HIGHWAY COMMISSION

Progress Report

USE OF PRECAST, PRESTRESSED CONCRETE FOR BRIDGE DECKS

TO: J. F. McLaughlin, Director
Joint Highway Research Project

July 25, 1969

File No: 7-4-14

FROM: H. L. Michael, Associate Director
Joint Highway Research Project

Project No: C-36-56N

Attached is a Progress Report on the HPR Part II research project titled "Precast, Prestressed Concrete for Bridge Decks". This report is titled "Use of Precast, Prestressed Concrete for Bridge Decks" and has been authored by Mr. James H. Ford, Graduate Assistant in Research on our staff. Professors Martin J. Gutzwiller and Robert H. Lee directed the research.

The report covers the initial research on this project which has been conducted in the laboratory since the completion of the feasibility report and the approval of the laboratory phase of the project. Laboratory work is continuing but on the basis of the work completed to date and reported in this report, a field phase of this research is being developed. A proposal will be submitted shortly on the construction of an experimental structural deck system as developed by this research project.

The report is submitted to the Board for acceptance as progress toward fulfillment of the objectives of this research. It will also be submitted to the ISHC and the BPR for their review, comment and acceptance.

Respectfully submitted,

Harold L. Michael
Associate Director

HLM/rg

cc: F. L. Ashbaucher, W. L. Dolch, W. H. Goetz, W. L. Grecco, G. K. Hallock, M. E. Harr, R. H. Harrell, J. A. Havers, V. E. Harvey, G. A. Leonards, F. B. Mendenhall, R. D. Miles, C. F. Scholer, M. B. Scott, W. T. Spencer, H. R. J. Walsh, K. B. Woods, E. J. Yoder

Progress Report

USE OF PRECAST, PRESTRESSED CONCRETE FOR BRIDGE DECKS

by

James H. Ford
Graduate Assistant in Research

Joint Highway Research Project
File No: 7-4-14
Project No: C-36-56M

Prepared as Part of an Investigation

Conducted by

Joint Highway Research Project
Engineering Experiment Station
Purdue University

in cooperation with the

Indiana State Highway Commission

and the

U.S. Department of Transportation
Federal Highway Administration
Bureau of Public Roads

The opinions, findings and conclusions expressed in this publication are those of the authors and not necessarily those of the Bureau of Public Roads

Not Released for Publication

Subject to Change

Not Reviewed By
Indiana State Highway Commission
or the
Bureau of Public Roads

Purdue University
Lafayette, Indiana
July 25, 1969

Digitized by the Internet Archive
in 2011 with funding from
LYRASIS members and Sloan Foundation; Indiana Department of Transportation

http://www.archive.org/details/useofprecastpres00ford

ACKNOWLEDGMENTS

Acknowledgment is made to the members of the Joint Highway Research Project for funding the project.

Special thanks are given to M. J. Gutzwiller and R. H. Lee, major professors, for their instructive guidance. Thanks are also given to Professors C. F. Scholer and E. O. Stitz for their suggestions.

The author wishes to thank W. B. Telfer, laboratory technician, and several graduate students for their help in the laboratory.

TABLE OF CONTENTS

LIST OF TABLES. v

LIST OF FIGURES vii

ABSTRACT. xii

INTRODUCTION. 1

PRECAST, PRESTRESSED DECK SECTIONS. 3

General Description. 3
Selection of Typical Design Section. 4
Typical Deck Design Calculations 4
Design Parameters 4
Moment Calculations 7
Stress Analysis 8
Ultimate Flexural Strength. 10
Stresses at Transfer and Handling 12
Roadway Drainage 15
Slab Tie-Down System 17
Anchors 17
Bolting 19
Spring Clip. 21
Post-Tensioning System 23
Cable 23
Anchorage 23
Transverse Continuity Joint 24
Photoelastic Joint-Shape Study. 25
Semicircular Joint Model 26
Circular Sector Joint Model. 28
Flat Key-Type Joint Model. 28
Joint Testing with Concrete Models. 38
Circular Sector Joint Model. 39
Flat Joint Model 44
Joint Materials. 45

DESIGN OF PRESTRESSED LABORATORY SPECIMENS. 48

Design for Beam Spacing of Four-Feet 49
Design for Beam Spacing of Eight-Feet. 51

CONSTRUCTION OF PRESTRESSED CONCRETE ELEMENTS 57

Formwork 57
Bolt Inserts 59

TABLE OF CONTENTS (Continued)

Concrete 60
Concrete Placement 64
Continuity Joint 64

LABORATORY TESTING OF FULL-SCALE DECK 67

Load Cell Design and Calibration 67
Longitudinal Forces on Deck. 70
Description of Test 78
Series I 78
Series II 79
Series III 79
Measurement of Movement. 83
Results of Slip Test. 83
Static Testing of Specimens Reinforced for 4'-0" Beam Spacing. 87
Description of Test 87
Measurement of Loads 87
Measurement of Deflection. 87
Measurement of Strain. 91
Sources of Error 99
Strain Gage Application. 99
Results 100
Static Testing of Specimens Reinforced for 8'-0" Beam Spacing. 110
Description of Test 110
Results 110

TESTING OF PRESTRESSED SPECIMENS UNDER REPEATED LOAD. 125

Repeated Load Test With 8'-0" Beam Spacing 125
Testing Procedure 125
Load Application 125
Strain Measurement 130
Results 130
Repeated Load Test With 4'-6" Beam Spacing 133

COST ANALYSIS 136

Precast, Prestressed System. 136
Reinforced Concrete System 136
Cost Comparison. 137

CONCLUSIONS 139

RECOMMENDATIONS 141

BIBLIOGRAPHY. 145

APPENDIX A 146

APPENDIX B 152

APPENDIX C 159

LIST OF TABLES

Table		Page
1.	Measured Strains on Flat Joint Photoelastic Model	35
2.	Principal Stress Determination on Flat Joint.	36
3.	Model to Prototype Scaling.	37
4.	Concrete Properties of Test Specimens	63
5.	Cable Tension Cell "A" Calibration.	71
6.	Cable Tension Cell "B" Calibration.	73
7.	Cable Tension Cell "C" Calibration.	75
8.	Resistance of Deck to Longitudinal Forces	85
9.	Load Stages During Testing of Sections Reinforced for 4'-0" Beam Spacing	92
10.	Load Stages During Testing of Sections Reinforced for 8'-0" Beam Spacing	114
11.	Static Bending Test, 4'-0" Beam Spacing, Deflections	147
12.	Strain Data, 4'-0" Beam Spacing Static Test, Top North-South Gages on Section 4-2.	148
13.	Strain Data, 4'-0" Beam Spacing Static Test, Bottom North-South Gages on Section 4-2	149
14.	Strain Data, 4'-0" Beam Spacing Static Test, Top East-West Gages on Section 4-2.	150
15.	Strain Data, 4'-0" Beam Spacing Static Test, Bottom East-West Gages on Section 4-2	151
16.	Deflections During Testing of Sections Reinforced for 8'-0" Beam Spacing.	153
17.	Strain Data, 8'-0" Beam Spacing Static Test, Top East-West Gages on Section 8-1.	154

LIST OF TABLES (Continued)

Table		Page
18.	Strain Data, 8'-0" Beam Spacing Static Test, Bottom East-West Gages on Section 8-1	155
19.	Strain Data, 8'-0" Beam Spacing Static Test, Top North-South Gages on Section 8-1.	156
20.	Strain Data, 8'-0" Beam Spacing Static Test, Bottom North-South Gages on Section 8-1	157
21.	Strain Data, 8'-0" Beam Spacing Static Test, Gages on Top Surface of Section 4-2	158
22.	Strain Gage Readings, Repeated Load Test With 8'-0" Beam Spacing	160
23.	Strain Gage Readings, Repeated Load Test With 4'-6" Beam Spacing	161

LIST OF FIGURES

Figure		Page
1.	Typical Design Section	5
2.	Typical Moment Design Section	6
3.	Typical Reinforcing Pattern - 250K Grade	8
4.	Calculated Concrete Stresses Under Service Load	9
5.	Strain Geometry and Stress-Force Relationships at Ultimate Capacity	11
6.	Slab Handling, Pick-up at Quarter Points	14
7.	Handling Stresses at Pick-up Point Immediately After Stress Transfer	14
8.	Applied Torque Versus Clamping Force, 3/4" Bolt	20
9.	Slab Tie-Down Arrangement	22
10.	Loading of Photoelastic Joint Models	26
11.	Principal Stress Directions on Semicircular Joint	27
12.	Photoelastic Model, Semicircular Joint	27
13.	Principal Stress Directions on Circular Sector Joint	29
14.	Photoelastic Model, Circular Sector Joint	29
15.	Principal Stress Directions on Flat Joint	31
16.	Photoelastic Model, Flat Joint	31
17.	Flat Joint Model Fringe Photograph, P = 100 lb	32
18.	Flat Joint Model Fringe Photograph, P = 200 lb	32
19.	Flat Joint Model Fringe Photograph, P = 300 lb	33
20.	Flat Joint Model Strain Gage Locations	33

LIST OF FIGURES (Continued)

Figure		Page
21.	Concrete Joint Testing Model	40
22.	Concrete Model Joint Shapes	42
23.	Laboratory Joint Testing Arrangement	43
24.	Calculated Concrete Stresses Due to AASHO Loading Applied to Laboratory Specimens Reinforced for 4'-0" Beam Spacing	50
25.	Calculated Concrete Stresses Due to AASHO Loading Applied to Laboratory Specimens Reinforced for 8'-0" Beam Spacing	52
26.	Laboratory Model Hardware Detail	53
27.	Detail A-A, Bolt Insert Arrangement	54
28.	Laboratory Model Joint Detail	55
29.	Laboratory Model Strand Placement Patterns	56
30.	Laboratory Model Lifting Loop Detail	56
31.	Precasting Method for Laboratory Specimens	58
32.	Concrete Strength Versus Time, Laboratory Sections	61
33.	Crack Patterns in Sections Reinforced for 4'-0" Beam Spacing	62
34.	Templates for Dimensional Control	65
35.	Post-Tensioning Arrangement in Laboratory	67
36.	Cable-Tension Load Cell Detail	68
37.	Cable-Tension Load Cell Circuitry	69
38.	Calibration Curve, Load Cell A	72
39.	Calibration Curve, Load Cell B	74
40.	Calibration Curve, Load Cell C	76
41.	Calibration Curve, 50 Kip Load Cell	77
42.	Longitudinal Slip Test, Bolting Arrangements 1,2,3	80

LIST OF FIGURES (Continued)

Figure		Page
43.	Longitudinal Slip Test, Bolting Arrangements 4,5,6.	81
44.	Testing Arrangement, Longitudinal Slip, Series I and II.	82
45.	Testing Arrangement, Longitudinal Slip, Series III . . .	84
46.	Horizontal Load at Slip vs. Bolting Force.	86
47.	Plan View of Static Test for Sections Reinforced for 4'-0" Center-to-Center Beam Spacing.	88
48.	Sections A-A and B-B, Static Test with 4'-0" Beam Spacing	89
49.	Locations of Deflection Measurement, Static Test, 4'-0" Beam Spacing	90
50.	Longitudinal Center Line Deflection, 4'-0" Beam Spacing, Load Stages 1 and 2.	93
51.	Longitudinal Center Line Deflection, 4'-0" Beam Spacing, Load Stages 3 and 4.	94
52.	Longitudinal Center Line Deflection, 4'-0" Beam Spacing, Load Stages 5 and 6.	95
53.	Transverse Line Deflection Near Load, 4'-0" Beam Spacing, Load Stages 1 and 2.	96
54.	Transverse Line Deflection Near Load, 4'-0" Beam Spacing, Load Stages 3 and 4.	97
55.	Transverse Line Deflection Near Load, 4'-0" Beam Spacing, Load Stages 5 and 6.	98
56.	Strain Gage Locations on Top Surface, Static Test, 4'-0" Beam Spacing	101
57.	Strain Gage Locations on Bottom Surface, Static Test, 4'-0" Beam Spacing	102
58.	Transverse Top Surface Strains, 4'-0" Beam Spacing, Load Stages 1 and 2.	103
59.	Transverse Top Surface Strains, 4'-0" Beam Spacing, Load Stages 3 and 4	104

LIST OF FIGURES (Continued)

Figure		Page
60.	Transverse Top Surface Strains, 4'-0" Beam Spacing, Load Stages 5 and 6	105
61.	Transverse Bottom Surface Strains, 4'-0" Beam Spacing, All Load Stages	106
62.	Longitudinal Strain Measured on Longitudinal Center Line, 4'-0" Beam Spacing, Load Stages 1,2, and 3, Top Surface	107
63.	Longitudinal Strain Measured on Longitudinal Center Line, 4'-0" Beam Spacing, Load Stages 4,5, and 6, Top Surface	108
64.	Plan View of Static Test for Sections Reinforced for 8'-0" Center-to-Center Beam Spacing	111
65.	Sections A-A and B-B, Static Test With 8'-0" Beam Spacing	112
66.	Locations of Deflection Measurement, Static Test, 8'-0" Beam Spacing	113
67.	Longitudinal Center Line Deflection, 8'-0" Beam Spacing, Load Stages 1 and 2	115
68.	Longitudinal Center Line Deflection, 8'-0" Beam Spacing, Load Stages 3 and 4	116
69.	Strain Gage Locations on Top Surface, Static Test, 8'-0" Beam Spacing	117
70.	Strain Gage Locations on Bottom Surface, Static Test, 8'-0" Beam Spacing	118
71.	Transverse Top Surface Strains, 8'-0" Beam Spacing, Load Stages 1 and 2	119
72.	Transverse Top Surface Strains, 8'-0" Beam Spacing, Load Stages 3 and 4	120
73.	Transverse Bottom Surface Strains, 8'-0" Beam Spacing, All Load Stages	121
74.	Longitudinal Strain Measured on Longitudinal Center Line, 8'-0" Beam Spacing, All Load Stages, Top Surface	122

LIST OF FIGURES (Continued)

Figure		Page
75.	Testing Arrangement for Repeated Load Test With 8'-0" Beam Spacing.	126
76.	Section B-B, Repeated Load Test.	127
77.	Section A-A, Repeated Load Test, 8'-0" Beam Spacing.	128
78.	Load-Time Relationship During Repeated Load Test	129
79.	Strain Gage Locations for Repeated Load Test With 8'-0" Beam Spacing.	131
80.	Repeated Load Test With 8'-0" Beam Spacing	132
81.	Strain Gage Locations for Repeated Load Test With 4'6" Beam Spacing.	134
82.	Recommended Modification of Joint Detail	143

ABSTRACT

Ford, James Harvey. MSCE, Purdue University, August 1969. Use of Precast, Prestressed Concrete for Bridge Decks. Major Professors: Martin J. Gutzwiller and Robert H. Lee.

A structural deck system composed of precast and prestressed concrete sections of a size permitting over-the-highway transportation was conceived; structural design calculations conforming to the "Standard Specifications for Highway Bridges 1965", American Association of State Highway Officials, were made for the deck supported by steel beams spaced at the maximum anticipated prototype beam spacing. The completed deck would consist of similar precast pieces, each being six inches deep, as long as the transverse dimension of the bridge, and of a convenient width, four feet being anticipated as a common width.

Each precast piece would be symmetrically prestressed in the direction of its longest dimension; when the pieces are in place, the prestressing is transverse on the bridge, the principal direction of bending. The several precast pieces would be post-tensioned normal to their prestress direction, in the longitudinal direction of the bridge. Following post-tensioning, the pieces would be tied to the supporting beams by bolting to complete the system.

The purpose of the investigation was to arrive at a structural system capable of carrying the required loads in which advanced technology in concrete mix design could be applied with the specific intent of increasing deck durability. Since concrete control is more easily

exercised in the plant than the field, a plant-produced deck is most attractive. Secondary advantages gained with a precast deck system would be quick erection times with less down-time for deck replacement and possible dead load weight savings resulting in a more economical overall bridge.

Specific areas of investigation included the slab tie-down system, the transverse continuity joint, the post-tensioning system, joint materials for waterproofing and reduction of stress concentration, and static and repeated load testing of full-scale specimens.

The investigation indicated that the system is workable and that the design procedures employed are adequate. Performance of the deck in flexure indicated that a wheel load would be nearly all carried by one prestressed section or by two adjoining sections for a wheel load near their junction. The bolting system was observed to reduce deflections and to increase resistance of the deck to horizontal motion.

Detailed designs of the prestressed sections evaluated in the laboratory are included as are the deck response data obtained for a simulated wheel load statically applied at midspan of the system for two different beam spacings.

This study constitutes the initial work in a continuing study of the concept which will ultimately be utilized in the construction of a monitored prototype.

INTRODUCTION

Repairs on highway bridge decks represent a major cost item as well as an inconvenience and sometimes a safety hazard to the traveling public. If deck replacement times could be measured in days rather than weeks, many benefits would be realized. The concept of using precast bridge decks is not entirely new for it has been used on several bridges as a working surface for additional paving but not as a part of the load carrying structure. It would be feasible, even in new construction, to use precast slabs; some dead load reduction in the deck could allow significant modifications of the structural requirements of a bridge. In addition, control of air entrainment and concrete placing and curing should be more easily controlled in a precasting situation.

The most immediate projected use of the precast deck system is in replacement of existing bridge decks. The concept herein presented is to use precast and prestressed deck elements which are placed on the supporting floor beams, then post-tensioned and tied mechanically to the supporting system to achieve a deck which demonstrates satisfactory structural characteristics. Economy on each bridge should be realized since the deck is formed of identical pieces. In some instances, special sections might be necessitated by peculiarities of the particular floor system but the repetition of elements elsewhere in the deck should make the overall project economical.

Bridge down-time for repairs should be minimized since the precast elements could be stockpiled at the jobsite in the order of their use and could be placed on the bridge as soon as the original deck had been removed. Each time enough existing deck had been removed to allow placement of a precast element, the element could be placed and secured. No time would be lost in waiting for the concrete to cure. The only concrete which would be cast in place would be the concrete in the approach pavement which would need to be removed to facilitate post-tensioning. For this small concrete volume, the additional cost of high early strength concrete would be justified.

The concept of using precast prestressed concrete for bridge decks will minimize the time of replacing or initially constructing bridge decks. Plant production should result in high quality materials with good durability. Since economy must also be measured in terms of value to the regular user of the structure, the short down-time is doubly attractive, since the cost of implementing the system is comparable to the cost of present methods.

PRECAST, PRESTRESSED DECK SECTIONS

General Description

Precast, prestressed concrete sections will form the bridge deck. The proposed sections are rectangular, four feet by six inches in cross-section and, depending on the width of the roadway, can be made in any reasonable length. The sections, being as wide as the bridge, will be placed across the beams; afterward, the sections will be post-tensioned in the longitudinal direction of the bridge to eliminate any space between adjacent sections. Prior to the post-tensioning operation, the placing of a material in the joint formed by abutting sections is proposed. The joint material would have as its purpose the prevention of surface water seepage through the joint onto the beams as well as reduction of stress concentrations on the joint faces. Upon completion of the post-tensioning operation, the several pieces form a composite bridge deck.

The precasting and pretensioning operation may best be done in a concrete plant where prior experience with precast and pretensioned beams serves as an equipment and technological base. Concrete control, including mix design, placement, and curing, is more easily controlled in a concrete plant than is possible under field conditions. Concrete control constitutes one of the major advantages for precasting a bridge deck; it is presently necessary to replace many bridge decks because the concrete which was initially placed was of non-uniform quality and

subsequently deteriorated, making replacement necessary.

Selection of Typical Design Section

Prior to the design of a typical deck section, a roadway width was arbitrarily chosen. Transverse beam spacing was set at eight feet; the eight foot spacing was chosen as a probable maximum beam spacing which would be encountered. If the system may be designed for the extreme set of parameters, intermediate and lower parameters may be met with corresponding reductions in reinforcing and other related hardware; the design procedure for the large beam spacing is intended to establish an upper bound on the pretensioning force.

A 32 foot roadway width (shown in Figure 1) was not chosen as a size limit on the practical deck section, but as a practical design section for the chosen eight foot beam spacing.

Design criteria were established for the deck wherein a state of compression would be maintained over the entire section under design loading. The elimination of tensile stresses under design loading was intended to minimize cracking due to flexure in the thin, six inch section.

Design calculations for the base design follow. Where applicable, AASHO specifications and their designation are included.

Typical Deck Design Calculations

Design Parameters

Concrete Properties

a) $f'_c = 5{,}000$ psi compressive strength of concrete at 28 days.

AASHO 1.6.7

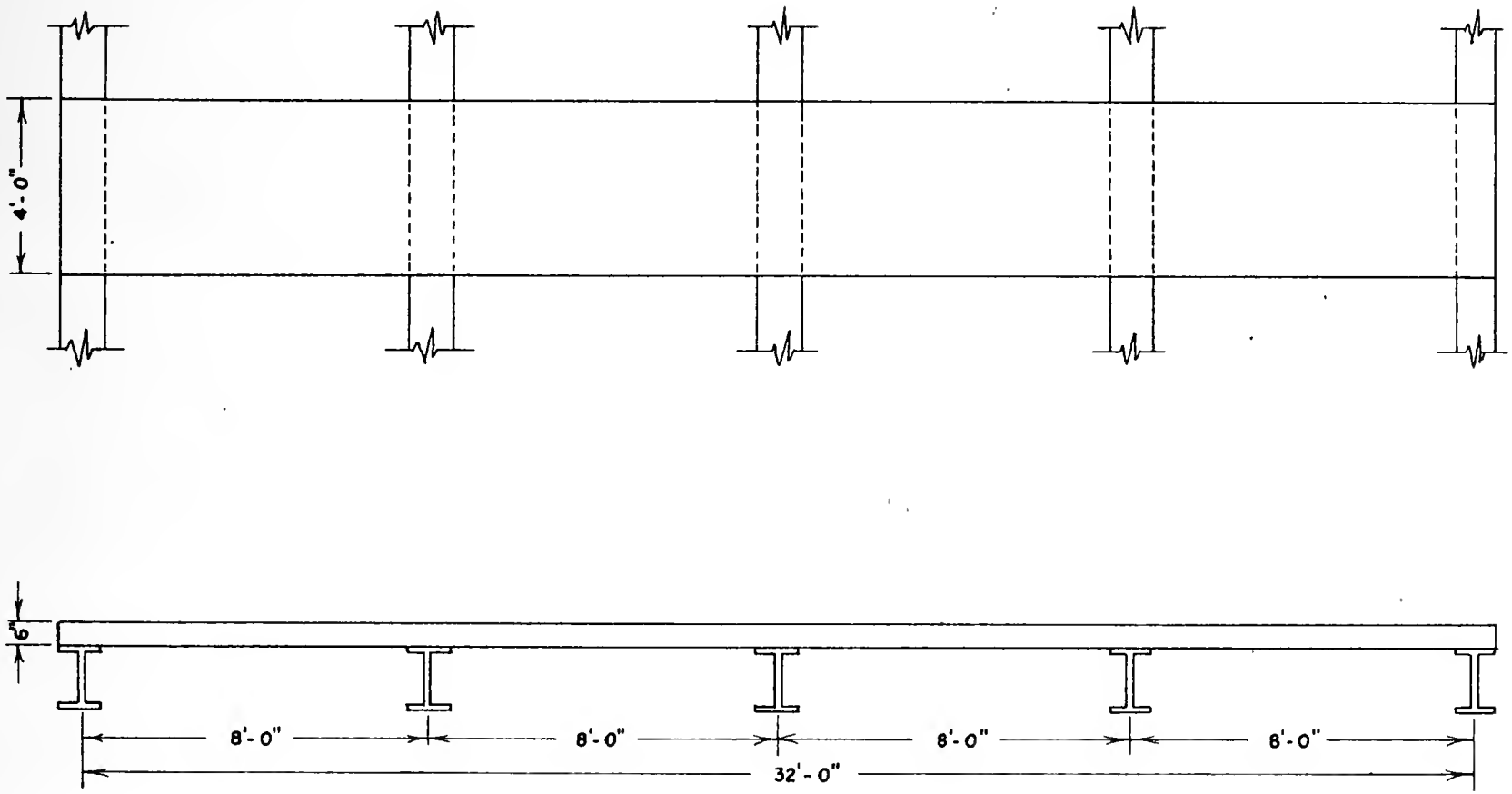

FIGURE 1. TYPICAL DESIGN SECTION

b) $f_t = 0$ tensile stress allowed at design load

c) $f'_{ci} = 4{,}000$ psi compressive strength of concrete at time of initial prestress

d) $f_c = 0.4\, f'_c = 2{,}000$ psi stress at design load after losses. AASHO 1.6.7 (B) (2)

Steel Properties

a) $f'_s = 250$ ksi ultimate strength of prestressing steel

b) 7/16" Φ strand

c) assume 20% losses

Conditions of Support

a) Wide-flange steel beams, flange width 8 3/4"

b) Beam spacing 8'-0" c to c, continuous over five supports

Loading

a) HS 20-44 $P_{20} = 16{,}000$ lb. AASHO 1.3.2 (C)

b) I - impact fraction = 30% of Live Load Moment

c) 6" deep concrete deck

c) 35 psf future wearing surface

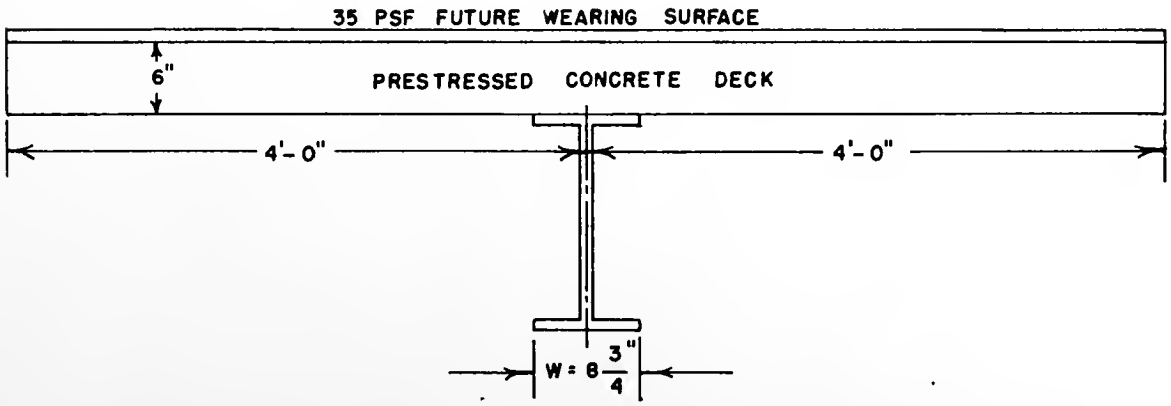

FIGURE 2. TYPICAL MOMENT DESIGN SECTION

Moment Calculations

AASHO Effective Span Length

According to 1.3.2 (A) for slabs supported on steel stringers, S = distance between edges of flanges plus one half of the stringer flange width.

$$S = (8'\text{-}0") - (8\ 3/4") + (8\ 3/4"\ /2) = 7.635'$$

AASHO Live Load Moment

By 1.3.2 (C) for HS20 loading, the moment in foot-pounds per foot width of slab, main reinforcement perpendicular to traffic,

$$LLM = 0.8\ \frac{(S + 2)}{32}\ P_{20} = \frac{0.8\ (9.635)\ 16{,}000}{32} = 3{,}850\ \text{ft-lb/ft}$$

AASHO Impact Moment

$$IM = 30\% \times (LLM) = 0.3\ (3850) = 1{,}155\ \text{ft-lb/ft}$$

Dead Load Moment

Using a value of 150 pounds per cubic foot for concrete and providing for a future 35 pounds per square foot wearing surface, uniform dead load moment, for a six inch slab becomes

$$DLM = 0.8\ \frac{(WS^2)}{8} = 0.1\ (110)\ (7.635)^2 = 641\ \text{ft-lb/ft}$$

Total Moment

The total moment to be provided for then becomes LLM + IM + DLM which is equal to 5,646 ft-lb/ft of slab. Considering a 4'-0" wide element which is six inches deep, total moment to be resisted is 4(5,646) = 22,584 ft-lb.

Stress Analysis

Section Properties

The moment of inertia of the concrete becomes the moment of inertia of a rectangle with a 4'-0" base and a six inch height.

$$I_c = bh^3/12 = (4)\ 12\ (6)^3/12 = 864\ in^4$$

The moment of inertia of the steel is the area-moment of the steel about the center of the section since the steel will be located in two rows, one at the top of the slab and one at the bottom of the slab, and will be uniformly distributed in those rows.

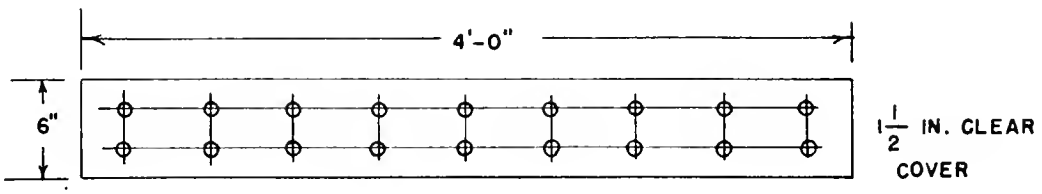

FIGURE 3. TYPICAL REINFORCING PATTERN—250K GRADE STRAND

If a 7/16 inch diameter strand, ASTM A-416 grade strand is assumed, the tensioning load per strand is 18,900 pounds; after 20 percent losses, the load is 15,110 pounds per strand.

The AASHO Code Section 1.6.16 (A) specified 1½ inches cover at the top of the slab and one inch cover at the bottom of the slab. Since it is desired to maintain a symmetrical distribution of pretensioning force, cover will be set at 1½ inches for both top and bottom. This establishes the steel location at 1.281 inches from the centroid of concrete area. Then, subtracting from the steel moment of inertia the effect of the displaced concrete,

$I_s = (nA_s - A_c)d^2$ where n is the modular ratio of 6. Assuming

18 - 7/16 inch strands,

$$I_s = 18\ (0.1089)\ (6 - 1)\ (1.281)^2 = 16.1\ in^4$$

The total moment of inertia for the section is then 880.1 in^4.

The transformed area in terms of concrete area is

$$A_t = A_c + (n - 1)\ A_s = 288 + 5\ (18)\ (.1089) = 297.8\ in^2.$$

Concrete Stresses at Working Load

The concrete stresses at service load are a combination of axial compression and bending moment. The combined stress equation is

$f_c = \frac{-P}{A_t} \pm \frac{M_c}{I}$ where the positive (+) sign indicates tension and the negative signs (-) indicate compression. Solving,

$$f_c = \frac{-(15{,}100)\ 18}{297.8} \pm \frac{22{,}588 \times 12 \times 3}{880.1} = -914 \pm 922$$

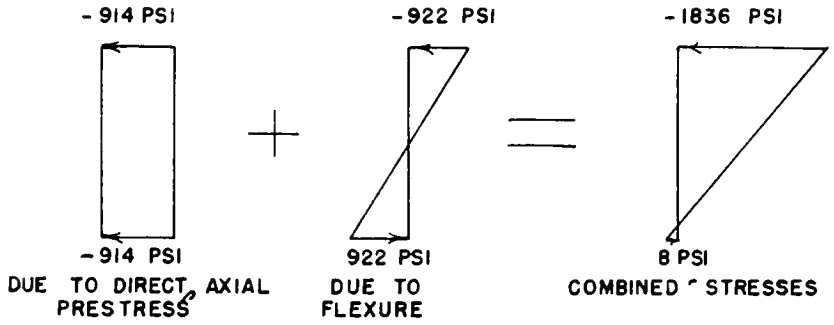

FIGURE 4. CALCULATED CONCRETE STRESSES UNDER SERVICE LOAD

Discussion of Concrete Combined Stresses

The AASHO code requirements have been met in both tension and compression. Allowable compression after losses have occurred is 0.40 f'_c or 2,000 psi. Allowable tension in a precompressed tension zone

is $3\sqrt{f'_c}$ or 212 psi. The allowable stresses are enumerated in AASHO 1.6.7 (B). Although the previously established limitation on tensile stress was to allow none, the 8 psi final tension stress is considered insignificant.

Ultimate Flexural Strength

Supplied Ultimate Flexural Strength

The AASHO specified ultimate flexural strength for rectangular members is assumed as

$$M_u = A_s f_{su}\, d\, (1 - 0.6\, \frac{p f_{su}}{f'_c}), \quad \text{by 1.6.10 (A).}$$

The ultimate steel stress for a bonded member by AASHO 1.6.10 (C) is $f_{su} = f'_s\, (1 - 0.5\, \frac{p f_s}{f'_c})$. Here, $f_{su} = 250\, (1 - .5\, p\, \frac{250}{5}) =$ 250 - 6,250 (p). Assume here that the top row of prestressing steel lies in the compression zone at ultimate load and hence, is being unloaded. Effectively, the steel percentage, p, is then one half of the steel area divided by the concrete area, bd, or 9 (.1089) ÷ 4.5 (48) = .00454. Then, f_{su} = 250 - 6,250 (0.00454) = 221.6 ksi.

The ultimate flexural strength becomes

$$M_u = 9\ (.1089)\ 222\ (4.5)\ (1 - 0.6\ (.00454)\ \frac{222}{5})$$

$$= 979\ (1 - .121) = 860 \text{ in-K} = 71{,}600 \text{ ft-lb.}$$

The value of $p\, \frac{f_{su}}{f'_c}$ = .201 and the steel percentage requirement set forth in 1.6.11 is satisfied, since the value of the expression for the reinforcement index is less than 0.3.

It is now necessary to check the previous assumption; that the

top row of prestressing strands lies in the compression zone is necessary. Equating compression in the concrete to tension in the bottom row of prestressing steel,

$$T = C = A_s f_{su} = 9\ (.1089)\ 222 = 217 \text{ kips}.$$

Using Whitney's stress block,[8]

$$C = a\ (0.85\ f'_c)\ b = a\ (4.25)\ 48 = 204\ a$$

$a = 1.062$ in. The depth of the compression zone to balance the bottom steel alone is $1.062 \div .80$ (for 5,000 psi concrete) or 1.33 inches. The distance from the extreme compressive fiber to the centroid of the top row of steel is 1.719 inches.

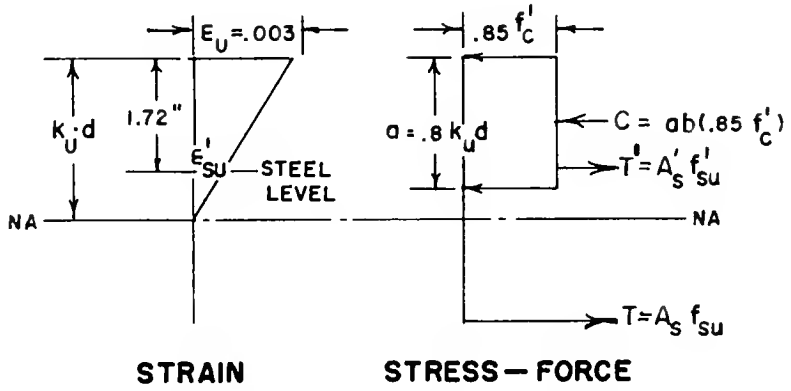

FIGURE 5. STRAIN GEOMETRY AND STRESS-FORCE RELATIONSHIPS AT ULTIMATE CAPACITY

Using strain compatability and internal force balance for the arrangement shown in Figure 5, assume $k_u d = 2.072$ inches. Then

$$C = 338 \text{ k}$$

$$T' = C - T = (338\text{-}217) \text{ k} = 121 \text{ k}$$

$$f'_s = \frac{T'}{A'_s} = \frac{121}{.98} = 123.4 \text{ ksi}$$

$$\varepsilon'_s \text{ (the total steel strain at ultimate)} = \frac{123.4}{29 \times 10^3} \frac{\text{ksi}}{\text{ksi}} = 4.25 \times 10^{-3} \frac{\text{in}}{\text{in}}$$

$$\varepsilon_s \text{ (the original steel strain)} = \frac{15.1 \text{ k}}{(.1089 \text{ in}^2)\ 29 \times 10^3 \text{ ksi}}$$

$$= 4.78 \times 10^{-3} \ \frac{\text{in}}{\text{in}}$$

$$\varepsilon'_{su} \text{ (the loss in steel strain)} = \varepsilon_s - \varepsilon'_s = .000530 \ \frac{\text{in}}{\text{in}}$$

From the strain diagram,

$$\varepsilon'_{su} = \frac{(k_u d - 1.72)\ (.003)}{k_u d} = \frac{(.352)\ .003}{2.072} = .000510 \ \frac{\text{in}}{\text{in}}$$

Therefore, it is evident that the top row of steel lies in the compression zone and is being de-tensioned at the accomplishment of ultimate moment. The previous assumption is thereby satisfied.

Required Ultimate Flexural Capacity

Using the load factors found in AASHO 1.6.6, the required ultimate flexural capacity is

1.5 DLM + 2.5 (LLM + IM)

1.5 (641) + 2.5 (5,005) ft-lb /ft

(961.5 + 12,512.5) ft-lb /ft = 13,474 ft-lb /ft.

For the four foot wide section under consideration, total capacity required is 53,896 ft-lb, less than the 71,600 ft-lb supplied. Hence, the section is adequate with respect to ultimate flexural capacity.

Stresses at Transfer and Handling

Initial Stresses

The stresses which are initially present in the slab sections are due to axial prestressing alone. There exist no stresses due to bending of the member since the member is fully supported by the bottom of the forms. The initial axial force is (18,900 x 18) pounds distributed over a transformed concrete area of 298 square inches. This

results in a uniform compressive stress of 1140 pounds per square inch. AASHO 1.6.7 (B) sets a limit of 0.6 f_{ci} on this stress, or 2400 pounds per square inch in this case.

The foregoing statements assume that the strands are detensioned symmetrically about the center line and that the resulting force is axial. The largest bending moment due to eccentricity of the strand would be the force in one cable times a lever arm of 1.28 inches. The stresses due to this eccentrically applied load are not significant for the first strand that is cut: $f_c = \pm \frac{Mc}{I} - P/A$

$\frac{Mc}{I} = \frac{(15{,}100 \times 1.28)}{880 \text{ in}^4}$ in - lb x 3 in = 65.9 psi (+ or -)

$\frac{-P}{A} = \frac{-15{,}100}{298} = -50.6$ psi and the eccentric effect is nearly cancelled by the direct compressive stress, resulting in very small tension stresses.

The resultant stresses are even less critical for strands which are cut and cause bending moments due to eccentricity after at least two strands have been symmetrically released.

Handling of Slab Sections

The determination of pick-up points for the slab pieces should be made with consideration for ease of handling. Choosing two pick-up points along the section as convenient it will be shown that the quarter-points of the section would be acceptable pick-up points.

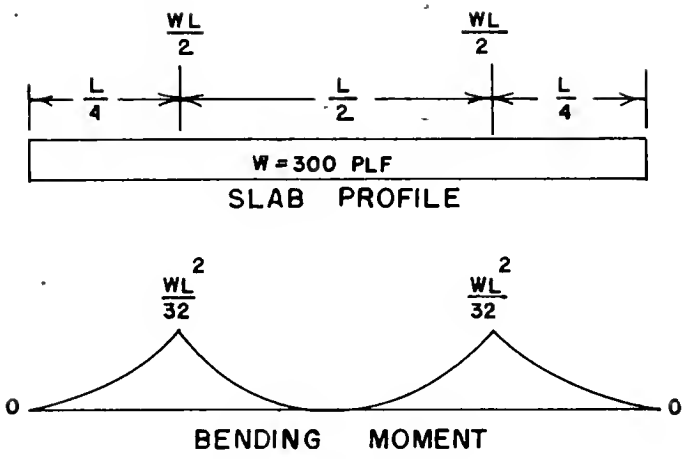

FIGURE 6. SLAB HANDLING, PICK-UP AT QUARTER POINTS

The maximum bending moment in this configuration is $\frac{WL^2}{32}$ or 300·32 = 9,600 ft-lb. This 9,600 ft-lb moment is 42.5 percent of the total service moment, and would provide approximately a 57.5 percent reserve for impact due to lifting.

Assuming that pick-up is made immediately after stress transfer, the uniform axial stress due to prestressing is 1,140 pounds per square inch. Stresses due to flexure are $\pm$ Mc/I = 9,600 x 12 x 3/880, resulting in a stress of $\pm$ 338 psi.

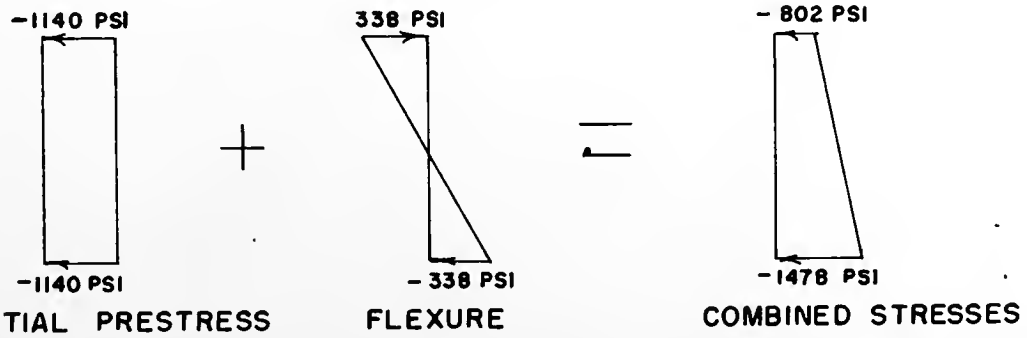

FIGURE 7. HANDLING STRESSES AT PICK-UP POINT IMMEDIATELY AFTER STRESS TRANSFER

The combined stresses due to handling immediately after transfer as shown in Figure 7, are within the allowable stresses set by the AASHO Code. After some time and all losses, stresses due to pick-up at the quarter point would be 572 psi on top and 1252 psi on the bottom, both compressive.

Roadway Drainage

The single most desirable condition to be met in providing roadway drainage is simplicity in its accomplishment. Ideally, the deck section would be of uniform thickness, would be planar, and would be uniformly prestressed with straight tendons.

The accomplishment of transverse drainage presents the largest problem since longitudinal drainage can easily be accomplished by providing gradient. Longitudinal drainage facilitated by camber would be tolerable but would be less desirable than drainage by gradient since the post-tensioning cable would necessarily have an arched profile.

If the prestressed deck system which is proposed was placed on a supporting system which was transversely flat and provided no natural drainage, there are three immediately evident ways in which transverse roadway drainage could be provided. The first and most easily accomplished method for providing transverse drainage would be the placing of an asphalt wearing surface which provides the desired crown. The typical structural design, which appeared above, provided for a future 35 psf wearing surface which could be the asphalt surface which provides the bridge crown. The disadvantages which might be experienced in the use of an asphaltic surface are: deck deterioration could take place unnoticed, causing eventual spalling of the concrete and distress

of the steel; since asphalt does not provide a waterproof seal, there is a possibility that water and de-icing chemicals could become trapped. Use of the asphalt wearing surface would be at the discretion of the agency in charge of the bridge and its code requirements, tempered by experience in other structures under its jurisdiction. Should the asphalt surface prove workable, it would provide an easy solution to the problem of lateral roadway drainage.

The second drainage method would consist of tilting the entire deck system to provide lateral drainage in one direction. This could be accomplished by specification in new construction or by releveling the supporting system on its piers when the deck system was being used in a replacement situation.

Drainage facility could be provided in another manner by casting the crown in the deck as an integral part of the roadway. The composite crown could be formed by casting the deck in an inverted position in order to provide a uniform slope to the crown (provided by the casting bed) as well as a horizontal working surface for the concrete finishers. This method would most likely increase the cost of the deck due to its additional forming requirement. The prestressing tendon profile could be altered to provide an axial prestressing force but at additional precasting cost. Also, the stress level in the top and bottom rows of prestressing steel might be adjusted to eliminate eccentricity of the prestressing force. Slight variability in concrete properties from point to point along the member could negate the effort of stress level adjustment, resulting in no characteristic structural improvement from stress level adjustment. Care would necessarily be exercised in this

instance to ensure proper performance at ultimate capacity. In implementing this method on bridges, alignment of the crown on the adjacent sections would be difficult because a small misalignment, although not critical from a structural standpoint, would be evident when one viewed the bridge longitudinally.

If it is desired to place the deck system on an existing bridge whose floor system is cambered, a natural drainage could be accomplished by stepping the bottom of the precast deck to match the camber in the floor system. The least depth dimension, occurring at the base of each step, would be the structurally designed uniform depth, and the prestressing cables could be draped at the center of the member, thereby maintaining an axial prestressing force.

Slab Tie-Down System

The slab tie-down system which has been examined and is herein proposed consists of a 3/4 x 2 7/8 in. steel anchor, a spring steel clip, and a 3/4 x 2 3/4 in. high strength steel bolt; see Figure 9. A similar arrangement is used by the Association of American Railroads to fasten rails to prestressed, precast concrete ties.

Anchors

The anchors recommended by The American Railway Engineering Association (AREA) are specified to be "formed from corrosion-resisting chromium-nickel steel, meeting the requirements of ASTM specification A-167." [6] Alloy steel is also recommended by the Association of American Railroads (AAR) for any metal to be encased in concrete. The specifications also include a requirement that the anchor should be

able to develop a vertical load of 20,000 lb or a 300 ft-lb torque without deformation of the anchor. These requirements are based on a specified concrete strength of 6,500 psi at seven days or a 28 day strength of 8,000 psi. (Two #2 stirrups are also placed 3 in. on each side of the anchor.) There would necessarily be a reduction of the anticipated pull-out strength of the anchors for lesser concrete strengths, or for the case of no shear reinforcement.

The anchor which was used during parts of the laboratory testing is a commercially available anchor which is formed by bending a 3 x 2 in. stainless steel plate to form a cylinder with a flared end, inside which threads are subsequently cut. This anchor was studied in the Portland Cement Association (PCA) research laboratory with regard to pullout strength.[4] Two identical anchors were cast in a block 10 in. deep 18 in. wide and 48 in. long with 24 in. separating the anchors; the concrete had an average cylinder strength of 6830 psi at the time of the pullout test. Loads were monitored by a 50 kip load cell and were applied to a 3/4 in. diameter threaded rod with a center-hole ram. The anchors (3/4 x 2 7/8 in. uncoated) were found to have an average pull-out strength of 12.8 kips and failed by tearing off the top surface of the concrete block. Similar anchors 3/4 x 1 7/8 in. (painted) were tested in the same manner and were found to have an average pull-out value of 6.6 kips, when failure by pull-out of a concrete cone around the anchor was observed.

The most desirable anchor for the precast deck is the 3/4 x 2 7/8 in. uncoated anchor. Applied torque in the bolt can be maintained at a level which will allow for an increase in load due to uplift of the

slab without danger of damage to the concrete in the vicinity of the anchor. The anchor in place under the slab should be virtually corrosion free since it is self draining.

Bolting

The bolts specified by the AREA specifications are 3/4 in. diameter, high strength steel bolts with hexagonal heads. Length is specified as 2 3/4 in. with a minimum engagement length of one inch but not to exceed 1½ inches. The specifications also require that the shanks of the bolts be dipped in petrolatum before engagement. The necessity for this requirement was demonstrated in the PCA testing where it was found that the force of friction between the bolt and anchor in the non-lubricated situation was large in magnitude. Achievement of the full intended tension in the bolts and the intended holding force of the fastener could not be realized with non-lubricated bolts where much of the applied torque was taken up by friction. Performance of the lubricated bolts was as intended and predicted. For this reason, the bolts which were used in the laboratory investigation were lubricated before any torque was applied.

The applied torque versus the clamping force realized when a 3/4 in. bolt is tightened is illustrated in Figure 8. The basis for the values illustrated follows: "When a bolt is torqued up, the initial axial load due to the torque is approximately $F_i = \frac{T}{0.2D_0}$." [2]

- F_i = initial force
- T = applied torque
- D_0 = major bolt diameter
- 0.2 = average factor for plain bolts

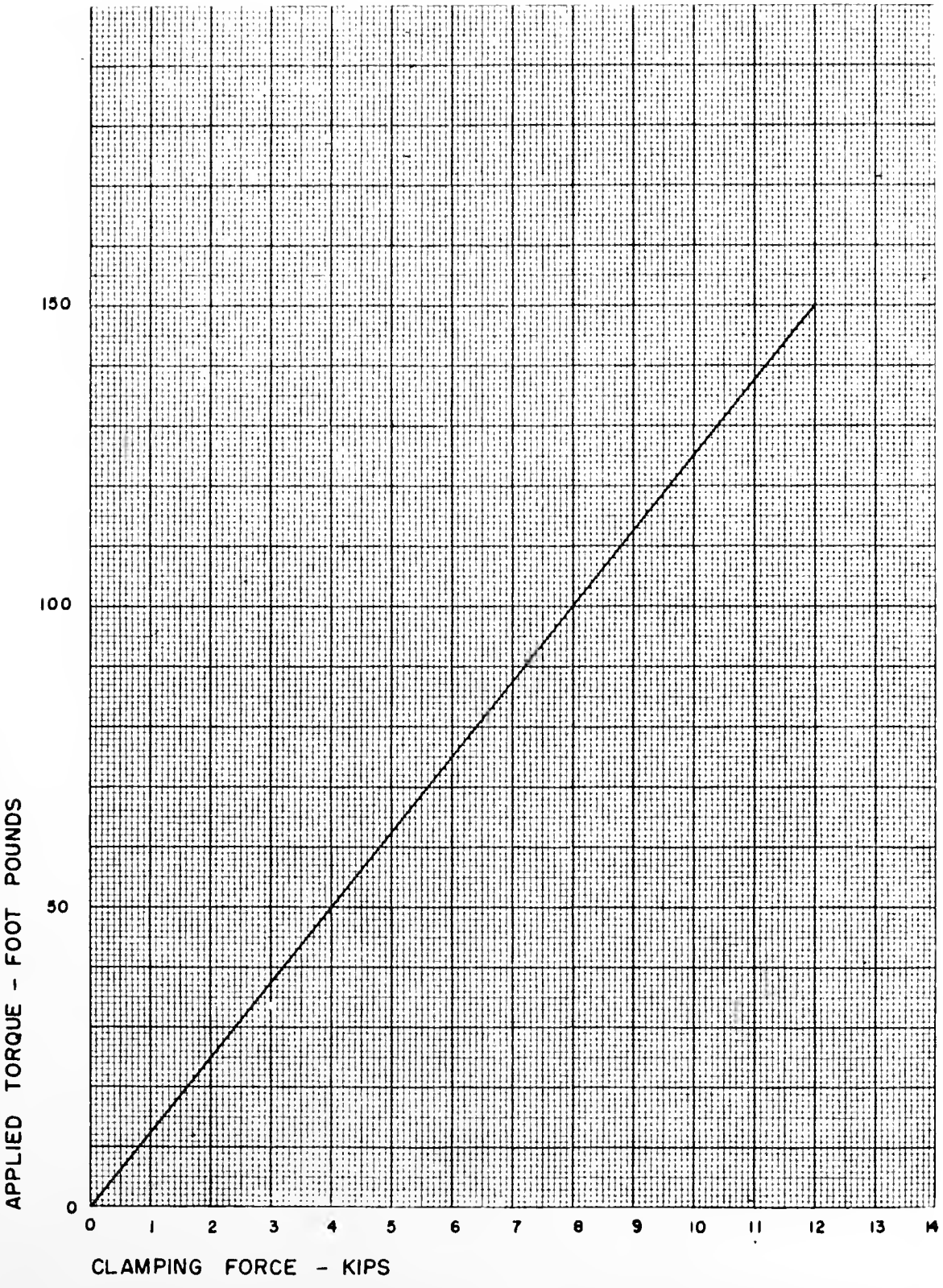

FIGURE 8. APPLIED TORQUE VERSUS CLAMPING FORCE, 3/4" BOLT

Hence, for a 3/4 inch diameter bolt, $F_i = \frac{T(\text{ft-lb}) \times 12\ (\text{in/ft})}{(0.2)\ (.75\ \text{in.})}$

$F_i = 80 \times T$ where T is measured in ft-lbs. Faupel also indicates a maximum torque (to bring the material just below yielding) of 1,259 in.-lb (104.9 ft-lb) for a 3/4 - 10 nominal size bolt of structural steel, or 1,530 in.-lb (127.5 ft-lb) for austenitic stainless steel, the values being approximate.

The testing in the PCA laboratories indicated a loss in applied torque (at the 150 ft-lb level) when the bolts were subjected to repeated loading. The bolts, upon a reapplication of the initially applied torque after approximately 0.6 million cycles of loading in one case and approximately 0.1 million cycles of loading in another case where observed to maintain the desired torque value to 3 million cycles of loading.[4]

Spring Clip

The spring clip, illustrated in Figure 9, is a commercially available clip which is used by the AREA to fasten, by bolting, precast concrete ties to rails. The clip is formed by hot-bending a strip steel bar. The suggested clip is intended by the AREA to be used with a 119CF&I rail section, on the field side of the rail. The tongue of this clip is the largest of the standard clips, being 2 5/16 in. from center of the bolt hole to point of bearing on the tongue. The largest lap of the tongue over the beam flange to which attachment was being made would be 1 1/16 in. No evidence of clip fatigue was observed during use in the laboratory.

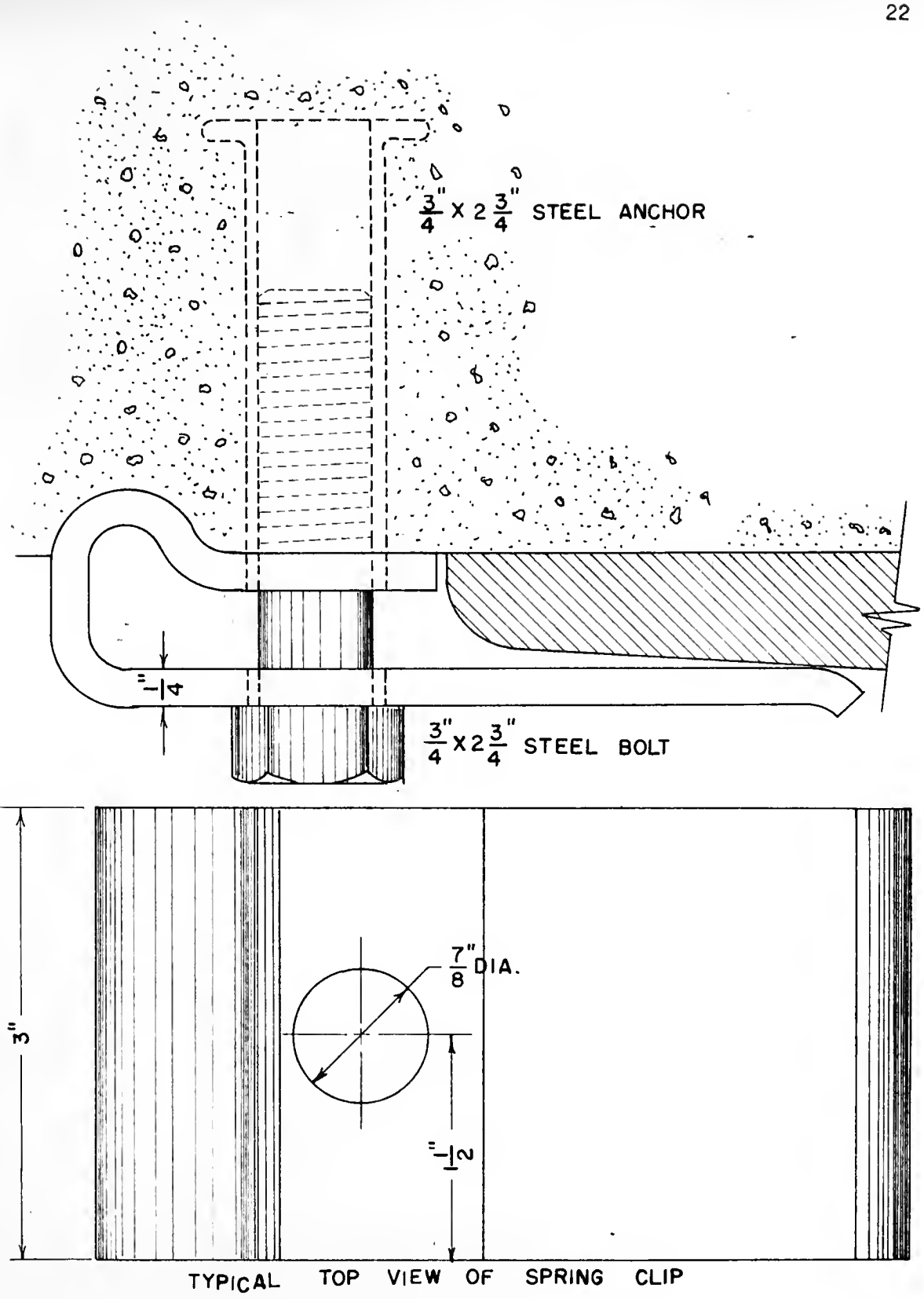

FIGURE 9. SLAB TIE-DOWN ARRANGEMENT

Post-Tensioning System

Cable

The post-tensioning of the several elements on a bridge deck to form a single unit will be accomplished by threading a series of cables through void spaces which have been accurately positioned during precasting. A post-tensioning cable of one-half inch diameter is proposed in order to minimize the number of cables and the size and number of void spaces. A small number of cables would also minimize the field labor required to erect the system. Since it would be most desirable to maintain an unbonded cable, a coated cable which has been treated with a rust inhibitor is necessary. A cable thus formulated would not be susceptible to the corrosive action of water in the void space or to friction in the void space due to construction or repeated loading. The void space would be placed at the center line of the slab and would be round. Size of the void space could be as much as 2 inches in diameter in the interior panels. In the special end panels containing the anchorage assemblies, the void space should be made no larger than necessary to accommodate the strand as any greater reduction will produce anchorage zone problems upon stressing.

Anchorage

Anchorage of the cable would be by means of anchors provided in special end sections. The anchorage assemblies would be cast into the end section and the section would be placed like any other section. By precasting the end sections, field time for erection would be minimized. An anchor which could satisfy the requirements of the post-tensioning system proposed must be shallow and must fit between the layers of

prestressing strand which will be in place. Special attention should be given to conventional steel reinforcing in the anchorage zone which may be recommended by the manufacturer. Special attention must also be given in the selection of a system as to the clearance requirement at the level of the slab for the post-tensioning jack; a minimum removal of approach paving is essential as it must be replaced before traffic is allowed to return to the bridge.

Transverse Continuity Joint

The necessity of choosing a joint configuration between adjacent deck sections which would allow a flexibility of application of the deck system became immediately apparent. For the system to find more than limited use, an easily fabricated joint shape which could meet the desired post-tensioning and rotation requirements imposed by the basic design was imperative.

The purpose of the joint would basically be to transfer load between adjacent sections as well as to permit the relatively small rotations which would necessarily take place between adjacent members. These small rotations could occur due to two dissimilar conditions; the first condition would be the requirement that the deck conform to a longitudinal deck profile as in the case of a vertical curve, and the second condition being rotations caused by moving loads which deflect the bridge floor and cause rotation between adjacent members. A contoured joint should permit these movements and profile conformance more easily than a flat joint. Planar joints would also have the undesirable condition of excessive bearing stresses between adjacent sections caused by line bearing during rotation or due to a longitudinal change

in deck profile.

The problem of supplying a satisfactory transverse joint was studied in the laboratory under two quite different circumstances. A two dimensional photoelastic investigation was conducted which quite precisely indicated the principal stress directions and the stress level at selected points and permitted a prediction of the probable mode of failure of the area adjacent to the joint due to post-tensioning the slabs in a direction normal to the joint. At the same time, full-size concrete joint models were cast in the laboratory and were subjected to qualitative observation when rotations were imposed on the post-tensioned joints by a repetitive load.

Photoelastic Joint-Shape Study* 9

The models which were selected for the photoelactic study were models whose shapes were considered to be feasible for the prototype concrete sections. The shapes of the models which were investigated are shown in Figures 11, 12, 13. For purposes of the laboratory investigation, the plastic models were made one half the size of the prototype concrete models; the dimensions of the models are shown in Figures 11, 12 and 13.

The photoelastic testing, which made use of a polariscope and photography, was limited to a study of the stress distribution in adjacent sections due to a compressive force applied in the plane of the model. The compressive force corresponded to the post-tensioning force in the proposed bridge deck. It was not possible to examine the

---

*The photoelastic joint study was conducted by Robert J. Craig, MSCE, Purdue University.

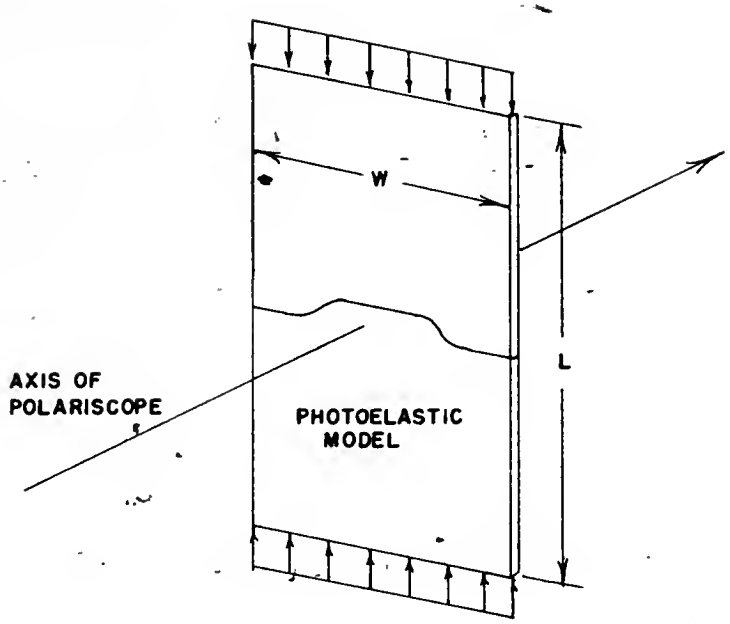

FIGURE 10. LOADING OF PHOTOELASTIC JOINT MODELS

effect of shear forces acting at the joint due to the limitations imposed by the loading apparatus.

The models were loaded as short columns with the length-to-width ratio of each model fixed at three-to-eight, in order that uniform stresses would develop in the model on both sides of the joint.

Semicircular Joint Model. The first model which was evaluated was the full semicircular section. A brittle-coating method of analysis using Stresscoat was used to determine the principal stress directions; Figure 11 indicates the direction of the principal stresses. The subscripts 1 and 2 in the figure refer to the algebraically largest and smallest plane stresses respectively at a point, where tension is positive.

One would expect to discover tension stresses normal to the

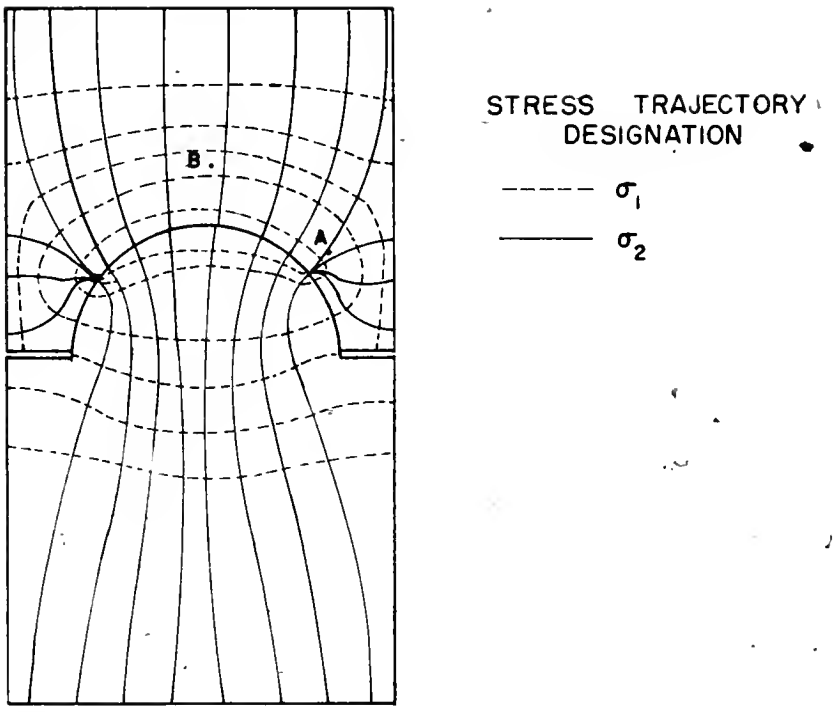

FIGURE 11. PRINCIPAL STRESS DIRECTIONS ON SEMICIRCULAR JOINT.

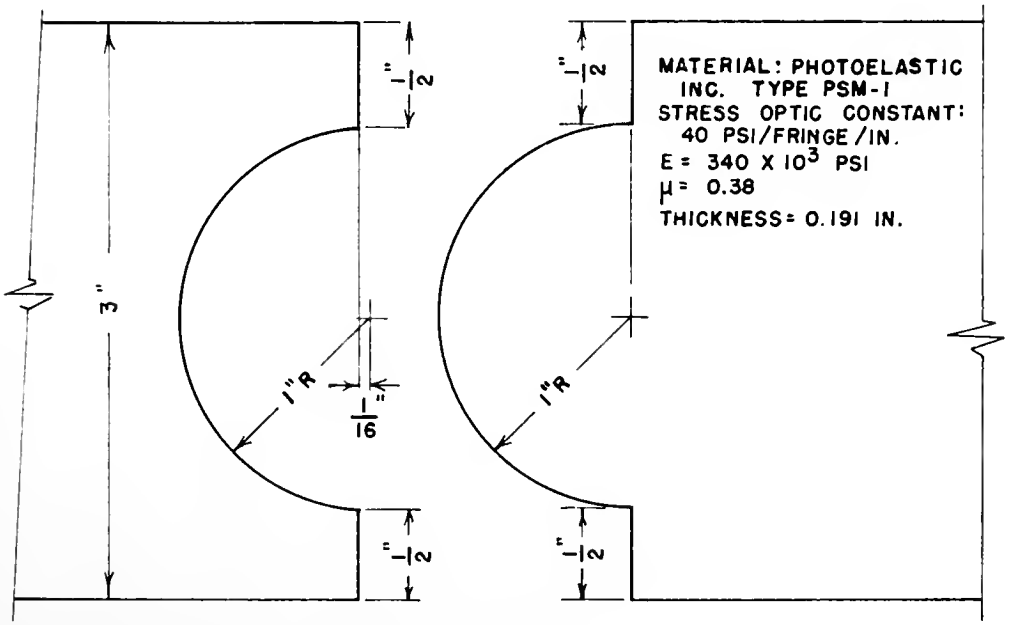

FIGURE 12. PHOTOELASTIC MODEL, SEMICIRCULAR JOINT

stresses labeled σ_2 , and tensile stresses of 144 psi at 30 degrees to the horizontal (joint under 100 pound load) were determined in the vicinity of point A in Figure 11. With an increase in the compressive load on the model, the tensile forces correspondingly increased; this indicated that in the concrete prototype, which is relatively weak in tension, the corners on the concave side of the joint would be expected to develop tension cracks and eventual spalling. The stress trajectories indicated a concentration of load at the head of the semicircle which would also be an undesirable likelihood in the concrete prototype.

Circular Sector Joint Model. The circular-sector model was loaded in the same manner as the semicircular model. The principal stress directions were similar to those of the semicircular model discussed above and the existence of tensile stresses in similar locations on both models was found. The tensile stress on the concave side of the joint in the vicinity of point A (in Figure 11) on the circular sector was of smaller magnitude at the same compressive load than in the semicircular joint. With the largest tensile stresses on the section tending to fracture the corners on the concave side of the joint, a secondary failure would be predicted at the center of the section since the tensile stresses at that location are of the next most critical magnitude. (point B of Figure 11) Although the circular-sector joint indicated lower stresses at similar load levels than the semicircular joint, the corner-splitting possibility in a concrete prototype led to dismissal of the section from further consideration.

Flat Key-Type Joint Model. The flat joint was found to distribute the stresses at the joint most uniformly. The stress

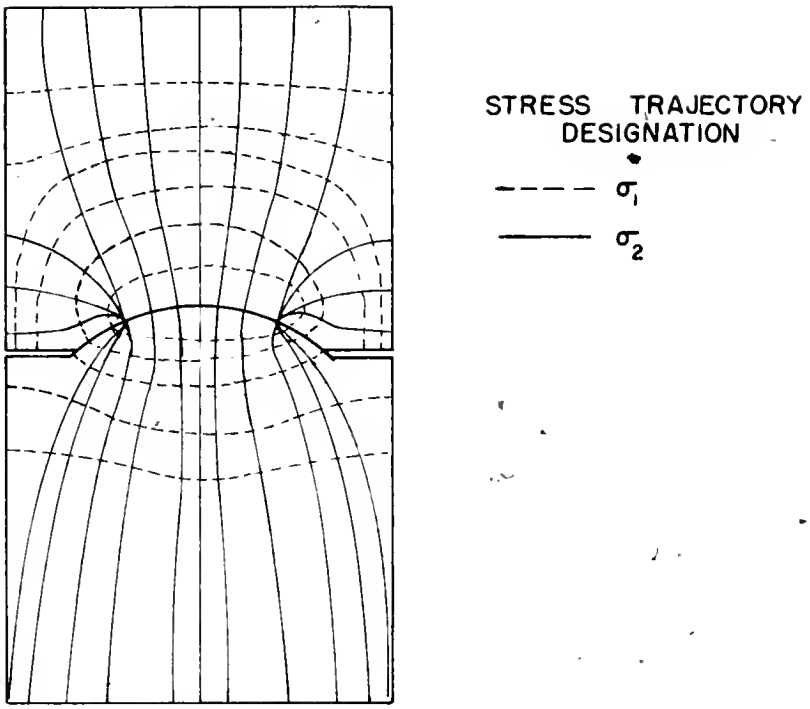

FIGURE 13. PRINCIPAL STRESS DIRECTIONS ON CIRCULAR SECTOR JOINT.

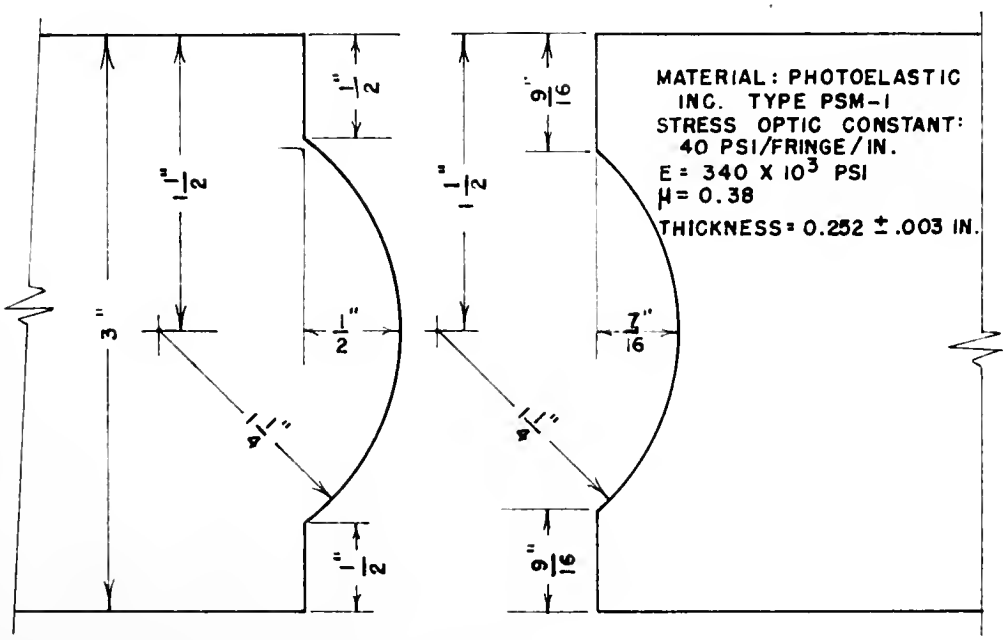

FIGURE 14. PHOTOELASTIC MODEL, CIRCULAR SECTOR JOINT

trajectories shown in Figure 15 were observed to become more uniform nearer the joint than was the case with the other models.

The flat joint displayed the most desirable characteristics of the three models for application to a concrete section; the flat joint, upon evaluation, showed tensile stresses at only one point, and these tensile stresses would not be detrimental to the performance of the system because of their small magnitude. Since this joint was selected for use, an evaluation of its performance as determined using photoelasticity and electrical resistance strain gages is presented.

Evaluation of Photoelastic Data for Flat-Joint Model. The photoelastic model, shown in Figure 16, was loaded in compression in the field of a polariscope and photographs of the resulting fringe patterns were made. The photographs are included as Figures 17, 18, and 19.

The evaluation of the data thus obtained was made using the theory of photoelasticity.[1] The stress optic law in two dimensions at normal incidence can be applied to the fringe photographs. The numbers on the fringe photographs indicate the fringe order at the point indicated, or the relative retardation at the point where one cycle of retardation is equal to 2π. The fringe order, N, is related to the principal stress difference, $(\sigma_1 - \sigma_2)$, at the point in question by the relation $(\sigma_1 - \sigma_2) = \frac{Nf\sigma}{h}$ where "$f\sigma$" is the material fringe value and "h" is the model thickness. The stress "σ_1" is the algebraically largest stress of the principal stresses σ_1 and σ_2, where tension is of positive sign.

For the model used (Figure 16), $(\sigma_1 - \sigma_2) = 158.9$ N. The points

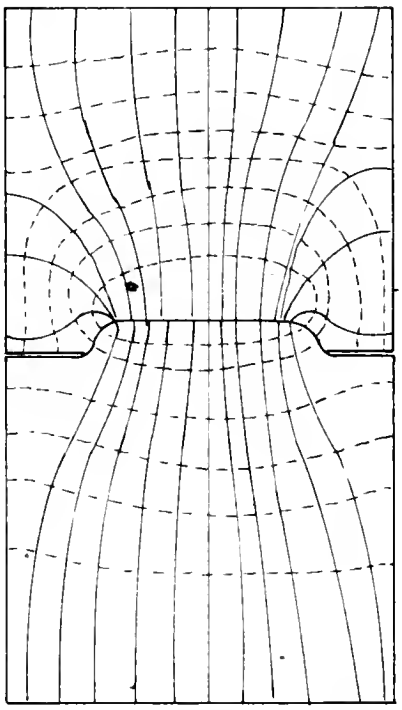

FIGURE 15. PRINCIPAL STRESS DIRECTIONS ON FLAT JOINT

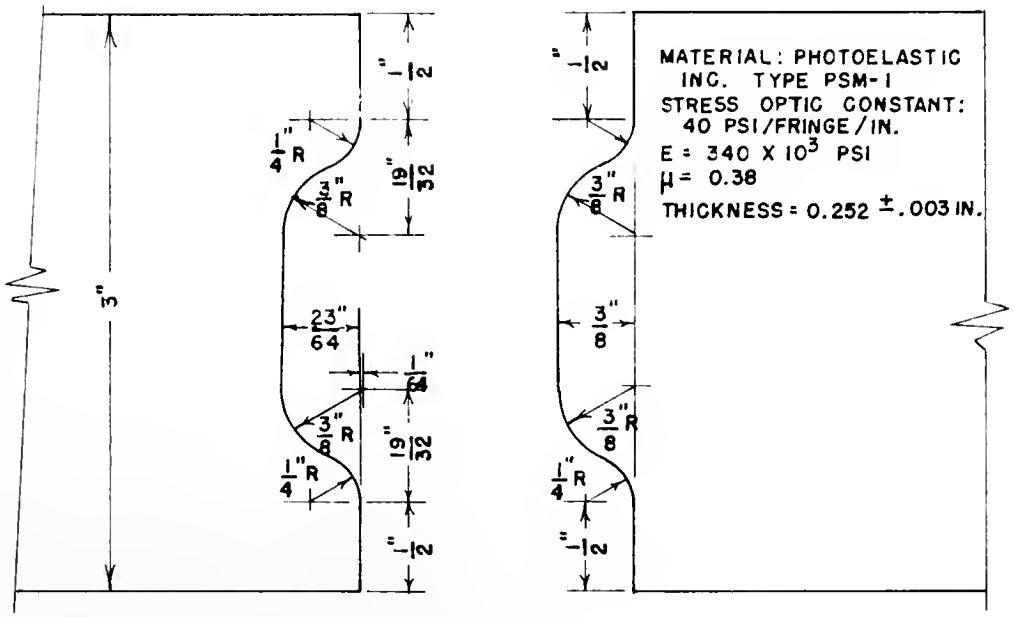

FIGURE 16. PHOTOELASTIC MODEL, FLAT JOINT

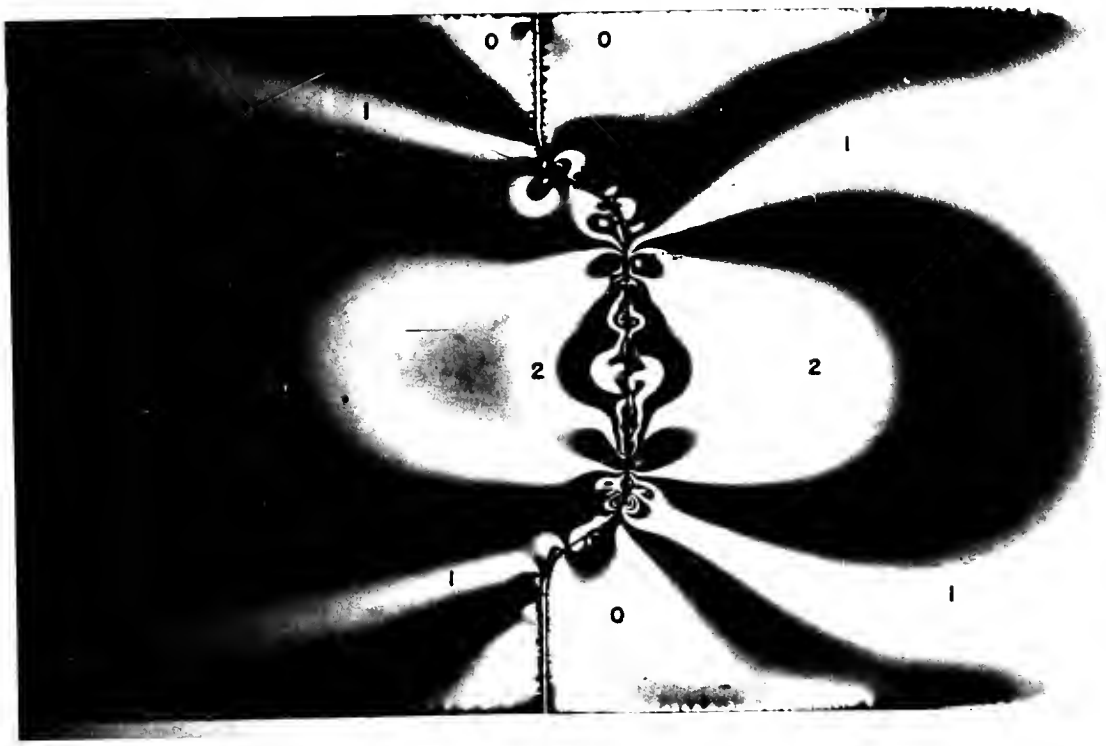

FIGURE 17. FLAT JOINT MODEL FRINGE PHOTOGRAPH , P=100 LB

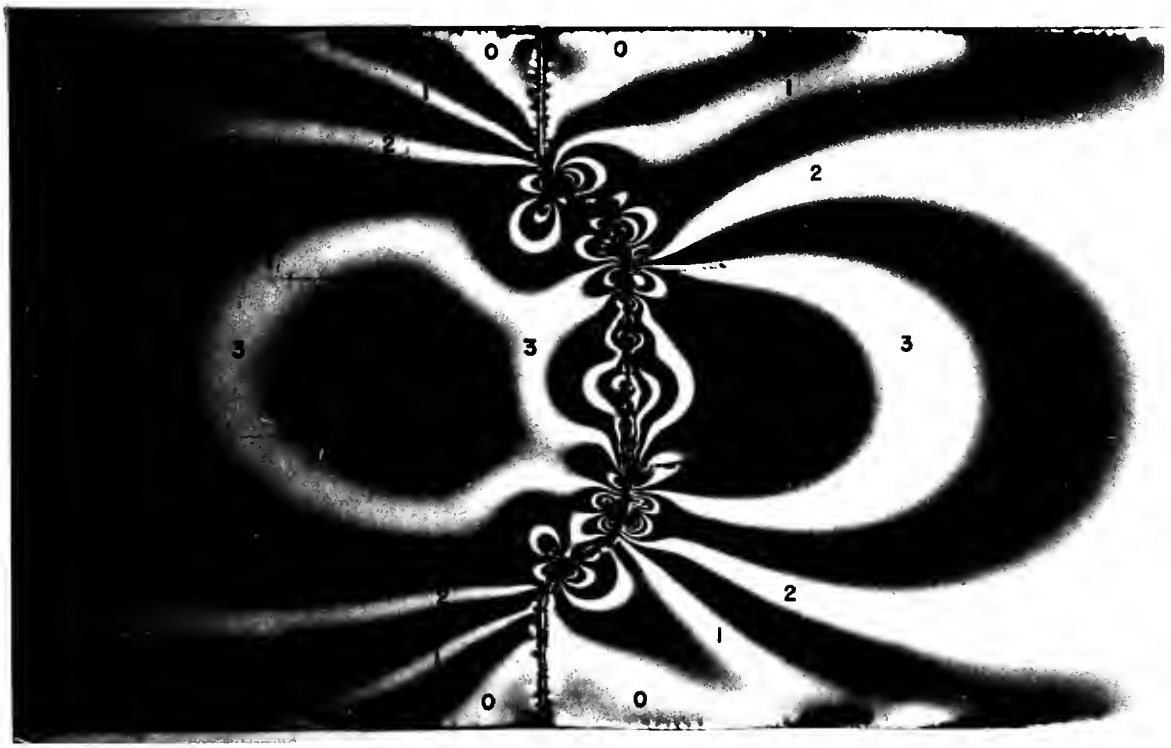

FIGURE 18. FLAT JOINT MODEL FRINGE PHOTOGRAPH, P=200 LB

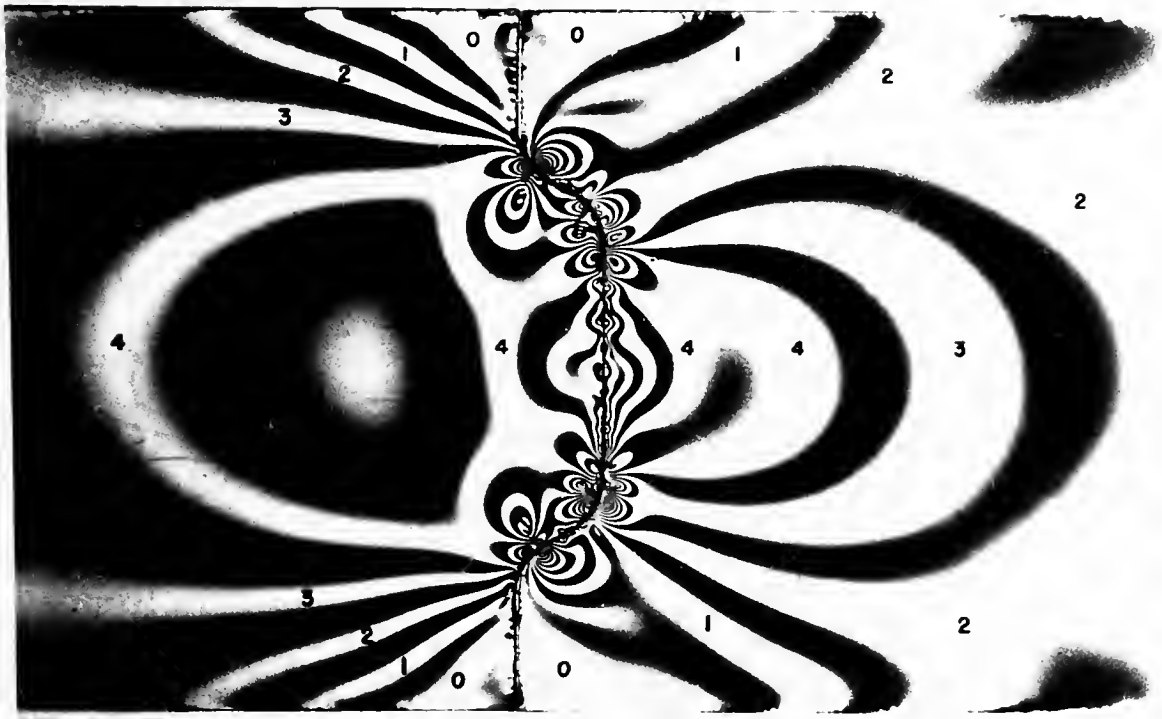

FIGURE 19. FLAT JOINT MODEL FRINGE PHOTOGRAPH, P=300LB

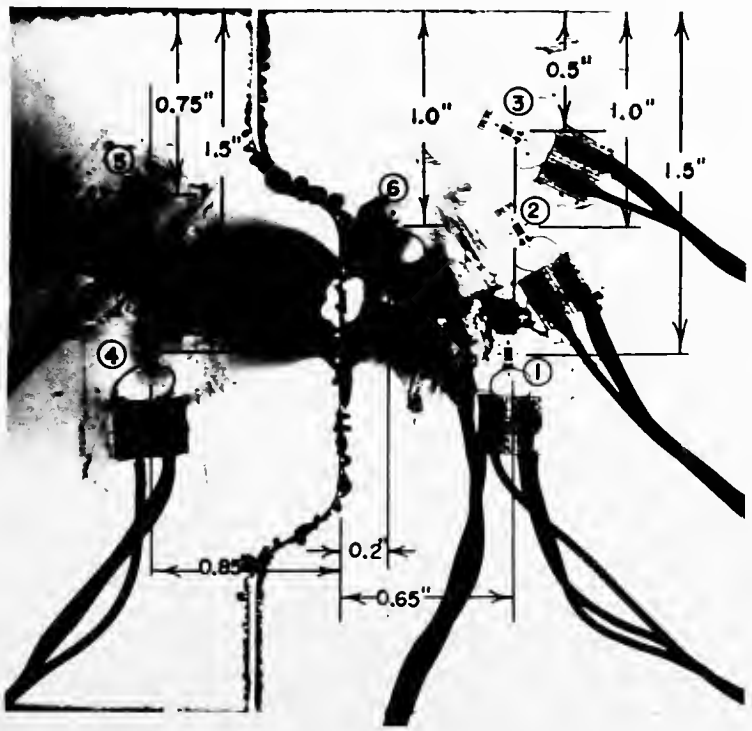

FIGURE 20. FLAT JOINT MODEL STRAIN GAGE LOCATIONS

which were studied are shown in Figure 20. In order to separate principal stresses, strain gages were mounted at each point to be examined in the direction of the previously determined stress trajectory, σ_1 in Figure 15.

The stress trajectories were determined by a photographic method,[3] based on the fact that a grid mounted at 45 degrees to the polarizer axis in a crossed plane polariscope will be visible in the light areas of a stressed-model image and the direction of the grid will indicate the direction of the principal stresses. A multiple exposure photograph, one image taken each time the analyzer, grid, and polarizer are rotated in the same direction through 90 degrees gives a complete stress trajectory picture of the stressed model.

Theory for Data Reduction. From the theory of photoelasticity, the equation relating the fringe order at a point in a stressed model and the principal stress difference at that point is known as $(\sigma_1 - \sigma_2) = \frac{Nf\sigma}{h}$. From elasticity, the relationship between stress and strain is known as $\varepsilon_1 = \frac{1}{E}(\sigma_1 - \nu\sigma_2)$. The principal stress difference is known from the fringe photographs, and the strain at selected points can be determined with electrical resistance strain gages. The strain ε_1 corresponds to the stress σ_1. Solving the relationships above for σ_2, one finds that $\sigma_2 (1 - \nu) = E\varepsilon_1 - \frac{Nf\sigma}{h}$; σ_2 can now be found directly as all quantities on the right-hand side of the equation are constant or are known from measurement. Strain gage data are presented in Table 1 and the photoelastic data are presented in Table 2. The fringe orders indicated in Table 2 are the result of graphical interpolation to arrive at the fractional fringe order.

Table 1. Measured Strains on Flat Joint Photoelastic Model

Load (lb)	Point on Flat Joint Model					
	1	2	3	4	5	6
0	0	0	0	0	0	0
100	325	200	-180	220	135	45
200	629	410	-300	475	305	230
300	1055	595	-500	700	485	400

Strain is measured in micro-inches per inch (tension positive)

Scaling Model to Prototype Stresses.[1] In any two dimensionally stressed body, the stress at a point in the body is related to the applied load by the relationship $\sigma = \frac{P}{bh}$ where σ is the stress, P is the applied load and b and h are a length dimension and thickness respectively. In dimensionless terms this becomes $1 = \frac{\sigma bh}{P}$. Using the subscripts p and m to represent the model and prototype respectively, dimensionless (and equal) quantities may be written for each item. Equating the two expressions, $\frac{\sigma_m b_m h_m}{P_m} = \frac{\sigma_p b_p h_p}{P_p}$. Solving this for the prototype stress, $\sigma_p = \sigma_m \frac{b_m h_m}{b_p h_p} \frac{P_p}{P_m}$.

Table 3 demonstrates the application of this equation to the principal stresses σ_1 and σ_2 where the prototype is twice the size of the model. Assuming the applied loads and the thickness of section were the same, $\sigma_p = \frac{\sigma_m}{2}$. Direct stress on the gross section would be halved by applying the same force to the prototype as to the model.

Conclusions. As illustrated in Table 3, stresses which will be encountered in the prototype concrete deck system due to post-tensioning

Table 2. Principal Stress Determination on Flat Joint

Load	Point	N	$\sigma_1 - \sigma_2$ (psi)		$(1 - \nu)\sigma_2$ (psi)	σ_2 (psi)	σ_1 * (psi)
0	1	0	0	0	0	0	0
100	1	2.05	191.5	110.5	-81.0	-130.6	+60.9
200	1	3.85	595.9	213.9	-382.0	-616.1	-20.2
300	1	4.30	683.3	358.7	-324.6	-523.5	+159.8
0	2	0	0	0	0	0	0
100	2	1.69	268.5	68.0	-200.5	-323.4	-54.9
200	2	2.95	452.9	139.4	-313.5	-505.6	-52.7
300	2	3.33	529.1	198.9	-330.2	-532	-2.9
0	3	0	0	0	0	0	0
100	3	1.07	170.0	-57.8	-227.8	-367.4	-197.4
200	3	1.90	286.0	-102.0	-388.0	-625.8	-366.8
300	3	2.05	325.7	-170.0	-495.7	-799.5	-473.8
0	4	0	0	0	0	0	0
100	4	2.20	349.6	74.8	-274.8	-443.2	-93.6
200	4	3.50	556.1	158.1	-398.0	-641.9	-85.8
300	4	4.80	746.8	238.0	-508.0	-819.3	-72.5
0	5	0	0	0	0	0	0
100	5	1.50	238.4	45.9	-192.5	-310.5	-72.1
200	5	2.70	413.1	103.7	-309.3	-498.9	-83.8
300	5	4.10	651.5	161.5	-490.0	-790.3	-138.8
0	6	0	0	0	0	0	0
100	6	1.65	246.3	15.3	-231.0	-372.6	-126.3
200	6	2.75	421.1	78.2	-342.9	-553.1	-132.0
300	6	3.25	516.4	136.0	-380.4	-613.5	-97.1

* tension positive

Table 3. Model to Prototype Scaling

Load	Point	Prototype Stress σ_2 (psi)	σ_1 (psi)	Prototype Gross Section Stress (psi)
100	1	-65.3	+30.5	-66.7
200	1	-313.0	-10.1	-133.3
300	1	-261.7	+79.9	-200
100	2	-161.7	-27.4	-66.7
200	2	-252.8	-26.3	-133.3
300	2	-266.0	-1.5	-200
100	3	-183.7	-98.7	-66.7
200	3	-312.9	-183.4	-133.3
300	3	-399.7	-236.9	-200
100	4	-221.6	-46.8	-66.7
200	4	-320.9	-43.9	-133.3
300	4	-409.6	-36.2	-200
100	5	-155.2	-36.0	-66.7
200	5	-249.9	-42.9	-133.3
300	5	-395.1	-69.4	200
100	6	-186.3	-63.1	-66.7
200	6	-276.5	-66.0	-133.3
300	6	-306.7	-48.5	-200

(+) tension

should not cause any problems near the joint section due to overstress in either tension or compression.

As shown in the photographs, contact is made only at the center of the deck on the flat portion of the joint; the stress distribution for an arrangement such as this would be expected in a prototype thus fitted but not necessarily for the case of the entire joint in bearing on adjacent sections.

Joint Testing With Concrete Models

In order to examine the behavior of the concrete models, it was decided to approximate the curvature of a typical steel girder highway bridge. By approximating the curvature of a typical bridge, the same relative rotations between selected points could be achieved with an appropriately chosen model beam. In this manner, the joint rotations which were the object of the study would realistically approximate a prototype situation.

The typical bridge on which the curvature calculations were made had a beam span of 50'-0"; the typical beam was taken as a 30 WF 124 beam. This simply supported beam was loaded with an HS 20-44 live loading and subsequent deflection calculations were made at 10 ft intervals throughout the 50'-0" span. The load was located so as to produce the absolute maximum moment in the span and the deflection at this point was calculated in addition to the deflections at 10 ft intervals.

Knowing the deflections at the selected points, a deflection diagram was drawn. Since laboratory space was a limitation in the length selection of a testing beam, a beam length for testing was established at 21'-0" to provide a simply supported 20'-0" clear span. This

beam, it was decided, should approximate the center 20'-0" of the typical bridge; this length included the point of maximum deflection. The deflection curve was then used to establish a desired deflection in the test beam; with the points at ten feet on each side of the center line of the actual beam set as the end points of the testing beam, the deflections of the center twenty feet of the actual beam were determined relative to the end points of that twenty feet. Knowing the required center line deflection of the proposed beam and the range of loads available in the laboratory, a moment of inertia was determined for the test beam. For a desired deflection of 0.175 in., an 18 WF 70 beam with an applied concentrated load of 20 kips was selected. This beam, using the recommended American Institute of Steel Construction elastic analysis procedure and 24 ksi allowable bending stress, was found to be sufficient to support a concentrated load of 51.4 kips applied at its center line. Therefore, the range of loadings and accompanying deflections and curvatures could be extended if required.

The chosen beam should accurately represent the actual joint rotation requirement which would be found in a deck which would be placed on an actual bridge.

Qualitative studies of the feasibility of the proposed deck design were then begun. The purpose of the work was to verify some of the techniques which were proposed for the deck system.

Circular Sector Joint Model. The first model which was cast and tested was a model of the circular sector joint. The testing configuration consisted of four concrete elements with three joints. A typical specimen element shown in Figure 21, was six inches deep, 34 inches wide,

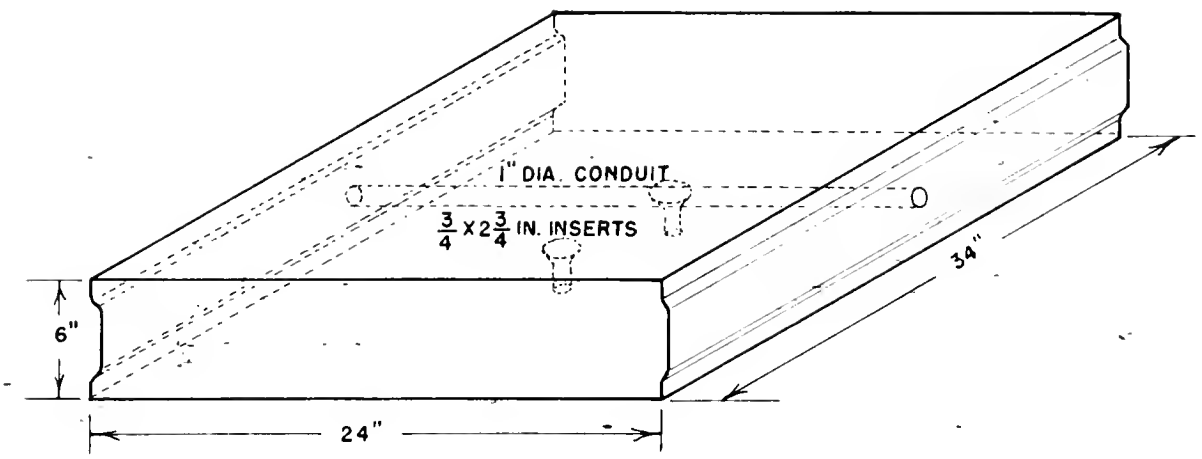

TYPICAL TEST SECTION

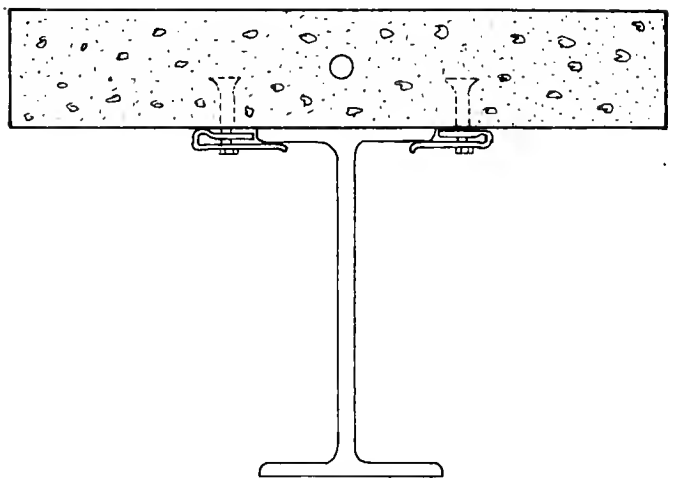

TYPICAL CROSS-SECTION AT
TIE DOWN

FIGURE 21. CONCRETE JOINT TESTING MODEL

and 24 inches long. No reinforcement was placed in the slab elements. A longitudinal, one inch void space was cast in the center of each specimen to accept a 3/8 in. diameter post-tensioning strand. The test section was placed on a simply supported 18 WF 70 lb beam spanning 20'-0". The beam thus approximated the curvature of a prototype bridge as was previously described. The testing arrangement is shown in Figure 23. The concrete strength at the time of testing was approximately 5,300 psi. A concentrated load, applied through a nine inch diameter aluminum plate and rubber pad, was applied at the center of the beam and slab configuration at a rate of 250 cpm.

The testing arrangement allowed a variation in applied load as well as in post-tensioning force. No material was included for reduction of stress concentration at the bare concrete joint. A good fit was assured as adjacent pieces were cast back to back, sharing a common 1/16 in. thick steel joint form, as shown in Figure 22.

A repetitive load of 16 kip maximum and 2.5 kip minimum was applied as indicated and a post-tensioning force of 5,000 lb was applied to the cable to start the test. The 5,000 lb load produced a stress on the gross concrete section of approximately 25 psi. The post-tensioning force was increased to 8,000 lb after two hours of continuous loading, during which no adverse performance of the joint was observed. The stress on the gross section was then approximately 40 psi. Five hours after the test was begun, the applied load was increased to 20 kips, while maintaining the 8,000 lb post-tensioning force and the test was run to completion at eight hours. Throughout the test, loading was maintained at a rate of 250 cpm and at the end of the test, 128,400

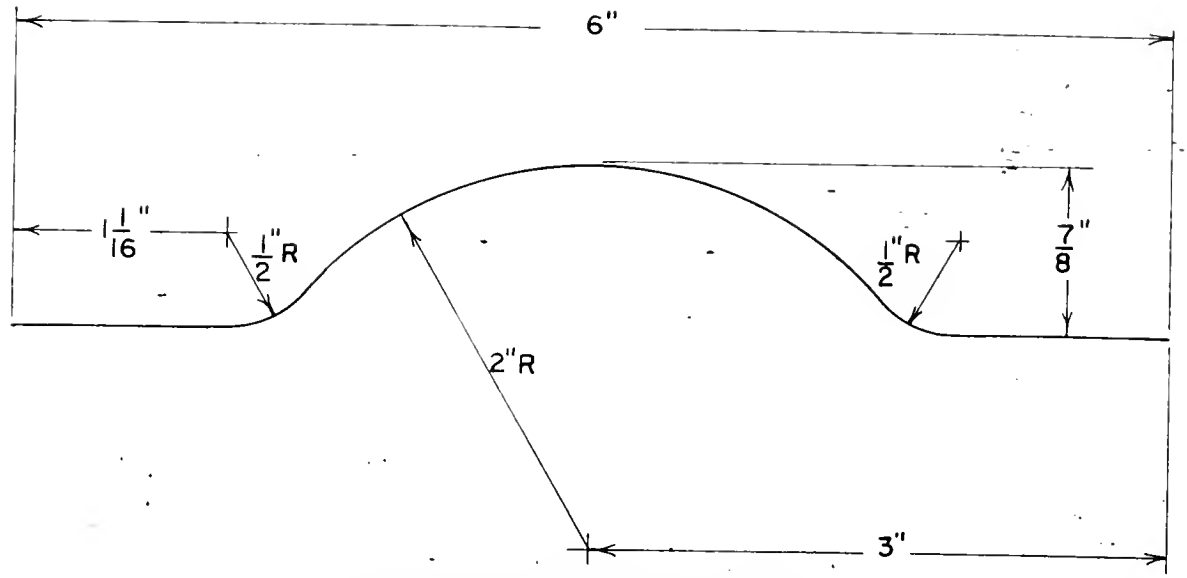

CIRCULAR SECTOR JOINT SHAPE

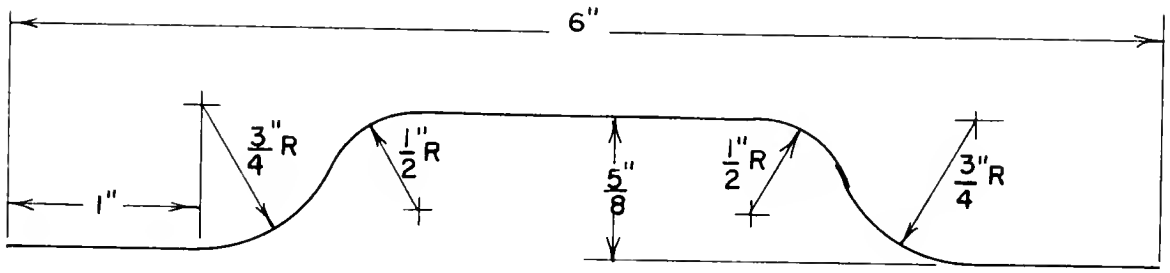

FLAT KEY-TYPE JOINT SHAPE

FIGURE 22. CONCRETE MODEL JOINT SHAPES

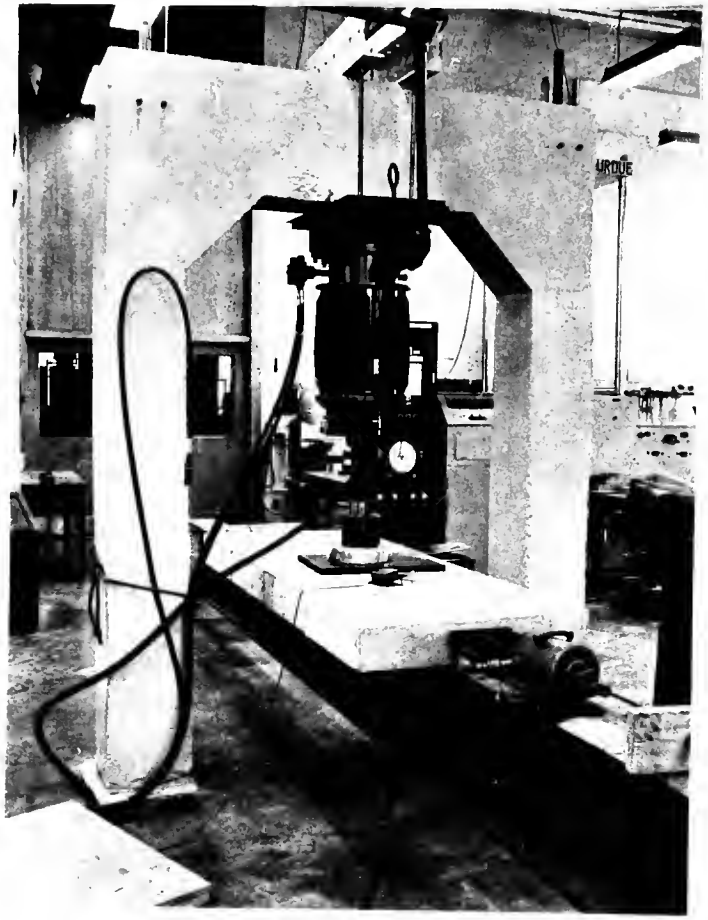

VIEW FROM STRESSING END

VIEW FROM "DEAD" END

FIGURE 23. LABORATORY JOINT TESTING ARRANGEMENT

cycles of loading had been completed. The loading varied sinusoidally between 2.5 kips and the maximum (described above) during each load cycle.

Flat Joint Model. The models for the flat joint examination were cast in the same manner as the models for the partial circle joint. The dimensions of the specimens were similar to those of the partial circle specimens. A maximum load of 12 kips and a minimum load of 2 kips were maintained throughout the test. The load was applied in the same manner and at the same rate, 250 cpm, as in the partial circle joint test. A post-tensioning force of 8,000 lb was maintained, creating a stress in the gross concrete section of 40 psi. The loading was continuously maintained for 2,255,800 cycles.

Both joint tests were conducted without instrumentation, with the exception of load indicators for the applied concentrated load and post-tensioning system. The object of the tests was to visually examine the performance of the joint under a repetitive load while approximating the conditions of joint rotation which would be realized in a prototype deck system.

The slab sections were held to the beams with the bolt-clip arrangement described previously. Two bolt inserts were cast in each slab section with one insert located on each side of the supporting beam.

Results. The limited results indicated that the two joint sections would perform satisfactorily when exposed to the conditions of an actual bridge. No concrete wear or cracking was realized at the joints. The photoelastically determined failure patterns were not in evidence;

this does not imply that the failure patterns would not be evident at higher post-tensioning loads, but would indicate that the failure patterns were not realized at the stress levels encountered during the testing.

The slab tie-down system was found to perform satisfactorily as the slabs were firmly held to the beam with no loosening of the lubricated bolts nor pull-out of the bolt anchors in evidence.

Joint Materials

A review of the photoelastic joint shape study indicated the desirability of a material to reduce the stress concentrations at the faces of the joint. The fringe photographs, Figures 17, 18 and 19, display quite vividly the presence of stress concentration at the joint. Another important factor is the desire to prevent moisture from entering the joint, creating problems due to freezing and thawing as well as concrete deterioration due to chemical action from thawing salts.

The requirements for a joint material are apparent. The material must have the ability to resist flow or creep under sustained load. This sustained load could be 20 years or more since the bridge deck with its post-tensioning is hoped to have a long service life. The material should be chemically resistant and should not deteriorate under the mild chemicals to be found on a deck mainly from de-icing chemicals. The material must be easily applicable to the joint and should conform easily to the joint; the material must be held in the joint at least until the adjacent section is in place whereupon it would be held by the adjoining sections. The material must also be stable under widely varying temperatures, displaying no creep or brittleness due to

situation where numerous identical pieces would be manufactured.

Design for Beam Spacing of Four-Feet

The 4'-0" center to center beam spacing was selected as a small beam spacing which would permit the examination of continuity over supports; the ten foot member length would permit two spans. The design parameters and calculations are presented:

Concrete Properties
a) f'_c = 5,000 psi
b) f_t = 0
c) f'_{ci} = 4,000 psi
d) f_c = 2,000 psi

Steel Properties
a) f'_s = 250 ksi
b) 7/16 in. diameter strand
c) assume 20-percent losses

Conditions of Support
a) wide-flange steel beams, flange width 8 3/4 in.
b) beam spacing 4'-0", continuous over three supports

Loading
a) HS 20-44 , P_{20} = 16,000 lb
b) I = 30-percent of live-load moment
c) 6 inch deep deck
d) 35 psf future wearing surface

Although the laboratory specimens were to be loaded with static or repeated point loads, it was considered potentially desirable to examine the specimens when loaded to failure, after the completion of all other tests. For that reason, the impact as well as future wearing surface loads and full live load were included in the design.

Moment Calculations

$$\text{AASHO effective span "s"} = 4.0 - \frac{8.75}{2(12)} = 3.636 \text{ ft}$$

$$\text{LLM} = 0.8 \left(\frac{S + 2}{32}\right) P_{20} = 2{,}260 \text{ ft-lb/ft}$$

$$IM = 0.3\ (LLM) = 678 \text{ ft-lb/ft}$$

$$DLM = \frac{110}{8}\ (3.636)^2 = 182 \text{ ft-lb/ft}$$

Total moment = 3,120 ft-lb/ft

Section Properties

For the 3'-0" x 6" slab, assuming 8 - 7/16 in. prestressing strands:

$$I = \frac{36(6)^3}{12} + 5\ (8)\ (.1089)\ (1.5)^2 = 658 \text{ in.}^4$$

$$A_c = 6 \times 36 + 5\ (8)\ (.1089) = 220.4 \text{ in.}^2$$

Stresses Under Service Load

Using the combined stress equation, $f_c = -\frac{P}{A} \pm \frac{Mc}{I}$ where negative signs (-) represent compression and positive signs (+) represent tension,

$$\frac{Mc}{I} = \frac{3{,}120\ (3)\ 3\ (12)}{658} = 512 \text{ psi}$$

$$\frac{P}{A} = \frac{8\ (15{,}110)}{220.4} = 548 \text{ psi}$$

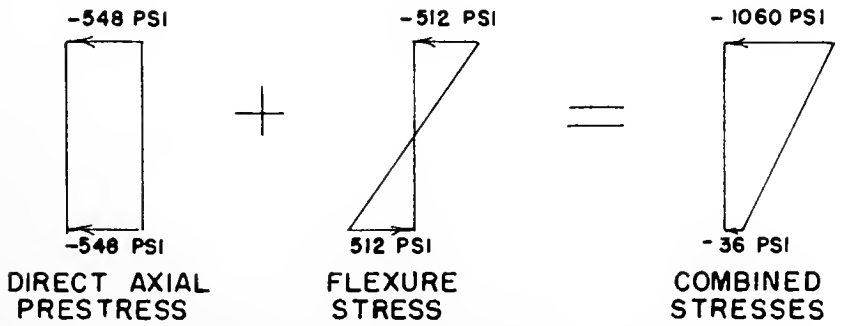

FIGURE 24. CALCULATED CONCRETE STRESSES DUE TO AASHO LOADING APPLIED TO LABORATORY SPECIMENS REINFORCED FOR 4'-0" BEAM SPACING

Ultimate Flexural Strength

Required flexural strength is 1.5 DLM + 2.5 (LLM + IM) or 22,869 ft-lb.

Neglecting the top row of prestressing steel, $P = \frac{A_s}{bd} = .00268$.

From before, $Mu = A_s f_{su}' d (1 - 0.6 p \frac{f_{su}}{f_c'})$ and $f_{su} = f_s' (1 - 0.5 p \frac{f_s'}{f_c'}) = 234$ ksi. The requirement that $p \frac{f_{su}}{f_c'}$ must be less than 0.3 is met as the quantity has the value 0.125. The ultimate moment, Mu, is then found to be 424 in. - k or 35,400 ft-lb. The required ultimate moment capacity is exceeded by the calculated capacity.

Design for Beam Spacing of Eight Feet

The design parameters remain the same as in the design for four-foot beam spacing with the following exceptions:

a) $f_s' = 270$ ksi
b) simply supported slab with 8'-0" beam spacing
c) $f_t = 3\sqrt{f_c'} = 212$ psi, AASHO 1.6.7 (B)

In this design it will be noted that the continuity factor (.8) for continuous slabs has not been used since the laboratory slab is essentially simply supported and is not continuous.

Moment Calculations

AASHO effective span "s" = 7.635 ft

$LLM = \frac{(S + 2)}{32} P_{20} = 4.810$ ft-lb/ft

$IM = .30 (LLM) = 1,442$ ft-lb/ft

$DLM = \frac{W (S)^2}{8} = \frac{110 (7.635)^2}{8} = 801$ ft-lb/ft

Total Moment = 7,053 ft-lb/ft

Section Properties

For the 3'-0" wide slab, assuming 12 - 7/16 in. diameter

temperature changes.

Laboratory Evaluation. The laboratory investigation consisted of placing the joint material in the joint of the flat-joint concrete model which had been used previously in the evaluation of the joint shape. A dike was constructed on top of the system shown in Figure 23 and was subsequently flooded in order to examine the effectiveness of the joint material with regard to protection of the joint from moisture. The flooded area measured approximately 24 inches by 6 feet, crossing all three joints in the model. By means of a flashing strip and flash-compound, the water within the dike was contained and could not flow laterally under the dike which was constructed of 2 in. by 2 in. wood strips. The joint material covered the entire width of the models and had a one-inch hole cut in it to facilitate passing of the post-tensioning strand.

The first material which was examined was asbestos cloth, both plain and wire reinforced. The cloth was held on the convex side of each joint with an MC 70 asphalt. The system was post-tensioned, then the dike was flooded with water to a depth of approximately one-half inch. The undesireability of the material was evident after a few hours of flooding as the capillarity of the cloth permitted the water to pass through the entire depth of the slab. One joint was faced with the wire-reinforced cloth and the other two were faced with the plain cloth.

Capillarity was very evidently at fault as the water passed laterally to the full depth of the unflooded portion of the joint. For this reason, the asbestos cloth was removed from further consideration.

The same specimens were then fitted with 1/16 in. U60 neoprene

sheet as the joint material. The dike was replaced on the top of the sections and water-tightness was again secured. The post-tensioning cable was tightened to seat the slab pieces and the joint material. Once assured that the joint was mechanically tight the post-tensioning cable was allowed to slacken and, the slab was flooded to a depth of one-half inch with water. No evidence of water passage was noted at any place on the three joints after 24-hours, this being accomplished with no post-tensioning force applied across the joint. The Neoprene sheet was sufficient to prevent water from entering the joint and was satisfactory in that respect.

Following the water test, the section was dried, and a post-tensioning force of approximately 8,000 pounds was applied. The system was then subjected to 3.5 million cycles of repeated load of 9,000 pound maximum and 1,000 pound minimum applied concentrated load similar to the concrete joint test, for which the testing arrangement is shown in Figure 23. The joint was dry in order that wear of the material could be observed without the lubricating effect of the water. Upon removal of the load and post-tensioning force, no significant change in the appearance of the material was noted. There was evidence present where slight irregularities in the joint shape had made depressions in the neoprene, but no tearing or buffing was found.

Neoprene is considered to be effective with regard to sealing and wearability for application on a bridge deck. Chemical resistance could be specified by American Society for Testing and Materials standards as could compression set and temperature performance desired.

DESIGN OF PRESTRESSED LABORATORY SPECIMENS

The laboratory specimens were designed for beam spacings of eight and four feet. It was desired to examine sections which were designed for small as well as large beam spacings in order to examine the response of the deck in likely configurations.

A size of 10 feet in the transverse direction and 12 feet in the longitudinal direction was chosen as a practical dimension with consideration given to the available laboratory testing and handling facilities. A deck element 3'-0" wide by 6 inches deep by 10 feet long was then selected. This would permit reinforcing two sections for the large beam spacing and two sections for the small beam spacing, thereby meeting the 12'-0" dimension.

In the following designs, reference is made to the general deck design calculations, which were presented above, for the applicable AASHO specifications. Where new specifications are applied, the specification and its designation are presented.

In both cases, the steel centroid is located at 1½ inches from both the top and bottom of the slab, as opposed to the 1½ inches clear cover in the previous general design. The steel location deviates from the general design case in order that the laboratory specimens could be fabricated in prestressing beds whose strand placement templates were already available. It should be noted that the cost of a template for forming for 1½ inches clear cover would be justified in a prototype

prestressing strands:

$$I = \frac{36\ (6)^3}{12} + 5\ (12)\ (.1089)\ (1.5)^2 = 663\ \text{in.}^4$$

$$A_c = 6 \times 36 + 5\ (12)\ (.1089) = 222.5\ \text{in.}^2$$

Stresses Under Service Load

$$\frac{P}{A} = \frac{12\ (17,360)}{222.5} = 935\ \text{psi}$$

$$\frac{Mc}{I} = \frac{7,053\ (3)\ 3\ (12)}{663} = 1,146\ \text{psi}$$

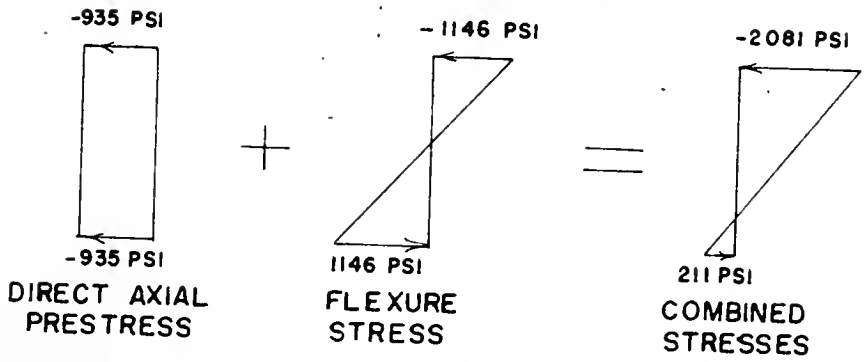

FIGURE 25. CALCULATED CONCRETE STRESSES DUE TO AASHO LOADING APPLIED TO LABORATORY SPECIMENS REINFORCED FOR 8'-0" BEAM SPACING

Ultimate Flexural Strength

The required flexural strength is 1.5 (DLM) + 2.5 (LLM + IM); the value of the expression is 50,550 ft-lb.

Neglecting the top row of prestressing steel, $P = \frac{A_s}{bd} = \frac{6\ (.1089)}{36\ (4.5)} = .00402$. Again, $Mu = A_s f_{su} d\ (1 - 0.6\ p\ \frac{f_{su}}{f'_c})$ and $f_{su} = f'_s\ (1 - 0.5\ p\ \frac{f'_s}{f'_c})$. Evaluating, $f_{su} = 270\ (.8915) = 241$ ksi. The requirement that $p\ \frac{f_{su}}{f'_c}$ must be less than 0.3 is met as the quantity has the value 0.194. The ultimate moment is then found to be 62,500 ft-lb; the required ultimate capacity is exceeded by the calculated capacity.

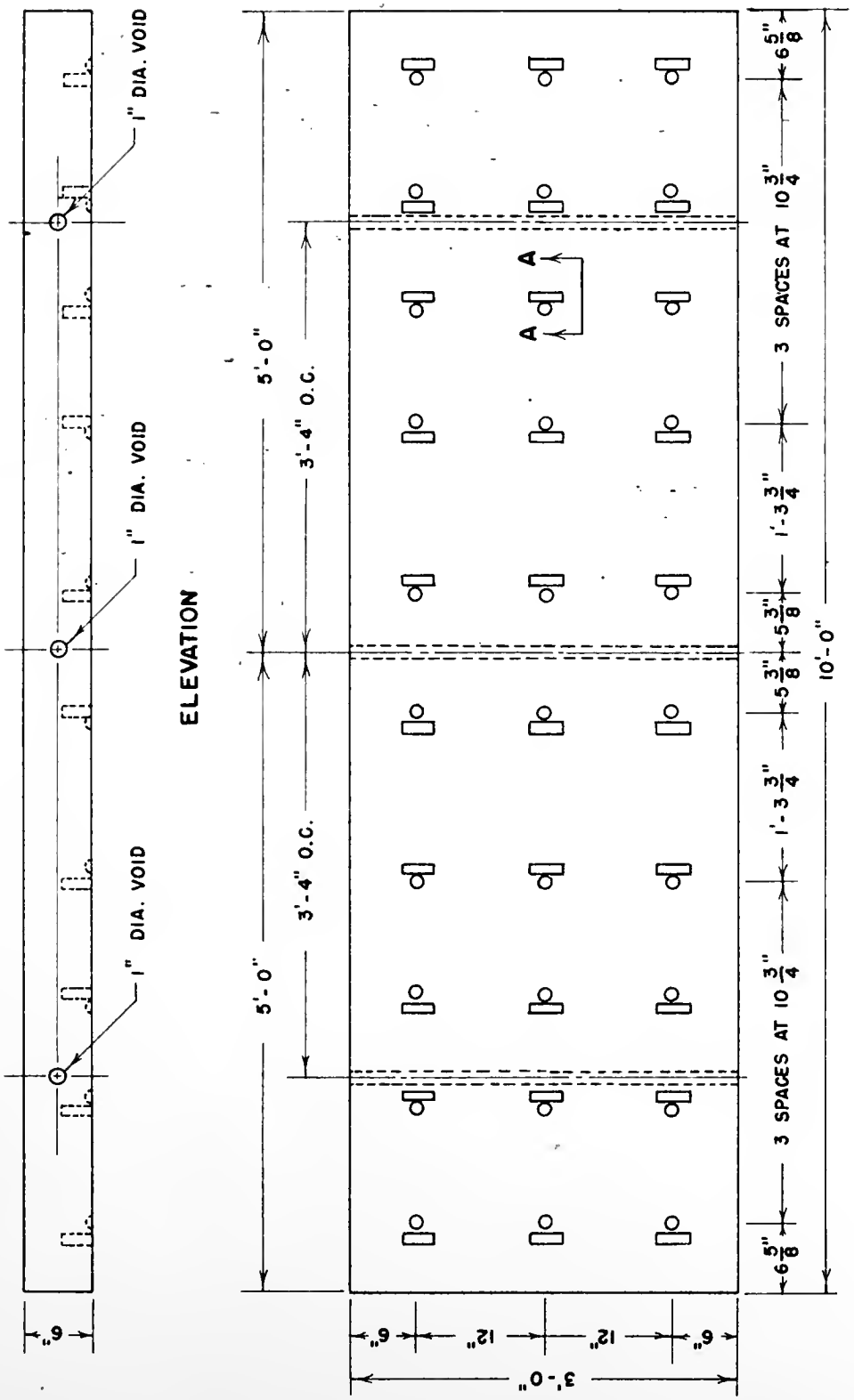

FIGURE 26. LABORATORY MODEL HARDWARE DETAIL

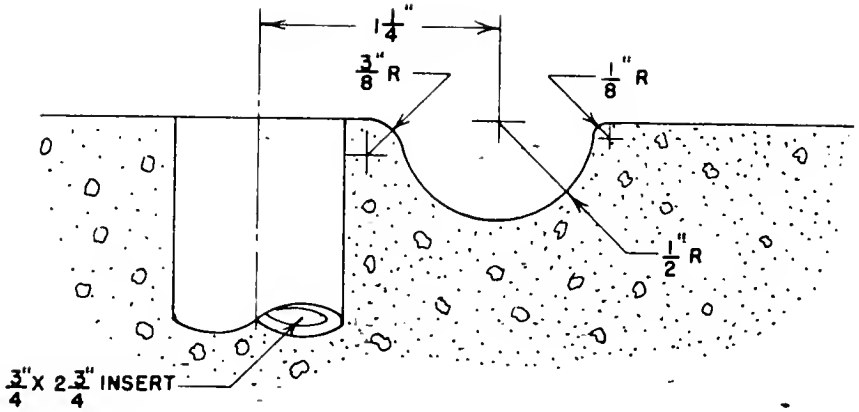

ELEVATION

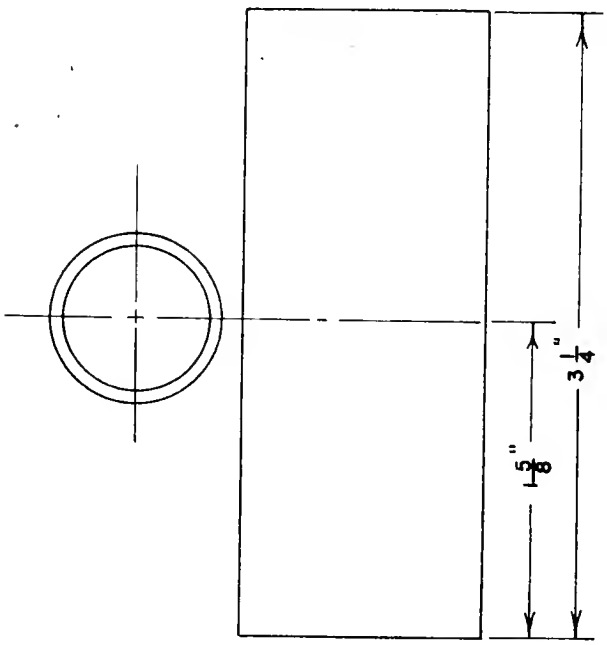

PLAN

FIGURE 27. DETAIL A-A, BOLT INSERT ARRANGEMENT

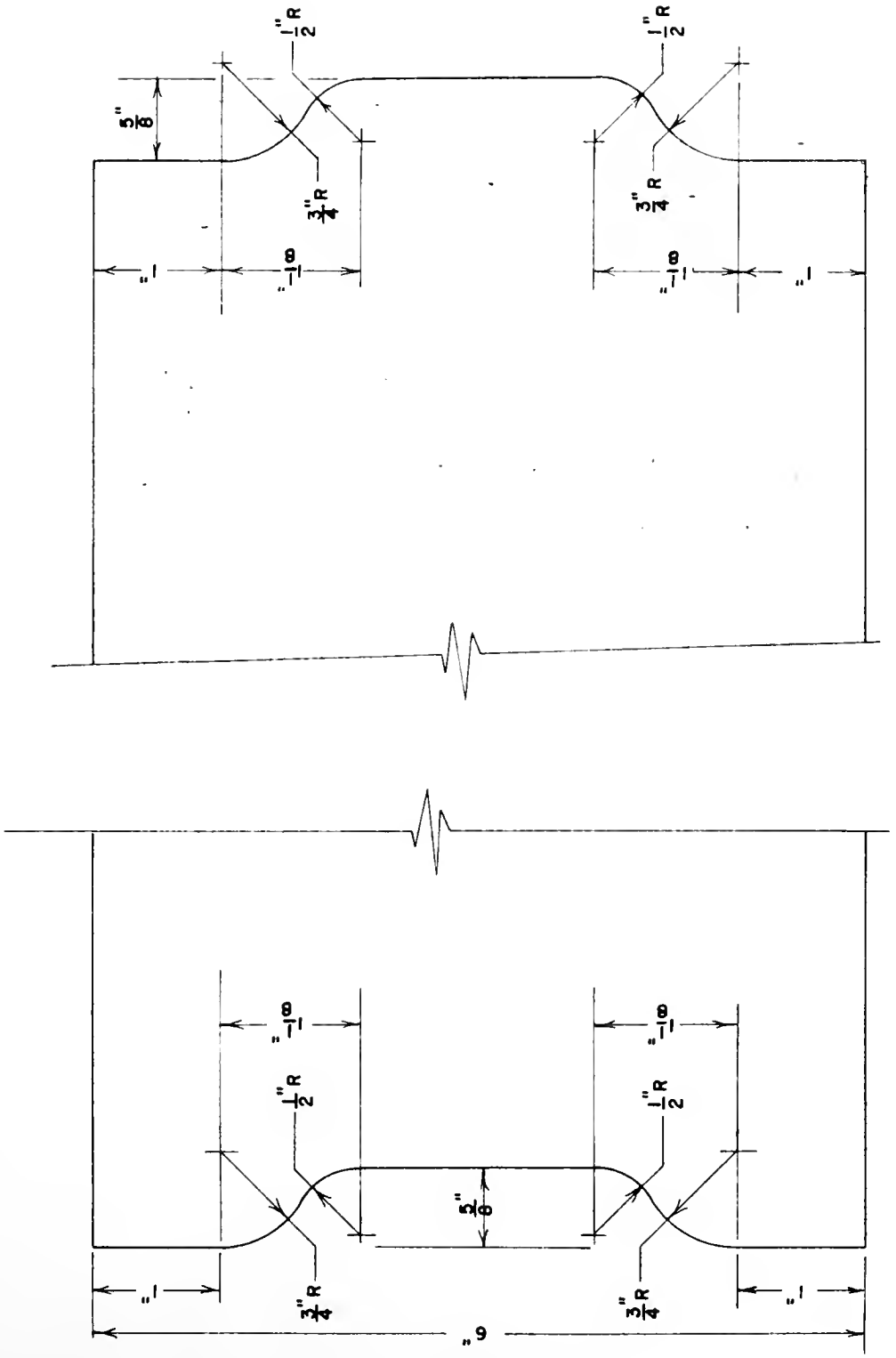

FIGURE 28. LABORATORY MODEL JOINT DETAIL

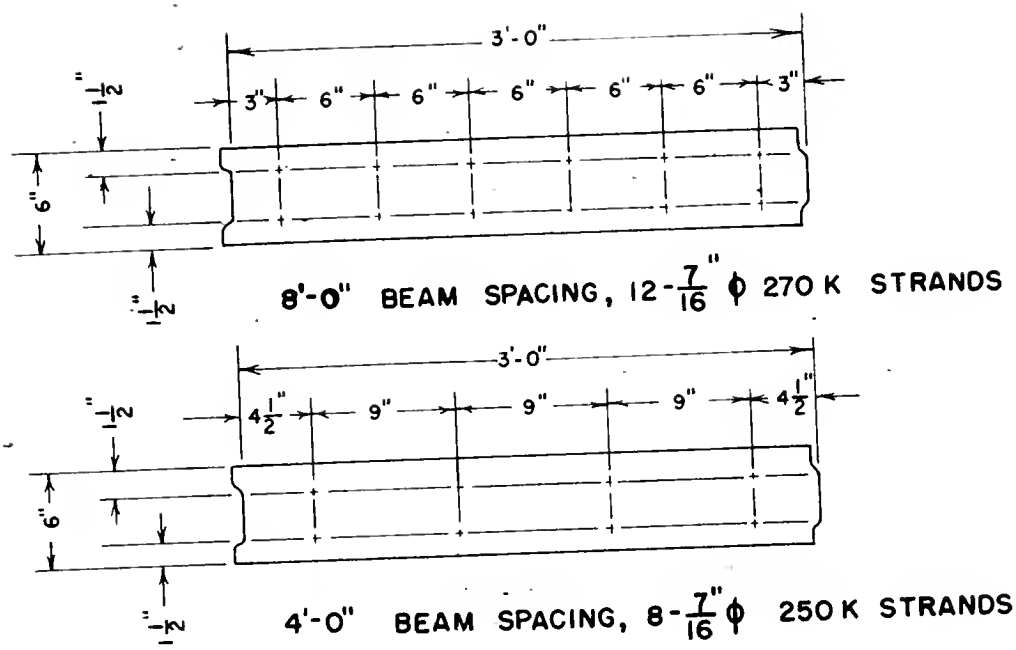

FIGURE 29. LABORATORY MODEL STRAND PLACEMENT PATTERNS

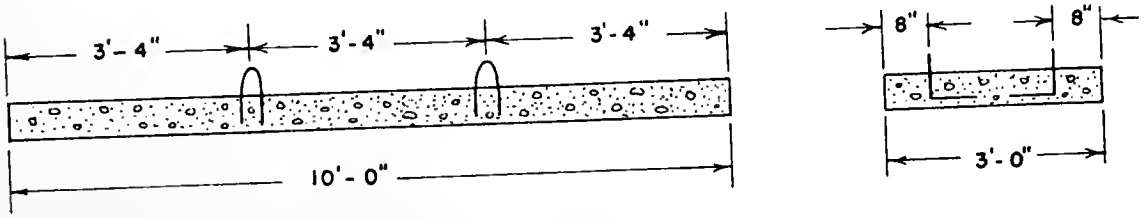

FIGURE 30. LABORATORY MODEL LIFTING LOOP DETAIL

CONSTRUCTION OF THE PRESTRESSED CONCRETE ELEMENTS

Precast construction of the highest quality is absolutely necessary if the concept of precast, prestressed concrete bridge decks is to succeed through actual application. The environment of the precasting yard is much more favorable for the mixing, placing, and curing of concrete than is the actual bridge site. Precasting in itself does not insure that the finished product will be of higher quality but all factors involved would point out the fact that a superior finished product should be realized. The precast, prestressed deck sections which were used for the laboratory testing were manufactured by Construction Products Corporation, Prestressed Concrete Division, of Lafayette, Indiana. The design of two differently reinforced elements which were manufactured appears above. Hereafter, the eight-foot section will refer to the two deck elements reinforced for eight-foot beam spacings, and the four-foot section will refer to the two deck elements reinforced for four-foot beam spacing.

Formwork

The formwork for the three-foot wide sections was provided by a prestressing bed which is normally used to cast 45 in. wide by 21 in. deep prestressed concrete box girders. Figure 31 indicates the forming procedure. The prestressing strands are placed in two rows running the entire length of the precasting bed. Diaphragms are placed along the

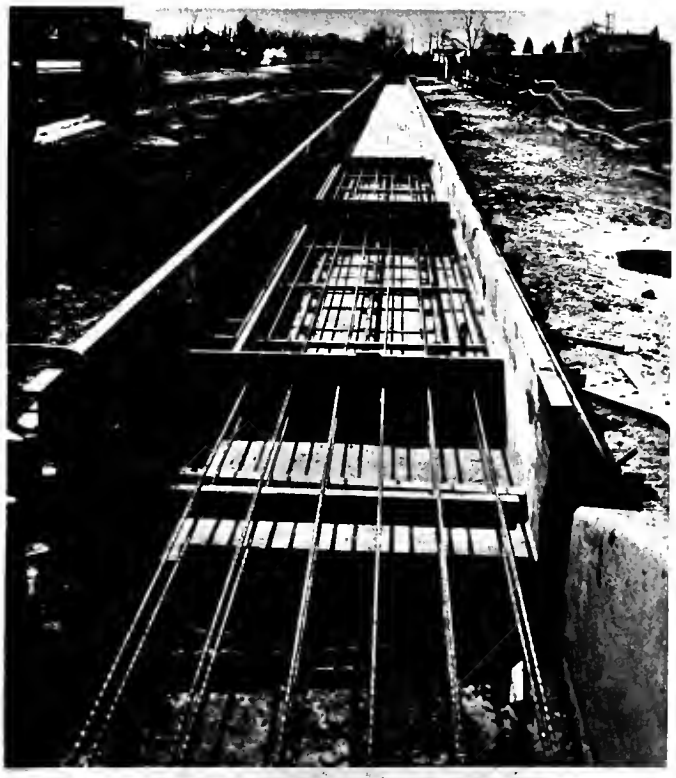

LONGITUDINAL VIEW OF PRECASTING BED WITH PRESTRESSING STEEL IN PLACE

CLOSE-UP OF PRECASTING BED SHOWING TWO ROWS OF PRESTRESSING STEEL, METHOD OF LOCATING BOLT INSERTS, LIFTING LOOP, VOID SPACE FORMER, AND SIDE FORM FOR TRANSVERSE CONTINUITY JOINT.

FIGURE 31. PRECASTING METHOD FOR LABORATORY SPECIMENS

length of the bed at the desired length of the member to be cast with approximately a one-foot space between sections to facilitate strand cutting between the members. The transverse continuity joint for the deck elements was cast in the longitudinal direction on the precasting bed, with one side of the joint form blocked away from the sidewall of the precasting bed in order to cut the 45 in. width of the precasting bed to the desired 36 in. dimension. Plywood sheet had been placed beneath the area of the elements to be cast to achieve the desired concrete cover while using the available end-block templates for the bed.

Bolt Inserts

The bolt inserts, capped on the bottom with a plastic cap, were positioned by welding to a frame constructed of 1/8 in. x 1 in. strap iron. The frame was welded outside the form and placed inside the form prior to concrete and strand placement. This method was observed in the laboratory to be dimensionally accurate and acceptable. Difficulty was encountered after casting, as in some instances water laden with cement had entered the insert, presumably from the top. After cleaning the threads with a 3/4 in. tap, no further difficulty was encountered. This problem could be eliminated either by capping the insert or by application of a bond-breaker to the threads of the insert; a petrolatum would probably be sufficient and would not tend to flow out of the insert.

Care must also be exercised in the forming of the indentation adjacent to the insert (see Figure 27) which accepts the projection on the spring clip. Some of the indentations on the laboratory specimens were found to be inaccurately located; this would not be acceptable in

a prototype situation as the full usefulness of the bolt-clip arrangement could not be realized. It is recommended that the 1¼ in. dimension of Figure 27, elevation view, be considered an exact or hold dimension, as the clip will only be accommodated by this dimension. The 3¼ in. dimension must also be centered for the full usefulness to be realized. An increase of this dimension to 4" is recommended.

Concrete

The concrete strength specified for the laboratory test specimens was 5,000 psi at 28 days; this strength was achieved in seven days and the strength versus time relationship for the eight-foot and four-foot sections appears as Figure 32. The curve appears to level-off at slightly above 6,500 psi compared to the specified 5,000 psi value.

The greatest precaution to be taken as far as concrete strength is concerned is to provide adequate concrete strength at the time that the prestressing strands are released. If the concrete does not have sufficient strength, cracks due to slip of the prestressing steel may occur along the surface of the slab immediately above or below the steel. The two eight-foot specimens had a 24-hour concrete strength of 4,140 psi and no cracking of the concrete along the prestressing steel was observed. However, the four-foot sections exhibited an evident crack pattern above the prestressing strand. (See Figure 33.) The one day strength at the time of release of the strand was tested by the manufacturer and found to be 4,570 psi. A seven-day strength test was performed in the laboratory and concrete strength was then indicated as 4,390 psi. The variation in cylinder strengths could indicate a discrepancy in casting, curing, or testing the concrete cylinders.

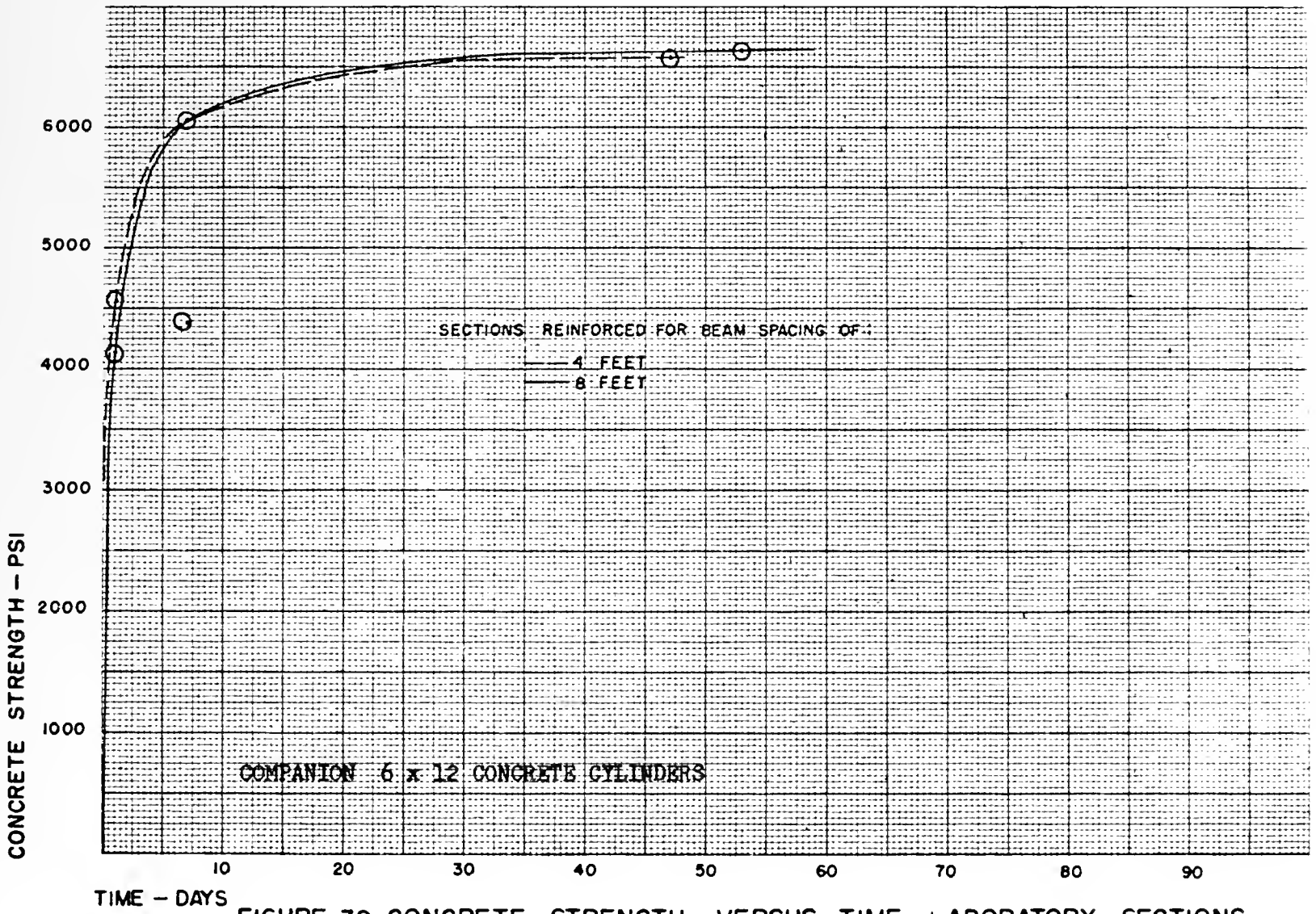

FIGURE 32. CONCRETE STRENGTH VERSUS TIME, LABORATORY SECTIONS.

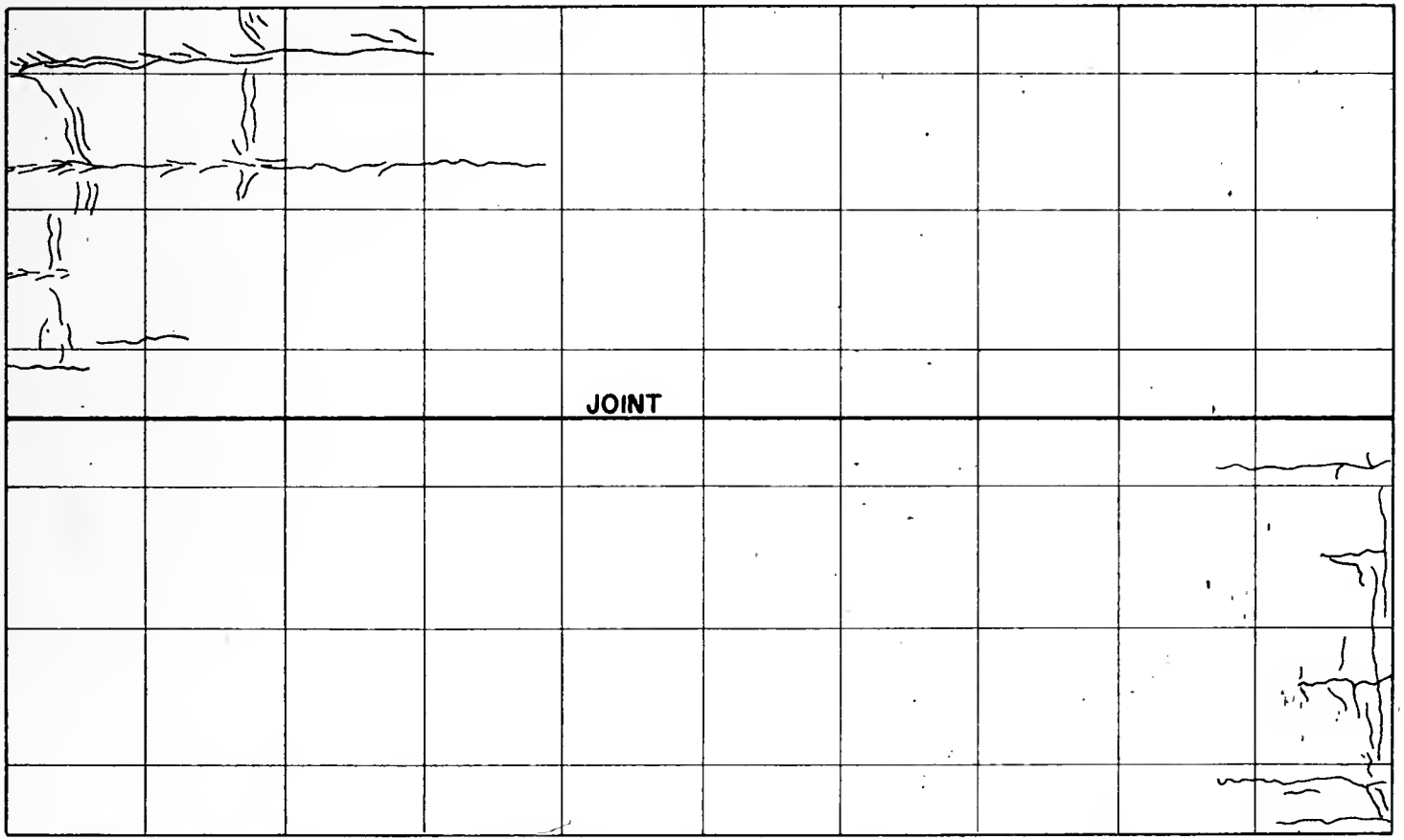

NOTES: GRID SIZE IS 12 INCHES. CRACKING OCCURRED ON TOP SIDE ONLY. IN GENERAL, CRACKING LIES ABOVE EITHER PRESTRESSING STRAND OR CONDUIT.

FIGURE 33. CRACK PATTERNS IN SECTIONS REINFORCED FOR 4'-0" BEAM SPACING.

In light of the cracking along the prestressing strand, it is possible that the full strength indicated by the test cylinder at one day was not attained by the slab.

An average value for the initial tangent modulus of elasticity of the concrete in the eight-foot sections, at 53 days, was found to be 3.65×10^6 psi and an average value for the four-foot sections tested at 47 days was found to be 3.86×10^6 psi. A split tension test was made for each pour and the eight-foot section showed a splitting tensile strength of 556 psi and the four-foot sections showed a splitting tensile strength of 615 psi, at the same ages as the modulus of elasticity tests.

Table 4. Concrete Properties of Test Specimens

Section Reinf. for Beam Spacing	Age (days)	f'_c (psi)	f_t (psi)	E_c (psi)	
8'	1	4140			
8'	7	6050			
8'	53	6625	556	3.65×10^6	(ave. of two)
4'	1	4570			
4'	7	4390			
4'	47	6585	615	3.86×10^6	(ave. of two)

Curing of the concrete is important as far as the driving surface is concerned. If steam curing is used, care should be exercised to protect the slab from water which condenses on the tarpaulin covering the slab and then drips to form pock marks on the surface of the slab. These irregularities cause not only a rough, unsightly surface but also would lead to further deterioration as the edges of the shallow hole would become worn and enlarged by traffic.

Concrete Placement

Concrete placement in the laboratory samples was accomplished by hauling, by fork lift, the concrete bucket which was filled at the plant concrete mixer. The bucket was carried approximately 200 ft. to the casting bed where the fork lift raised the bucket over the form to deposit the concrete. Once in the form the concrete was internally vibrated, then trowelled and finished by hand.

When sections are cast which use the full width of the precasting bed, some difficulty may be encountered in providing a uniform thickness. In the laboratory samples, variations in thickness were observed, particularly at the ends of the specimens. The producer must provide a specimen which is uniform in thickness or the rideability and structural soundness may be adversely affected. A means of checking the thickness seems necessary to bring about uniformity. Assuming that the precasting bed used is dimensionally uniform, a skid, such as the one illustrated in Figure 34 could be used to check the depth dimension over the entire width of the member.

Continuity Joint

The transverse continuity joint which was cast in the laboratory specimens (for shape see Figure 28) was found to be dimensionally varying along its length. It is believed that the joint form which was blocked (on the left side of the longitudinal view, Figure 31) did not have sufficient strength between blocks to resist the torsion induced between the blocks by the plastic concrete. As a result, the sideform rotated irregularly from point to point. This led to joints which did not fit when butted together in the laboratory and were brought to rough

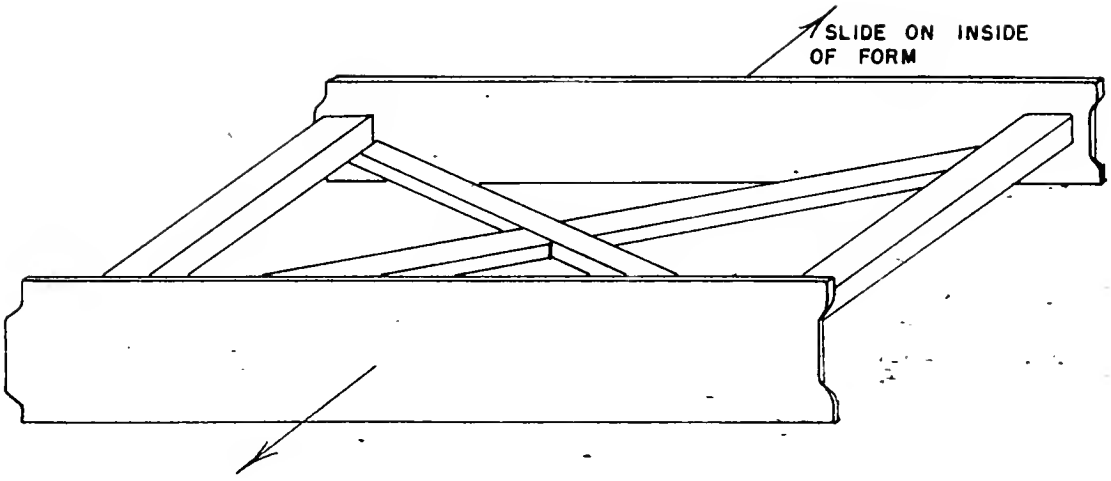

TEMPLATE FOR CHECKING DIMENSIONAL ACCURACY OF FORMWORK PRIOR TO PLACEMENT OF INTERNAL HARDWARE.

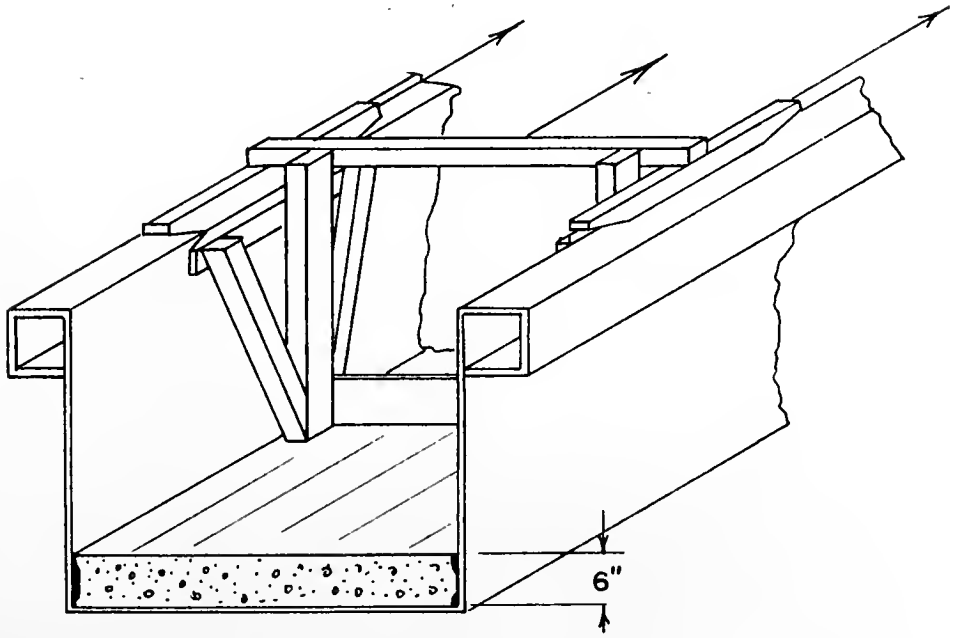

TEMPLATE FOR CHECKING DEPTH DIMENSION OF SECTIONS IMMEDIATELY AFTER CASTING.

FIGURE 34. TEMPLATES FOR DIMENSIONAL CONTROL

fit only after grinding. This problem should be self-rectifying in future applications as the form for both the joint faces will be fixed to the sidewall of the box beam form.

To ensure a uniform product, the formwork should be checked with a template prior to placing the slab hardware. A template, constructed similar to the one shown in Figure 39 would be easy to construct and simple to use. If the formwork was arranged such that the template could be passed while maintaining contact with the form, a uniform section, whose faces were in the correct dimensional relationship should be realized.

In an application on an actual bridge, it would prove worthwhile to butt and mark adjacent pieces to allow any necessary grinding or rearranging to be done prior to actual assembly where the working platform would be girders and stringers.

LABORATORY TESTING OF FULL-SCALE DECK

Load Cell Design and Calibration

Cable Tension Cells. In order to monitor the force in each of the post-tensioning cables under all stages of loading, a load cell was designed and built for each of the three post-tensioning cables. The cells were used in a configuration where the load measured by the cell was the actual cable load. (See Figure 35)

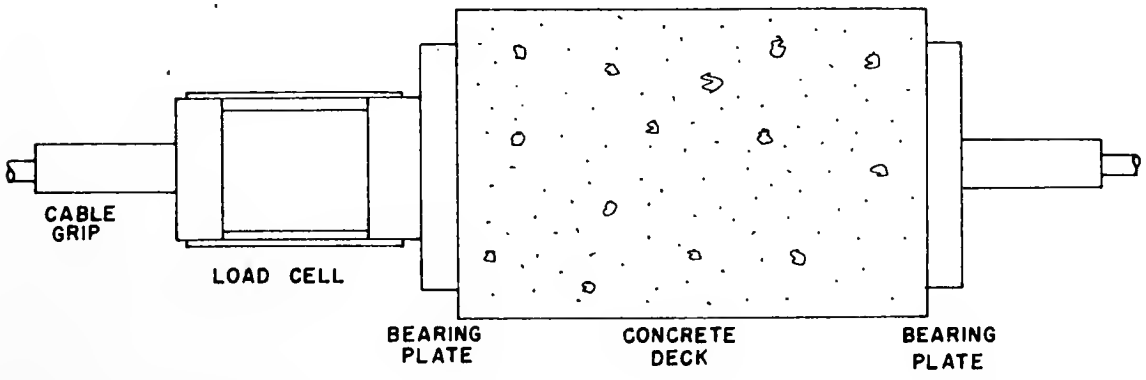

FIGURE 35. POST-TENSIONING ARRANGEMENT IN LABORATORY

Detailed drawings showing the construction of the load cells as well as the strain gage circuit which was used appear in Figures 36 and 37. The cells are constructed of 6061-T6 aluminum.

Excellent output and sensitivity were obtained as indicated by the calibration curves, appearing as Figures 38, 39, 40. Linearity is

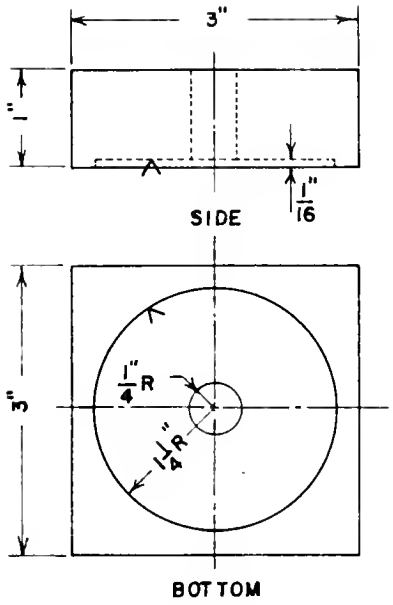

END BEARING BLOCK, 2 REQ'D PER CELL

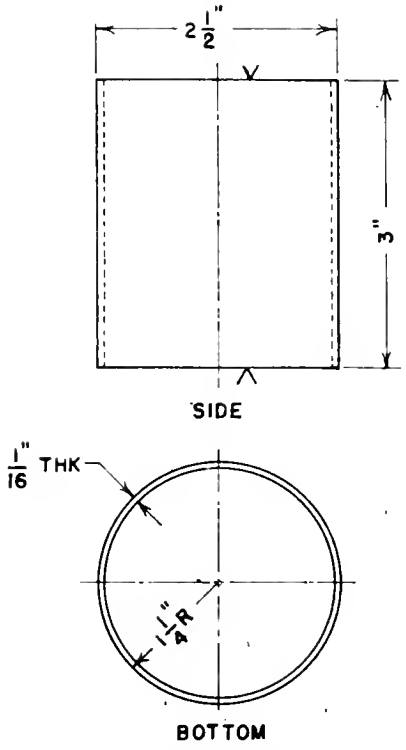

COMPRESSION CYLINDER, 1 PER CELL

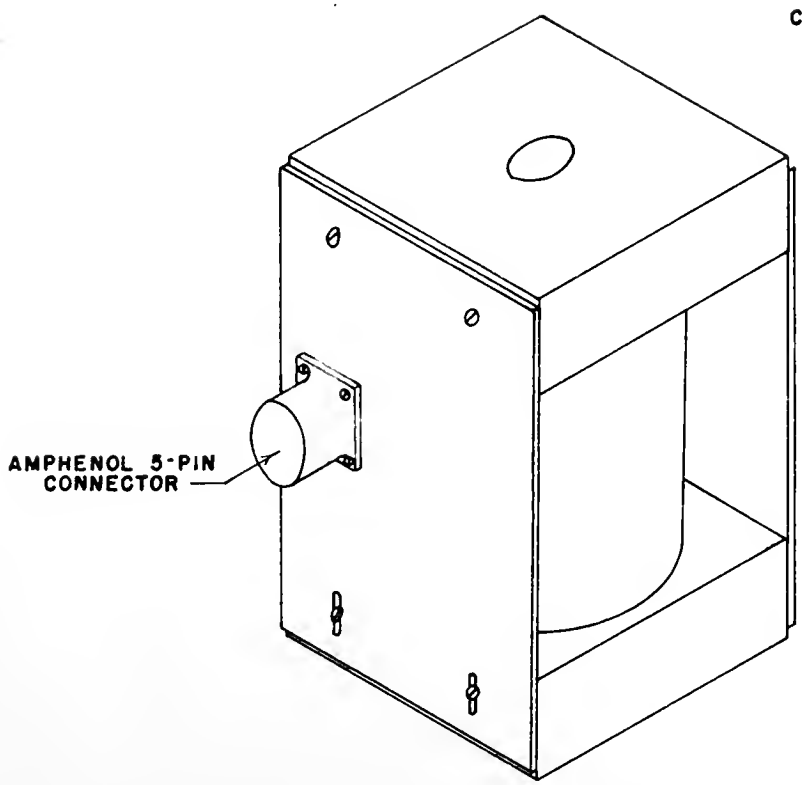

ASSEMBLED LOAD CELL

FIGURE 36. CABLE-TENSION LOAD CELL DETAIL

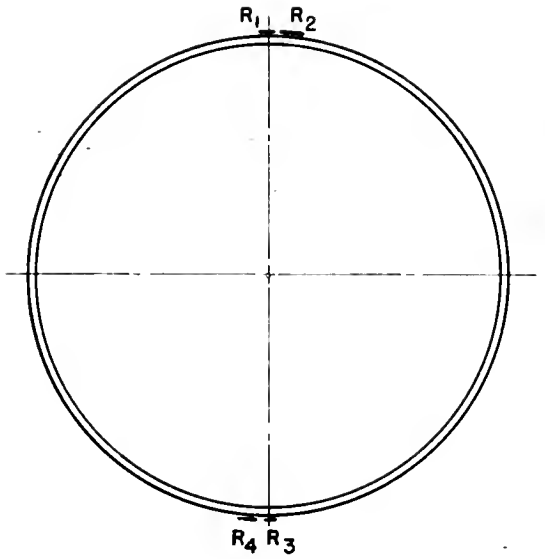

1. GAGES R_1 AND R_3 MEASURE LONGITUDINAL STRAINS.
2. GAGES R_2 AND R_4 MEASURE HOOP STRAINS.
3. GAGE GRIDS ARE EQUIDISTANT FROM THE CYLINDER ENDS AND ARE DIAMETRICALLY OPPOSED.
4. GAGES R_1 AND R_2 , R_3 AND R_4 . ARE ON A COMMON BACKING AND ARE NORMALLY ORIENTED ON THAT BACKING.

TOP VIEW OF COMPRESSION CYLINDER SHOWING GAGE LOCATIONS

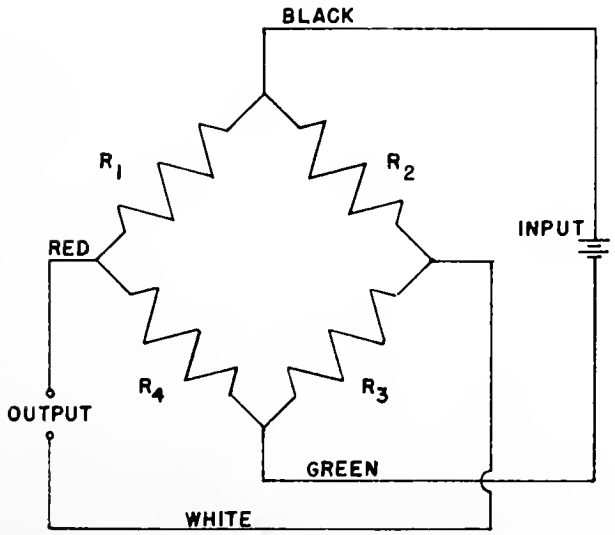

1. GAGE RESISTANCES ARE 350 OHMS
2. COLOR NAMES REFER TO WIRE USED IN ACTUAL CIRCUIT.
3. GAGES USED ARE MICRO-MEASUREMENTS (T.M.) TYPE 250 BB.

BRIDGE CIRCUIT USED FOR LOAD CELL STRAIN GAGES

FIGURE 37. CABLE-TENSION LOAD CELL CIRCUITRY

evident throughout the recommended 10,000 pound range. The maximum load which could be carried by the cell is 15,500 pounds whereupon the cell would fail by local buckling.

The three cable tension load cells were calibrated using two cycles of loading and unloading with readings made at every 500 pounds. Prior to calibration, the cells were loaded several times to the 10,000 pound maximum load in order to assure proper seating of the parts of the cells during the calibration runs, for which Tables 5, 6, and 7 contain the calibration data.

Load Measuring Cell. The calibration curve for the 50,000 pound load cell which was used to measure applied loads during the static portion of the testing appears as Figure 41. Design and calibration were performed by Mr. K. E. Wehr, a previous laboratory investigator. The curve appears as an aid to the reader who wishes to interpret the data which are presented.

Longitudinal Forces on Deck

The AASHO code specifies in section 1.2.13 that "provision shall be made for the effect of a longitudinal force of five percent of the live load in all lanes carrying traffic headed in the same direction.... the load used, without impact, shall be the lane load plus the concentrated load for moment specified in article 1.2.8."

The live load specified as the AASHO lane load for HS 20-44 loading is 640 pounds per lineal foot plus an 18,000 pound concentrated load. The deck width used in the experimental investigation was 10 feet or one lane width. The total lane load on the 10 foot wide by 12 foot long section used for the experimental investigation would be

Table 5. Cable Tension Cell "A" - Calibration

Load	Loading - Cycle 1		Unloading - Cycle 1		Loading - Cycle 2		Unloading - Cycle 2	
	Strain Reading	Strain με	Strain Reading	Strain με	Strain Reading	Strain με	Strain Reading	Strain με
Zero	30,110	-	30,105	5	30,105	-	30,107	2
0.5k	29,805	305	29,850	260	29,825	280	29,850	255
1.0	29,530	580	29,580	530	29,545	560	29,565	540
1.5	29,245	865	29,310	800	29,260	845	29,290	815
2.0	28,970	1140	29,020	1090	28,990	1115	29,015	1090
2.5	28,685	1425	28,745	1365	28,725	1380	28,740	1365
3.0	28,435	1675	28,465	1645	28,450	1655	28,465	1640
3.5	28,155	1955	28,200	1910	28,170	1935	28,185	1920
4.0	27,890	2220	27,925	2185	27,910	2195	27,915	2190
4.5	27,610	2500	27,655	2445	27,630	2475	27,650	2455
5.0	27,335	2775	27,380	2730	27,350	2755	27,370	2735
5.5	27,070	3040	27,115	2995	27,090	3015	27,110	2995
6.0	26,805	3305	26,850	3260	26,820	3285	26,860	3245
6.5	26,535	3575	26,575	3535	26,535	3570	26,580	3525
7.0	26,275	3835	26,310	3800	26,280	3825	26,315	3790
7.5	26,000	4110	26,045	4065	26,010	4095	26,040	4065
8.0	25,740	4370	25,775	4335	25,745	4360	25,775	4330
8.5	25,480	4630	25,515	4595	25,480	4625	25,515	4590
9.0	25,220	4890	25,245	4865	25,220	4885	25,255	4850
9.5	24,970	5140	24,990	5120	24,970	5135	24,990	5115
10.0	24,700	5410			24,700	5405		

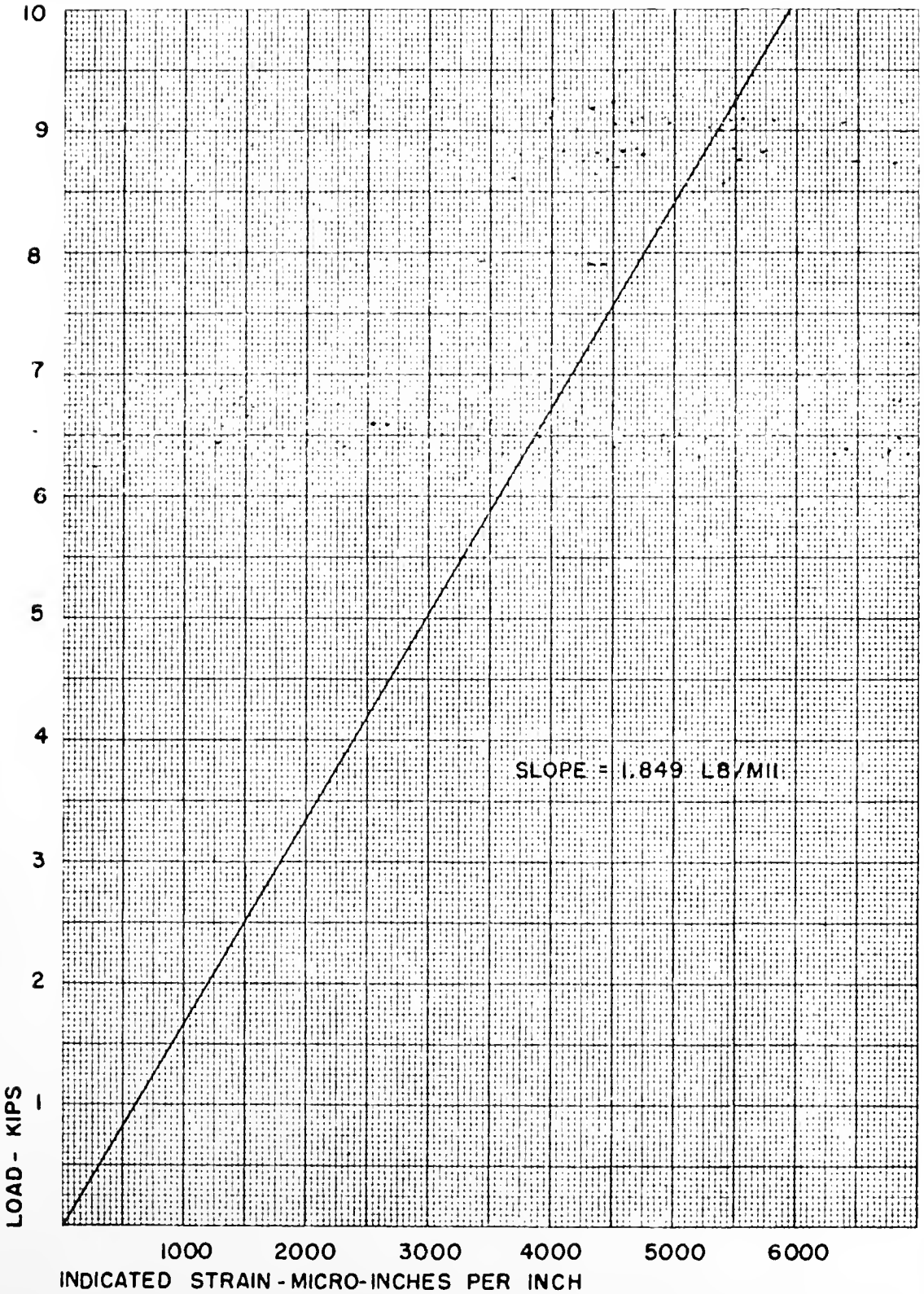

FIGURE 38. CALIBRATION CURVE , LOAD CELL A

Table 6. Cable Tension Cell "B" - Calibration

Load	Loading - Cycle 1		Unloading - Cycle 1		Loading - Cycle 2		Unloading - Cycle 2	
	Strain Reading	Strain με	Strain Reading	Strain με	Strain Reading	Strain με	Strain Reading	Strain με
Zero	30,385	-	30,365	20	30,365	-	30,362	-
0.5k	30,670	285	30,625	240	30,615	250	30,620	255
1.0	30,920	535	30,865	471	30,870	505	30,875	510
1.5	31,185	800	31,105	720	31,160	795	31,115	750
2.0	31,415	1030	31,350	965	31,430	1065	31,375	1010
2.5	31,665	1280	31,610	1225	31,675	1310	31,635	1270
3.0	31,915	1530	31,870	1485	31,920	1555	31,895	1530
3.5	32,165	1780	32,125	1740	32,190	1825	32,150	1785
4.0	32,425	2040	32,390	2005	32,445	2080	32,410	2048
4.5	32,680	2295	32,645	2260	32,700	2335	32,670	2305
5.0	32,940	2555	32,910	2525	32,960	2595	32,935	2570
5.5	33,200	2815	33,165	2780	33,225	2860	33,195	2830
6.0	33,465	3080	33,425	3040	33,490	3125	33,450	3085
6.5	33,725	3340	33,685	3300	33,750	3385	33,720	3355
7.0	33,980	3595	33,940	3555	34,005	3640	33,980	3615
7.5	34,250	3865	34,200	3815	34,270	3905	34,240	3875
8.0	34,515	4130	34,460	4075	34,525	4160	34,500	4135
8.5	34,765	4380	34,725	4340	34,785	4420	34,760	4395
9.0	35,030	4645	34,985	4600	35,050	4685	35,030	4665.
9.5	35,270	4885	35,240	4855	35,300	4935	35,285	4920
10.0	35,535	5150			35,575	5210		

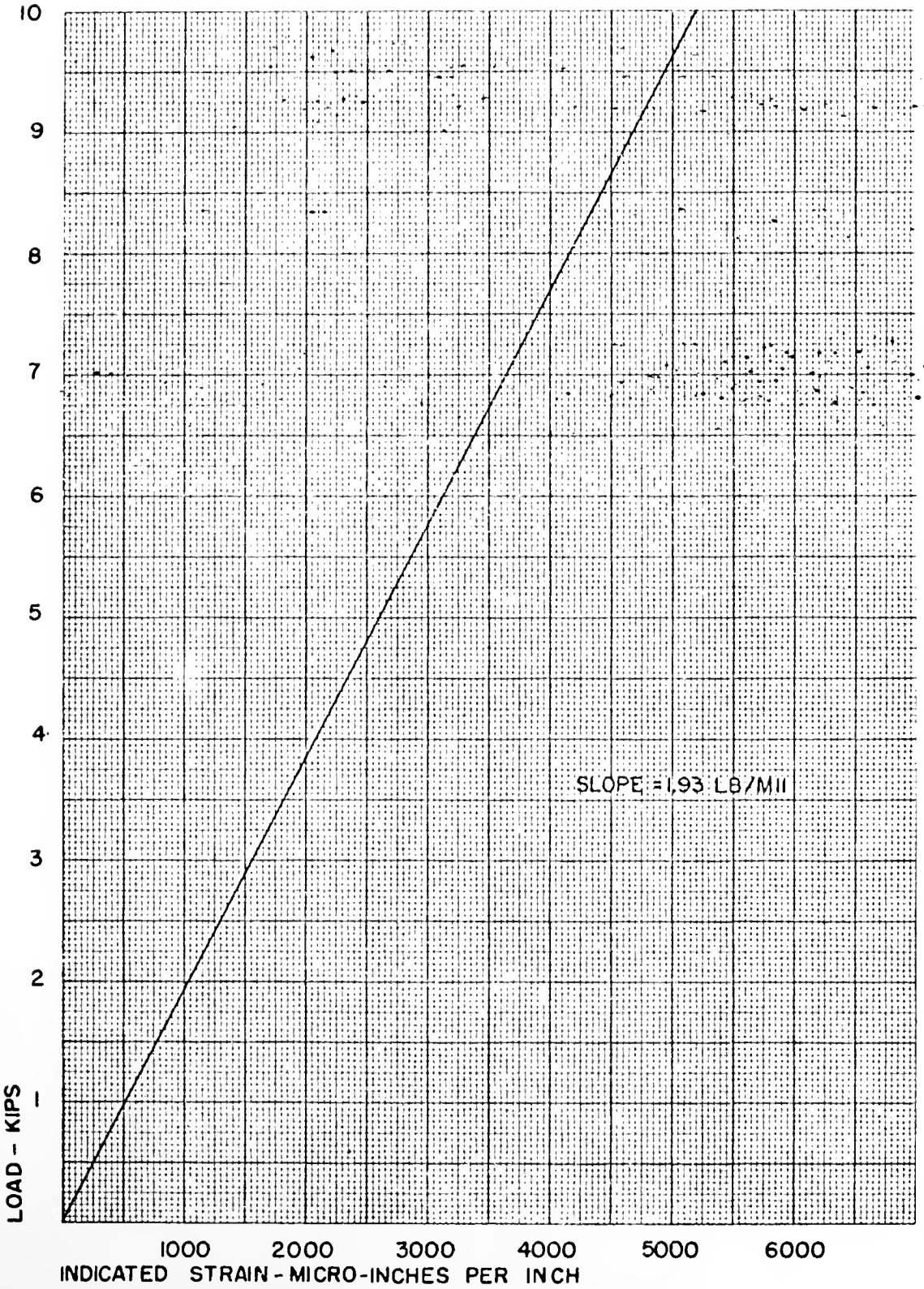

FIGURE 39. CALIBRATION CURVE, LOAD CELL B

Table 7. Cable Tension Cell "C" - Calibration

Load	Loading - Cycle 1		Unloading - Cycle 1		Loading - Cycle 2		Unloading - Cycle 2	
	Strain Reading	Strain με	Strain Reading	Strain με	Strain Reading	Strain με	Strain Reading	Strain με
Zero	29,740	-	29,740	-	29,740	-	29,710	-
0.5	29,460	280	29,495	245	29,465	275	29,490	250
1.0	29,190	550	29,230	510	29,180	560	29,215	525
1.5	28,910	830	28,960	780	28,915	825	28,955	785
2.0	28,675	1065	28,710	1030	28,650	1090	28,700	1040
2.5	28,420	1320	28,465	1275	28,405	1335	28,455	1285
3.0	28,170	1570	28,205	1535	28,145	1595	28,205	1535
3.5	27,905	1835	27,960	1780	27,905	1835	27,950	1790
4.0	27,665	2075	27,710	2030	27,650	2090	27,700	2040
4.5	27,410	2330	27,450	2290	27,390	2350	27,445	2295
5.0	27,150	2590	27,195	2545	27,140	2600	27,190	2550
5.5	26,895	2845	26,950	2790	26,880	2860	26,935	2805
6.0	26,650	3090	26,690	3050	26,625	3115	26,685	3055
6.5	26,395	3345	26,445	3295	26,375	3365	26,425	3315
7.0	26,140	3600	26,170	3570	26,115	3625	26,190	3550
7.5	25,865	3875	25,930	3810	25,810	3930	25,925	3815
8.0	25,620	4120	25,670	4070	25,560	4180	25,665	4075
8.5	25,375	4365	25,415	4325	25,350	4390	25,410	4330
9.0	25,115	4625	25,155	4585	25,100	4640	25,150	4590
9.5	24,885	4855	24,900	4840	24,840	4900	24,890	4850
10.0	24,620	5120	24,620	5120	24,610	5130	24,610	5130

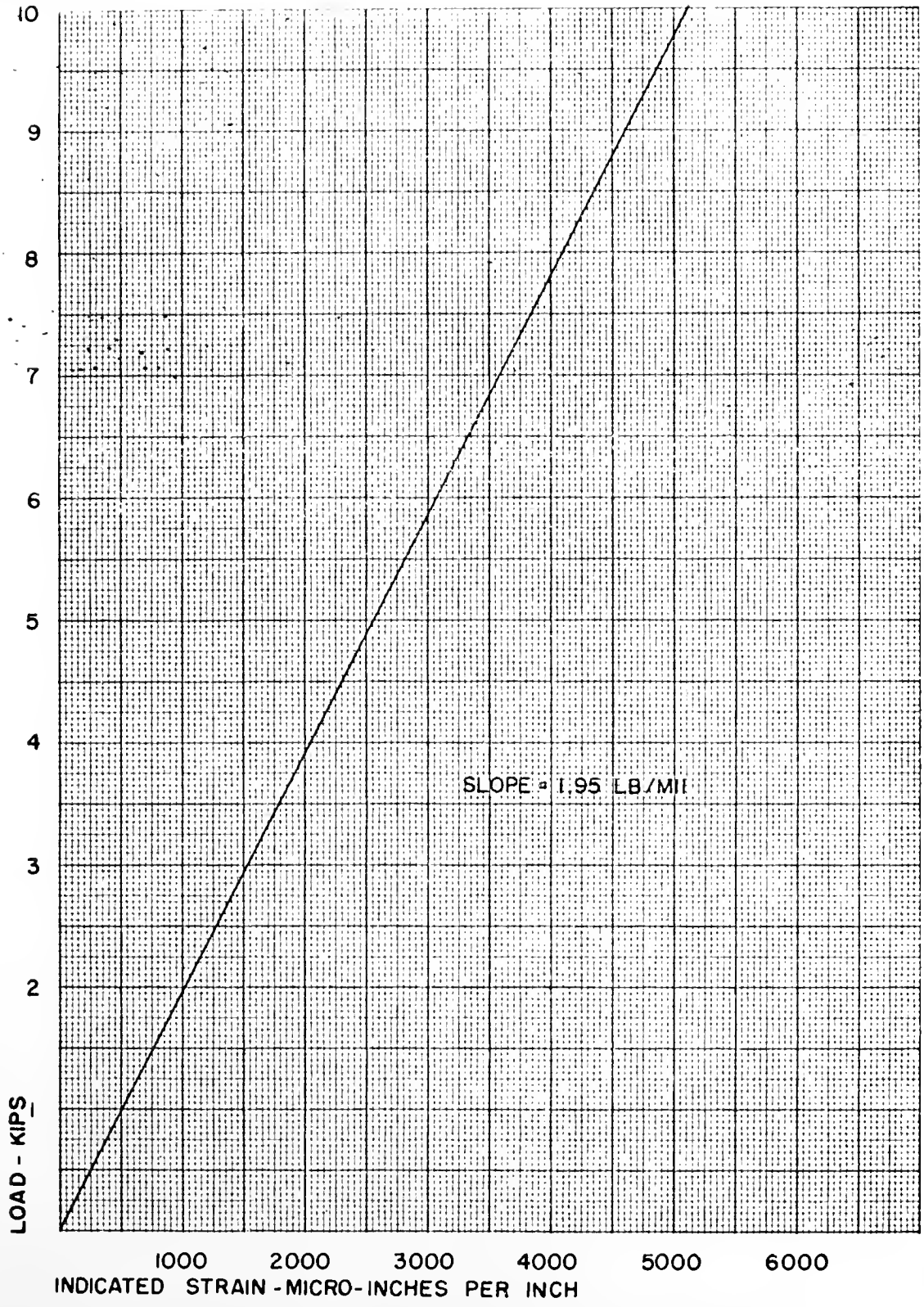

FIGURE 40. CALIBRATION CURVE, LOAD CELL C

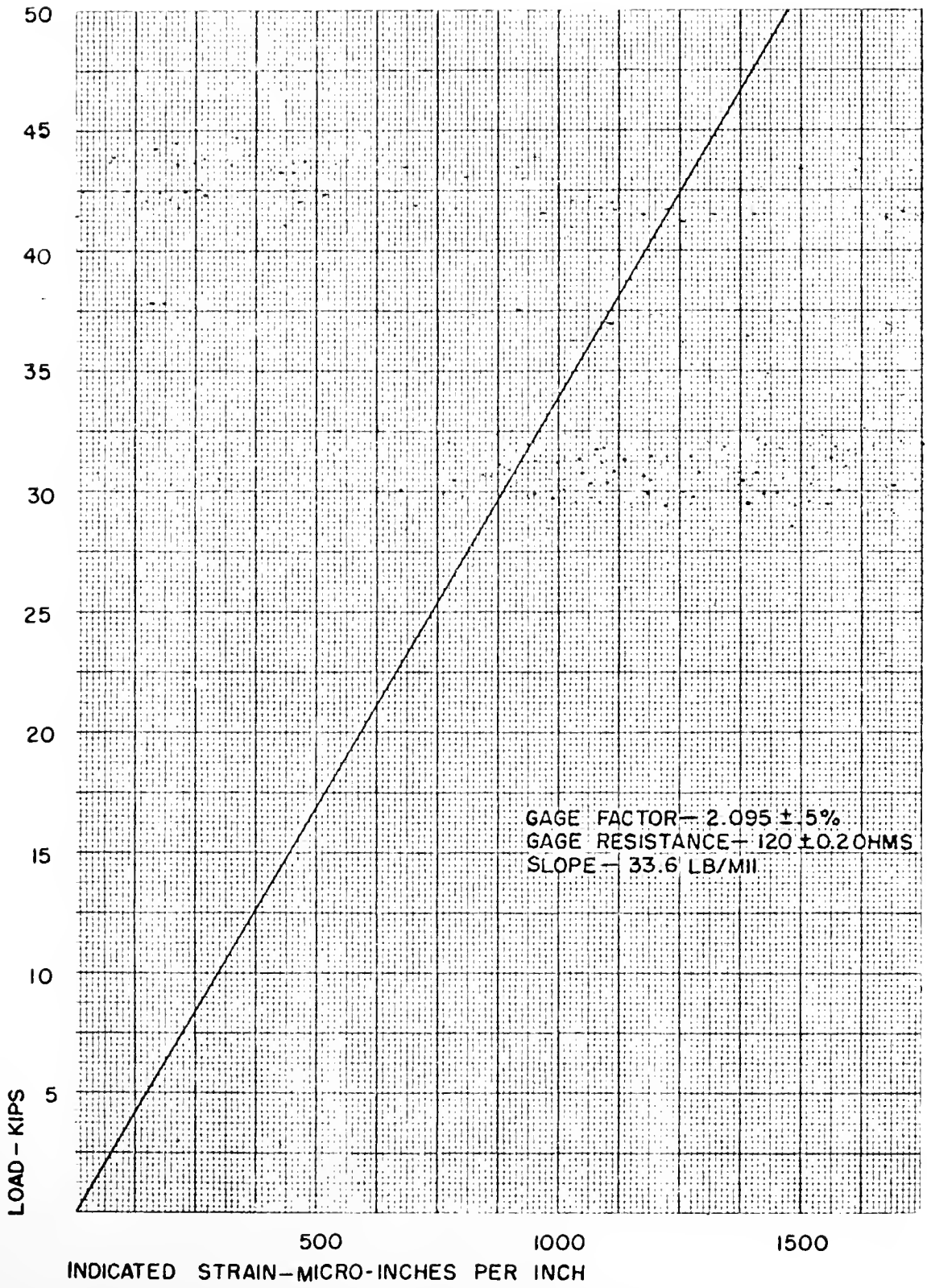

FIGURE 41. CALIBRATION CURVE, 50 KIP LOAD CELL

18 + 0.64 (12) = 25.68 kips. Taking five percent of this load as the longitudinal force to be resisted, the force to be transmitted from the deck to the supporting girders is 1,284 pounds on the experimental section.

Description of Test for Resistance to Horizontal Load

A 10 foot wide by 12 foot long deck section made up of four 3 foot by 10 foot sections was used for the horizontal slip test. The test was made up three series which varied with regard to support conditions. Support was provided by 18 WF 70 lb. beams. The testing arrangement for the three series of tests are shown in Figures 44 and 45.

Series I. In Series I, support for the slab was provided by three 18 WF 70 lb. beams spaced at 4'-0" center to center of web. The top flanges of the beams were leveled prior to the test by grout which was placed under the bottom flanges of the beams. The surface of the beams had been painted with a rust-proofing primer. The conditions approximated the conditions existing in a bridge which had a level floor system (or the case in which the floor system was not level and the irregular void space had been filled with a leveling course which was bonded to the deck slab but was not bonded to the floor system). The jacking system was arranged as shown in Figure 44. The load supplied to the deck was continuously monitored by means of a 50 kip capacity (See calibration curve, Figure 41) load cell which was coupled to a switch and balance unit and a strain indicator. The only motion in the system was between the deck and its supporting beams since the supporting beams were prevented from moving by a restraining beam resting on

the floor, oriented normal to the supporting beams. The restraining beam was held motionless by braces inserted into shear plugs in the laboratory floor. A post-tensioning force was maintained in the two outermost cables in order to close the joints and to ensure that the entire deck moved at first slippage. The cable tension load cells were also connected to the previously mentioned switch and balance unit and strain indicator.

The bolting force in the hold-down clip system was varied by not only changing the number of bolts but also by varying the applied torque in each bolt. The pattern of bolting systems was also varied in Series I. The bolting arrangements referred to in Table 8 are illustrated in Figures 42 and 43.

Series II. In Series II, support for the slab was provided by three 18 WF 70 lb. beams spaced at 4'-0" center to center of web but the grout used to level the Series I beams had been removed, making the slab support uneven and the bearing area variable. In Series II, the condition of an non-level floor system without a leveling course was approximated. All other conditions of load monitoring, jacking, and support were the same in Series II as in Series I. The bolting arrangement indicated in Table 8 is illustrated in Figures 42 and 43.

Series III. In Series III, support for the deck was provided by two 18 WF 70 lb. beams at 8'-0" center to center of web. The beams were supported off the laboratory floor at their ends by one-half inch steel bar stock. The support for the slab was uneven and the bearing area between the deck and beams was variable. The jacking beam in this case was restrained by another restraining beam, held by supports installed

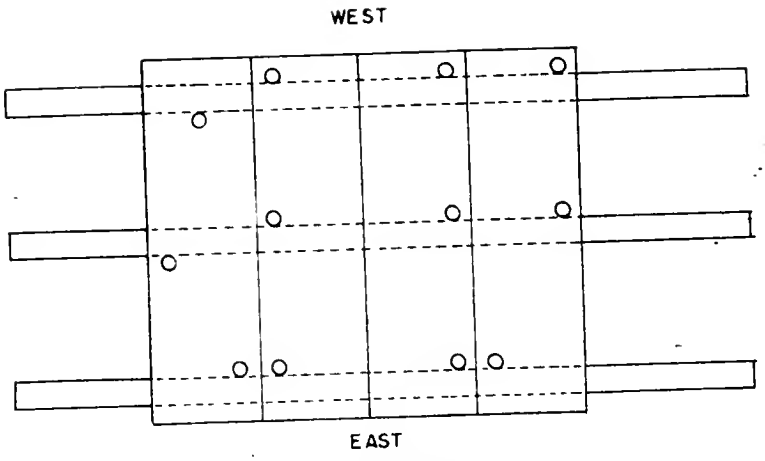

BOLTING ARRANGEMENT 1

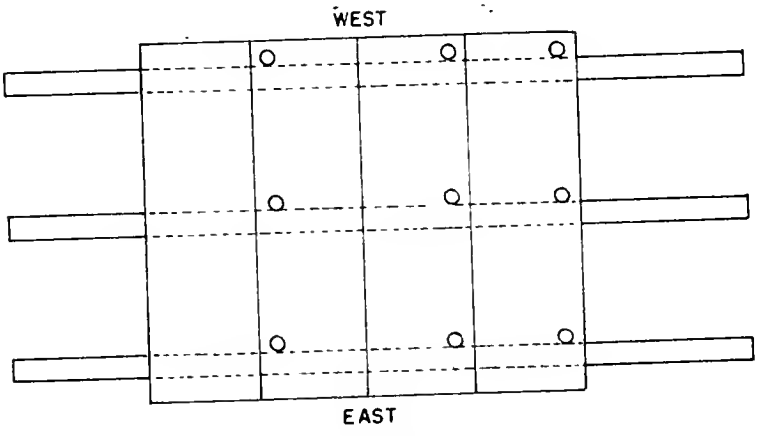

BOLTING ARRANGEMENT 2

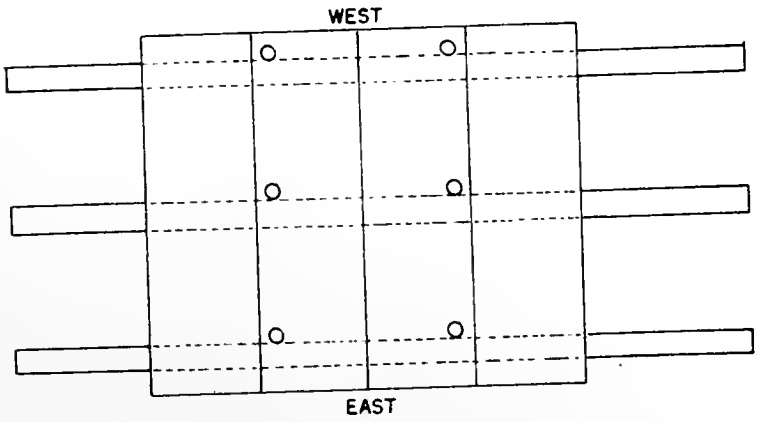

BOLTING ARRANGEMENT 3

FIGURE 42. LONGITUDINAL SLIP TEST, BOLTING ARRANGEMENTS 1,2,3

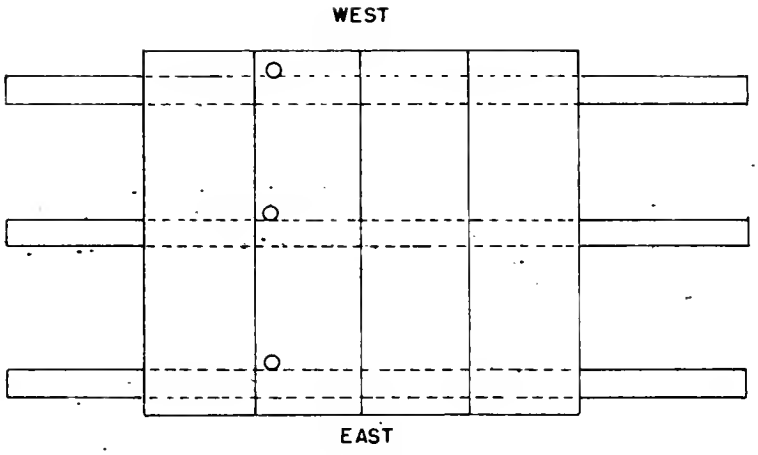

BOLTING ARRANGEMENT 4

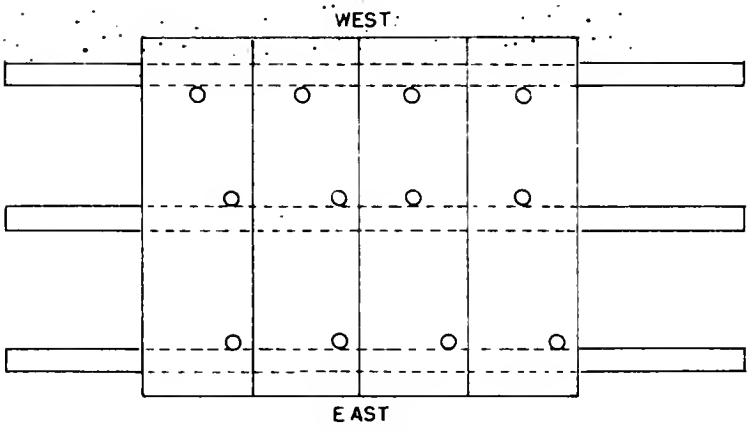

BOLTING ARRANGEMENT 5

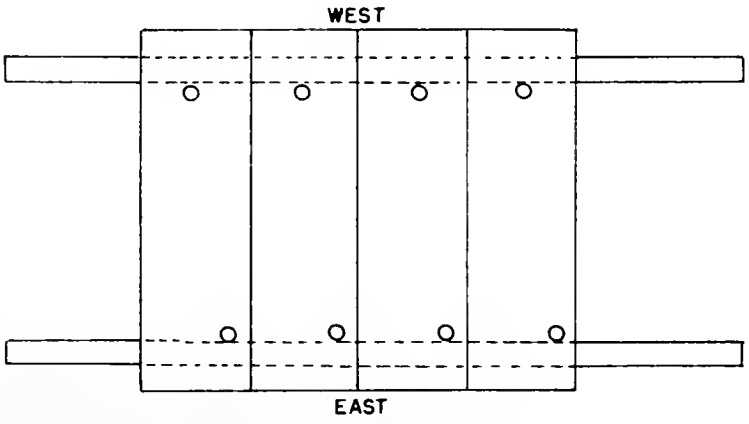

BOLTING ARRANGEMENT 6

FIGURE 43. LONGITUDINAL SLIP TEST, BOLTING ARRANGEMENTS 4,5,6

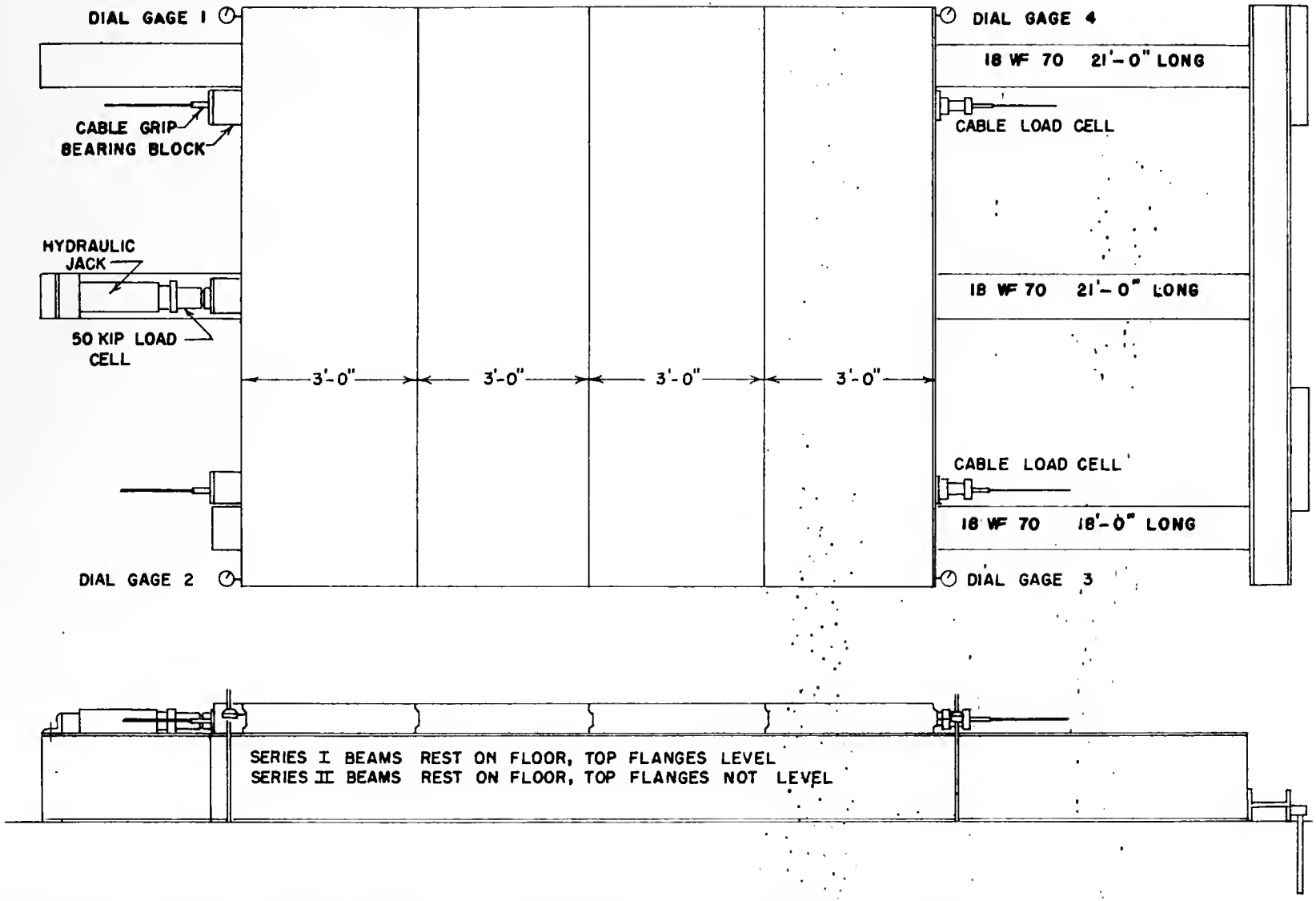

FIGURE 44. TESTING ARRANGEMENT, LONGITUDINAL SLIP, SERIES I AND II

in the floor of the laboratory. The jacking beam remained on the laboratory floor and the jack and load cell were raised in order to apply the horizontal load at mid depth of the deck. See Figure 45.

Measurement of Movement. The motion of the deck system was measured by four .001 inch dial gages placed at the four extreme corners of the section at mid depth of the deck. Longitudinal motion was measured at each point after each increase in applied load. The occurrence of slip was noted not only by the dial gages but also in the inability of the deck to resist an increase in load as noted by the strain indicator coupled to the load cell.

Results of Slip Test

The results of the slip test appear as Table 8 and graphically as Figure 46. In all cases, the horizontal load resistance of the deck system exceeds the AASHO code requirement of 1,284 pounds for the deck section analyzed. In all cases, an increase in bolting force produced an increase in horizontal resistance with the most pronounced increase occurring in Series I, the case of level beam flanges. For this reason, beam flanges which are nearly level or are essentially level due to the placement of a filler between the beams and slab would offer the greatest resistance to horizontal motion in a bridge. Although bolting was done on only one side of the beam flange, the bolting could be accomplished on both sides of the supporting beam if desired.

The bolting force predicted will not be realized if the bolts have not been lubricated; lubrication is always recommended before tightening the bolts.

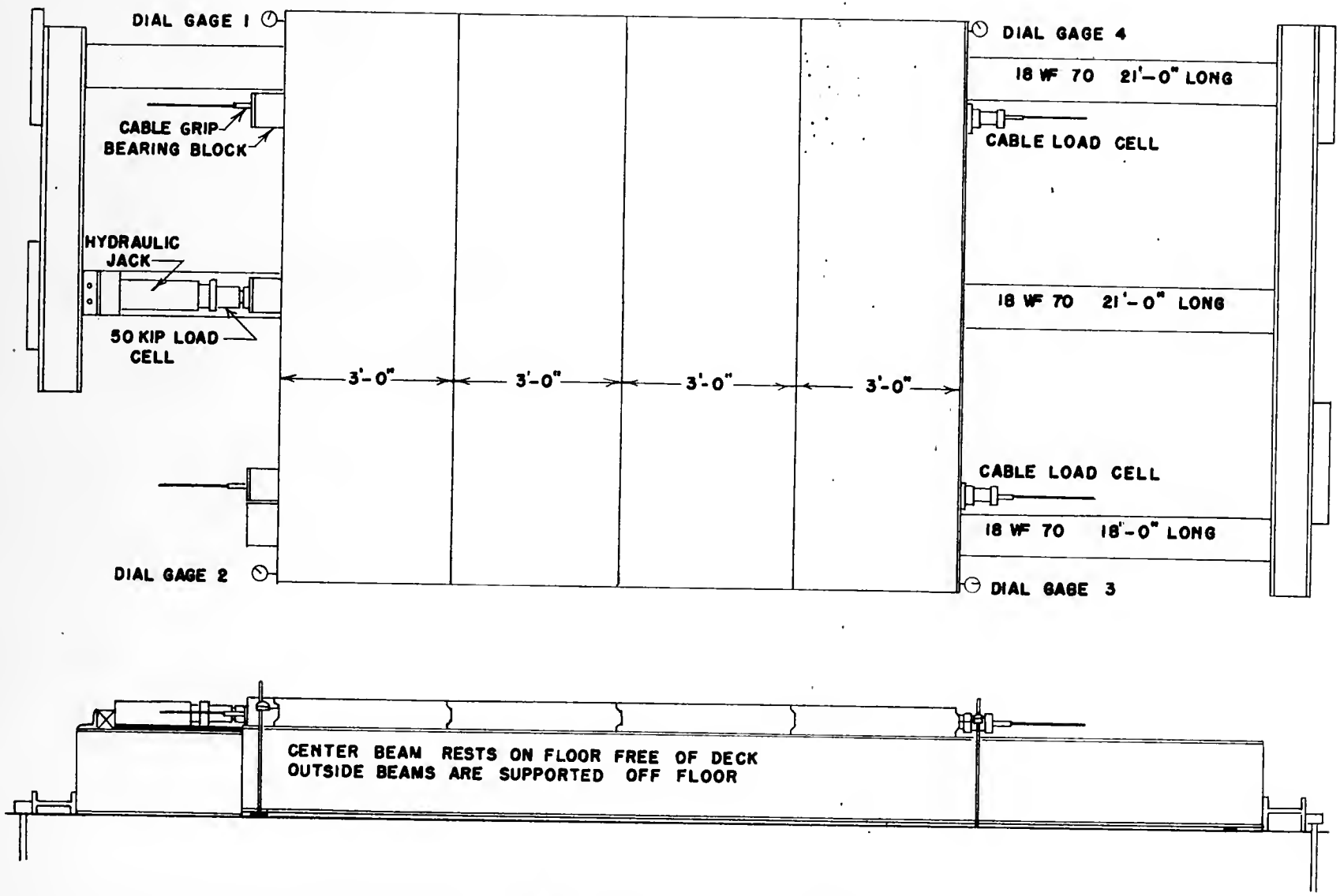

FIGURE 45. TESTING ARRANGEMENT, LONGITUDINAL SLIP, SERIES III

Table 8. Resistance of Deck to Longitudinal Forces

Series	Horizontal Load at Slip lb	Bolting Arrangement	Bolting Force lb	Number of Bolts
I	4,502	-	0	0
I	4,502	-	0	0
I	8,064	1	24,000	12
I	11,760	1	48,000	12
I	12,096	1	48,000	12
I	12,230	1	48,000	12
I	11,256	2	36,000	9
I	10,450	2	36,000	9
I	10,080	3	24,000	6
I	10,248	3	24,000	6
I	7,392	4	12,000	3
I	7,896	4	12,000	3
I	2,822	-	0	0
I	3,763	-	0	0
II	3,220	-	0	0
II	3,260	-	0	0
II	5,380	5	24,000	12
II	5,380	5	24,000	12
II	6,320	5	48,000	12
II	6,600	5	48,000	12
III	3,430	-	0	0
III	3,360	-	0	0
III	3,760	6	16,000	8
III	3,830	6	16,000	8
III	4,170	6	32,000	8
III	4,200	6	32,000	8

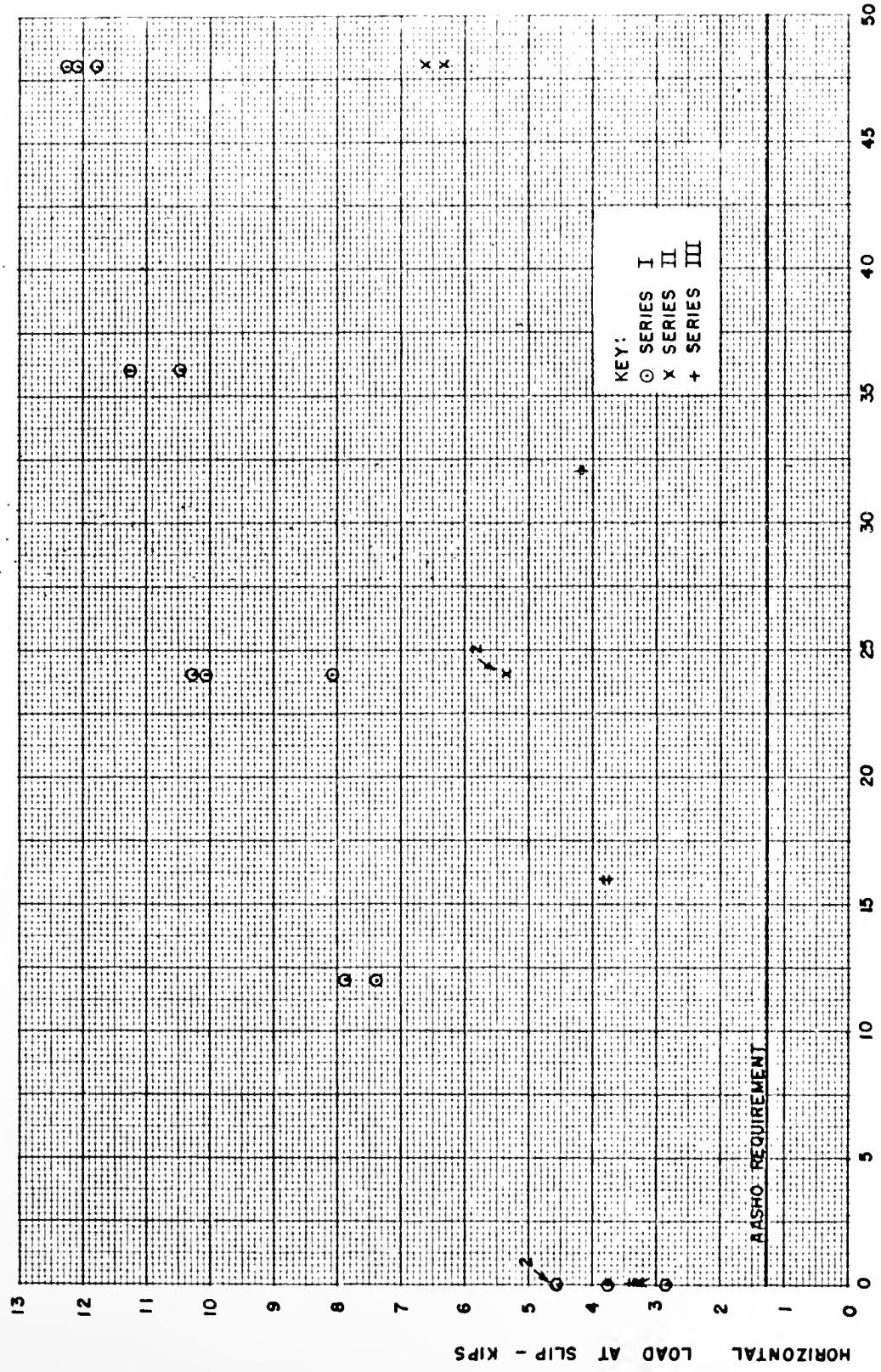

FIGURE 46. HORIZONTAL LOAD AT SLIP VS. BOLTING FORCE

Static Testing of Specimens Reinforced for 4'-0" Beam Spacing

Description of Test

Figures 47 and 48 indicate the testing arrangement used for the static test with 4'-0" beam spacing. The supporting beams, previously used in the longitudinal slip test, rested on the floor of the laboratory; grout was placed between the floor and the bottom flanges in order to level the top flanges for the test. Load was applied at midspan of the slab with a hand-operated hydraulic jack through a 10 inch diameter steel plate and rubber pad. Prior to any loading the joints were closed.

Measurement of Loads. A constant monitor of applied load was made with the 50 kip load cell connected to a switch and balance unit and strain indicator. The same switch and balance unit and strain indicator were used to monitor the cable tension load cells without any adjustment since gage factors for the several load cells were identical.

Measurement of Deflection. Deflection points on the slab consisted of quarter-inch hardwood dowel pegs cemented to the concrete with Duco (T.M.) Cement. A 0.10 inch graduated rod was held on these pegs and read with a self-leveling level fitted with an optical vernier, permitting deflection measurements to 0.001 inch. Points where deflection measurements were made are illustrated in Figure 49. Before and after each series of readings, the elevation of a fixed point was taken and compared to the elevation which had been observed at the start of the test to ensure that the level had not moved during the test. With no load at the beginning of each load stage the elevation of each point was read and subsequent readings were made after a change in applied

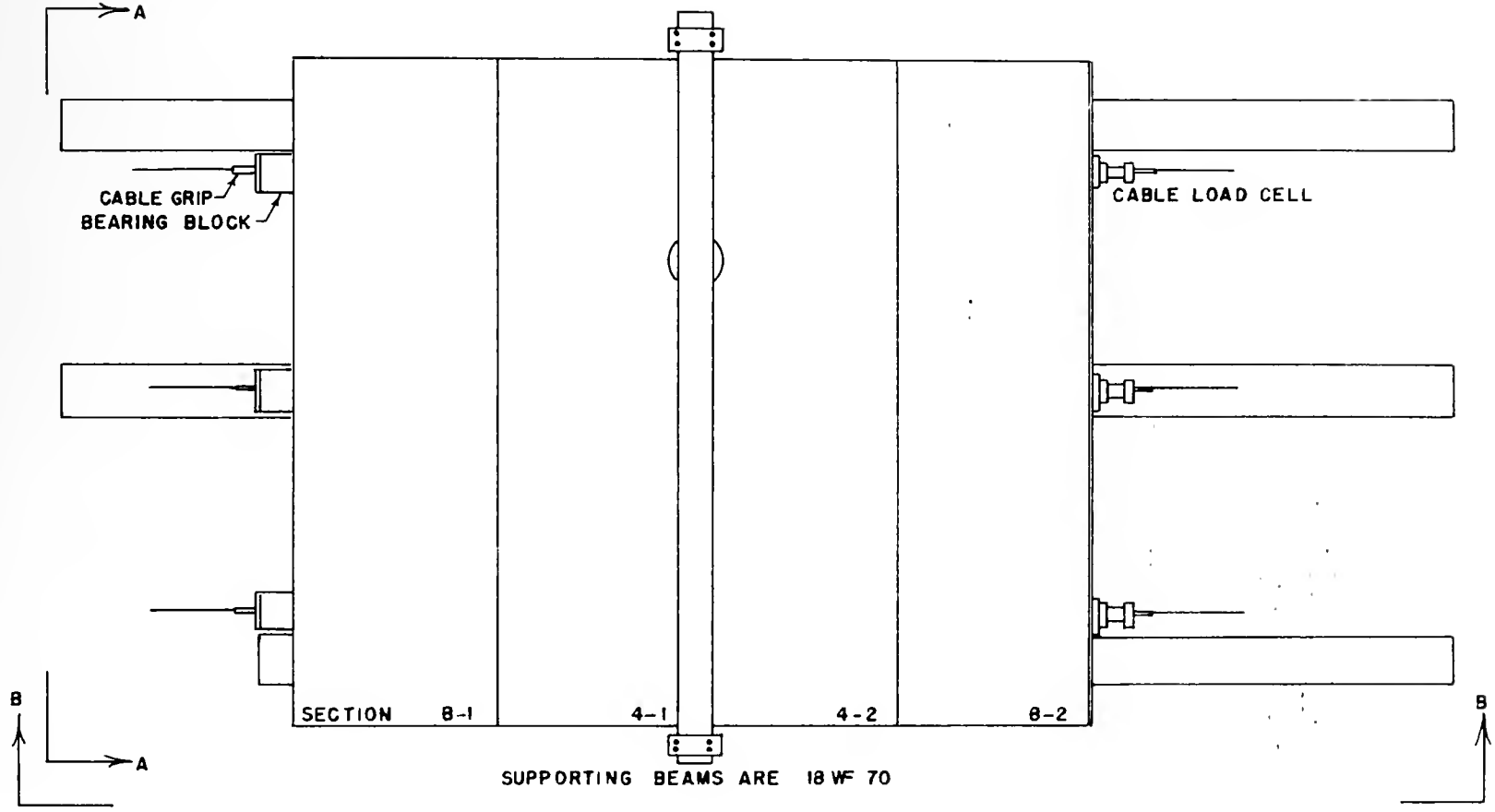

FIGURE 47. PLAN VIEW OF STATIC TEST FOR SECTIONS REINFORCED FOR 4'-0" CENTER-TO-CENTER BEAM SPACING

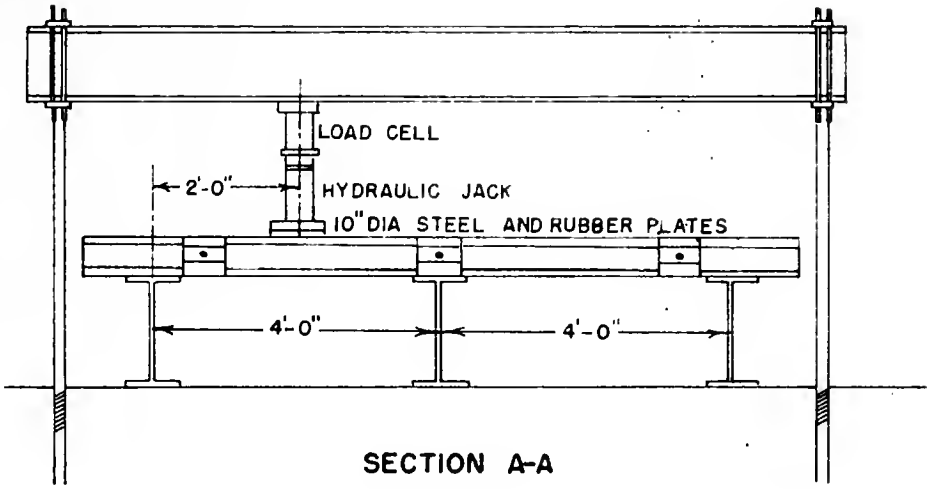

SECTION A-A

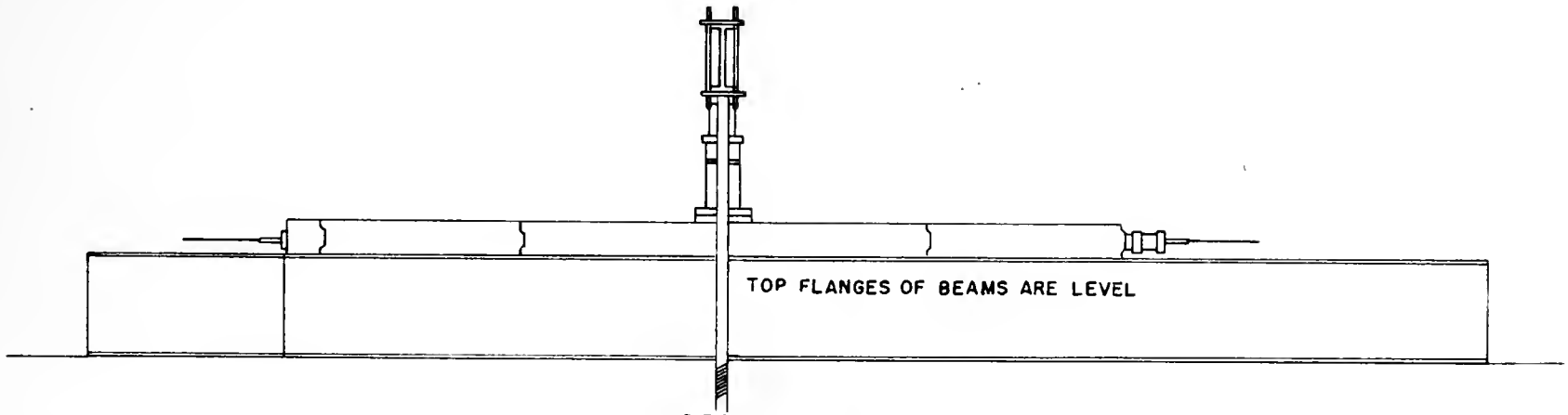

SECTION B-B

FIGURE 48. SECTIONS A-A AND B-B, STATIC TEST WITH 4'-0" BEAM SPACING

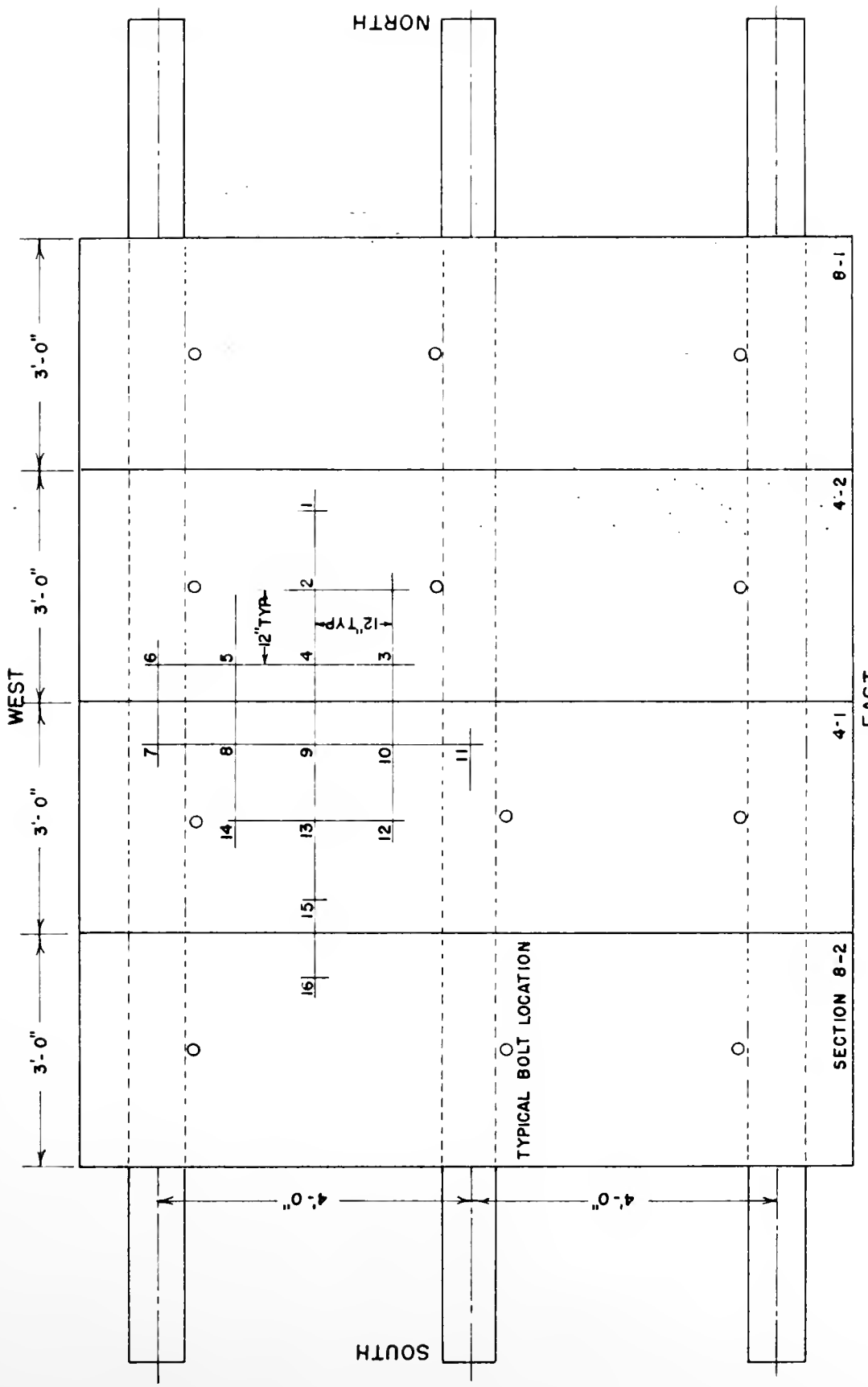

FIGURE 49. LOCATIONS OF DEFLECTION MEASUREMENT, STATIC TEST, 4'-0" BEAM SPACING

load. The difference between the original reading and the reading after load application gave the deflection due to loading. Figures 50 thru 55 contain deflection information as does Table 11.

Measurement of Strain. SR-4 (T.M.) electrical resistance strain gages were used in a basic Wheatstone bridge circuit with one active arm; attached to the other arms of the bridge were a compensating gage attached to an unstressed concrete cylinder, and two precision wire-wound resistors. Nominal resistance for all gages was 120 ohms; gage factor for the gages was 2.04 ± 1%.

The strain was not measured directly due to the large number of gages and the relative slowness of the method compared to other methods available. The method used consisted of measuring the voltage across the basic Wheatstone bridge with a digital volt meter, a method which permits reading of a large number of gages in a short period of time.

A constant voltage power supply was used to power the circuit and the applied voltage was maintained at 4 volts. The choice of 4 volts was made after examination of the equation for output in the Wheatstone bridge: $E = \frac{VR_1R_2}{(R_1 + R_2)^2}\left(\frac{\Delta R_1}{R_1} - \frac{\Delta R_2}{R_2} + \frac{\Delta R_3}{R_3} - \frac{\Delta R_4}{R_4}\right)$.[1]

In applying this equation to the circuit used, V is the 4 volts supplied, R_1 is the active gage, R_2 is the compensating gage, and R_3 and R_4 are precision wire-wound resistors. All resistors in the circuit are nominally 120 ohms. The only resistance change occurred in R_1, the active gage, which reduces the expression for the output to:

$E = \frac{VR_1R_2}{(R_1 + R_2)^2}\left(\frac{\Delta R_1}{R_1}\right)$. Since $R_1 = R_2$, the expression further reduces to $E = \frac{V}{4}\left(\frac{\Delta R_1}{R_1}\right)$. The strain causing the resistance change,

Table 9. Load Stages During Testing of Sections Reinforced for 4'-0" Beam Spacing

Load Stage	Post-Tensioning (psi on gross section)	Bolting Force (kips)	Applied Load (pounds)
1	0	0	5,040
	0	0	10,080
	0	0	15,120
2	20.2	0	5,040
	20.2	0	10,080
	20.2	0	15,120
3	33.6	0	5,040
	33.6	0	10,080
	33.6	0	15,120
4	33.6	48	5,040
	33.6	48	10,080
	33.6	48	15,120
5	20.6	48	5,040
	20.6	48	10,080
	20.6	48	15,120
6	0	48	5,040
	0	48	10,080
	0	48	15,120

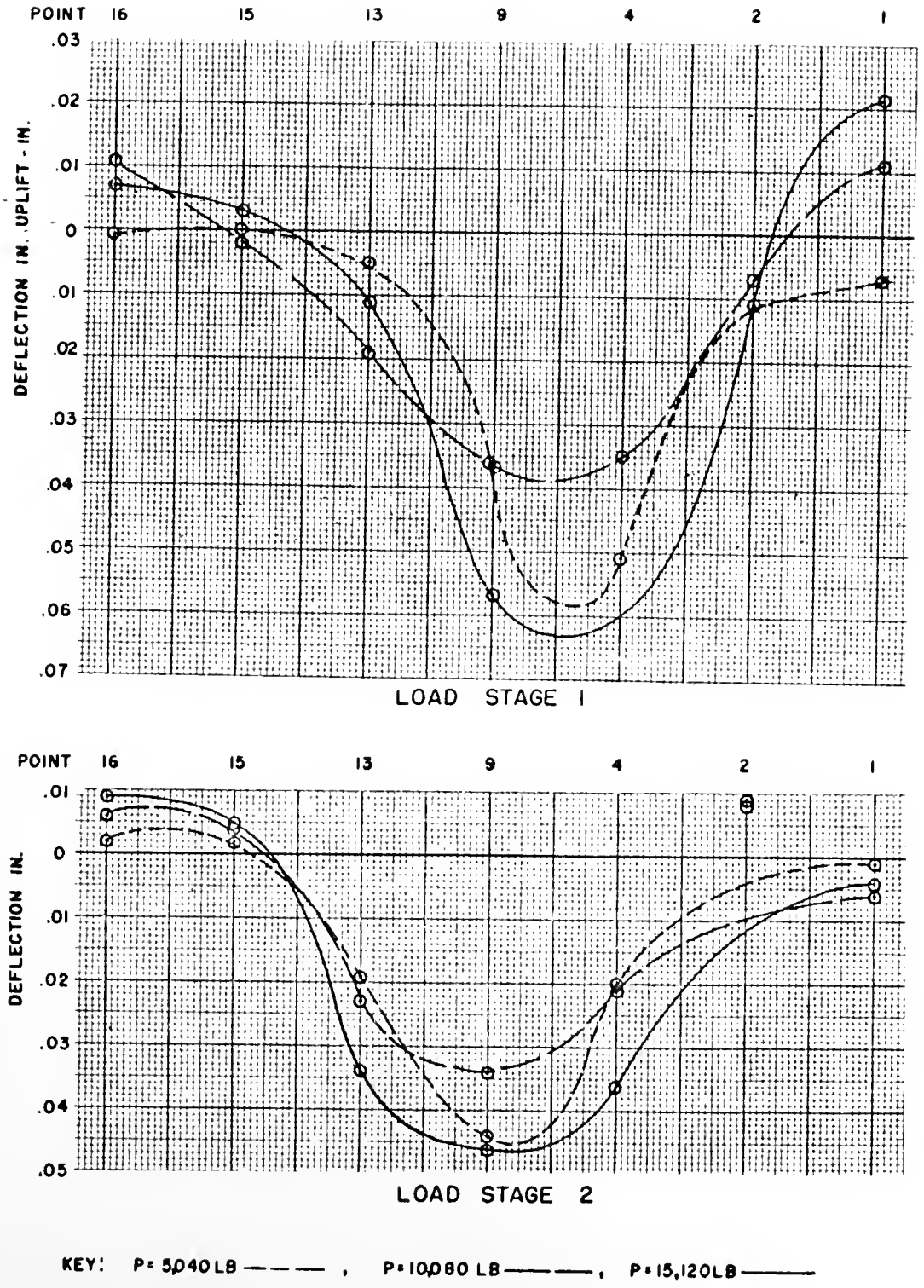

FIGURE 50. LONGITUDINAL CENTER LINE DEFLECTION, 4'-0" BEAM SPACING, LOAD STAGES 1 AND 2

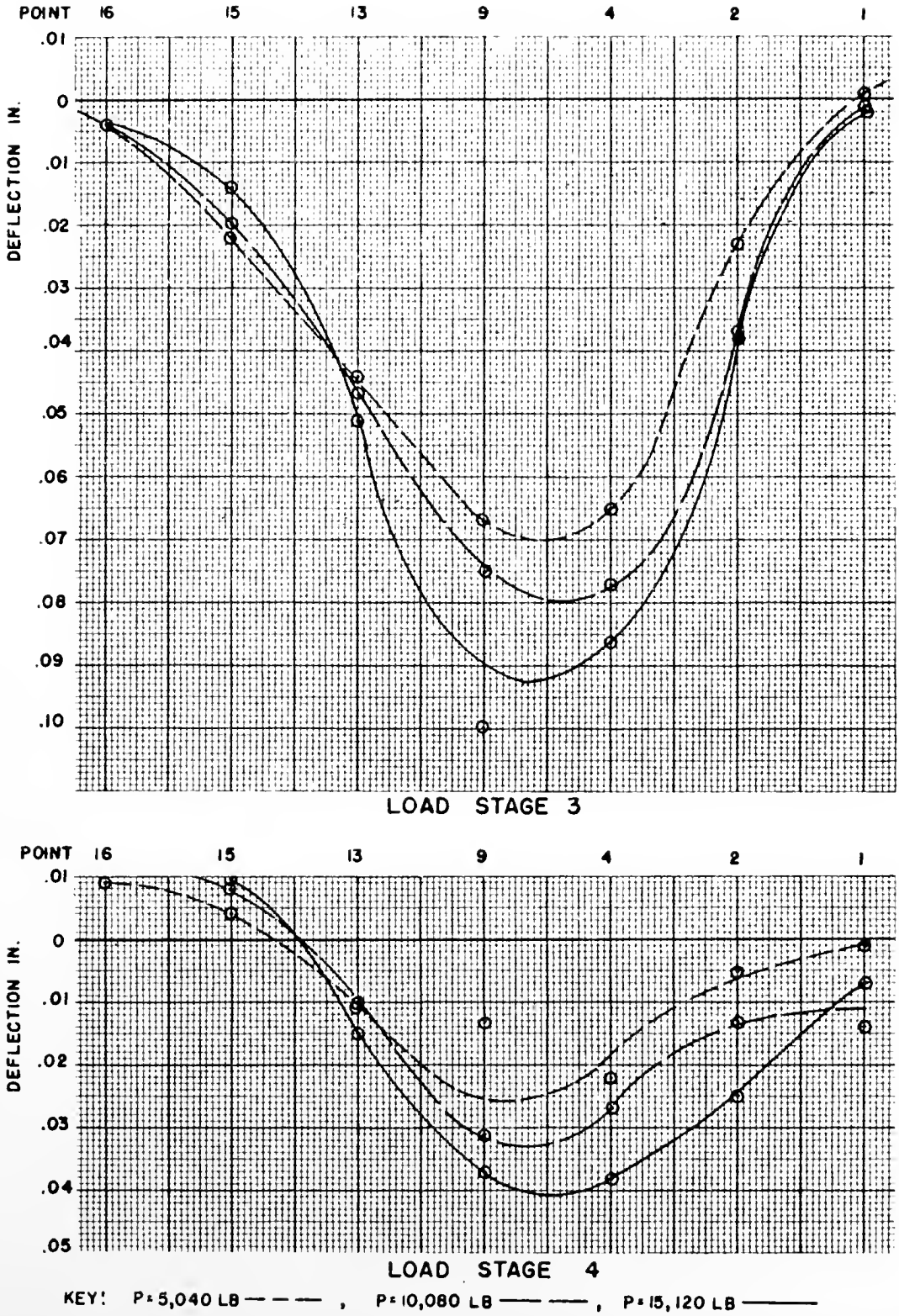

FIGURE 51. LONGITUDINAL CENTER LINE DEFLECTION, 4'-0" BEAM SPACING, LOAD STAGES 3 AND 4

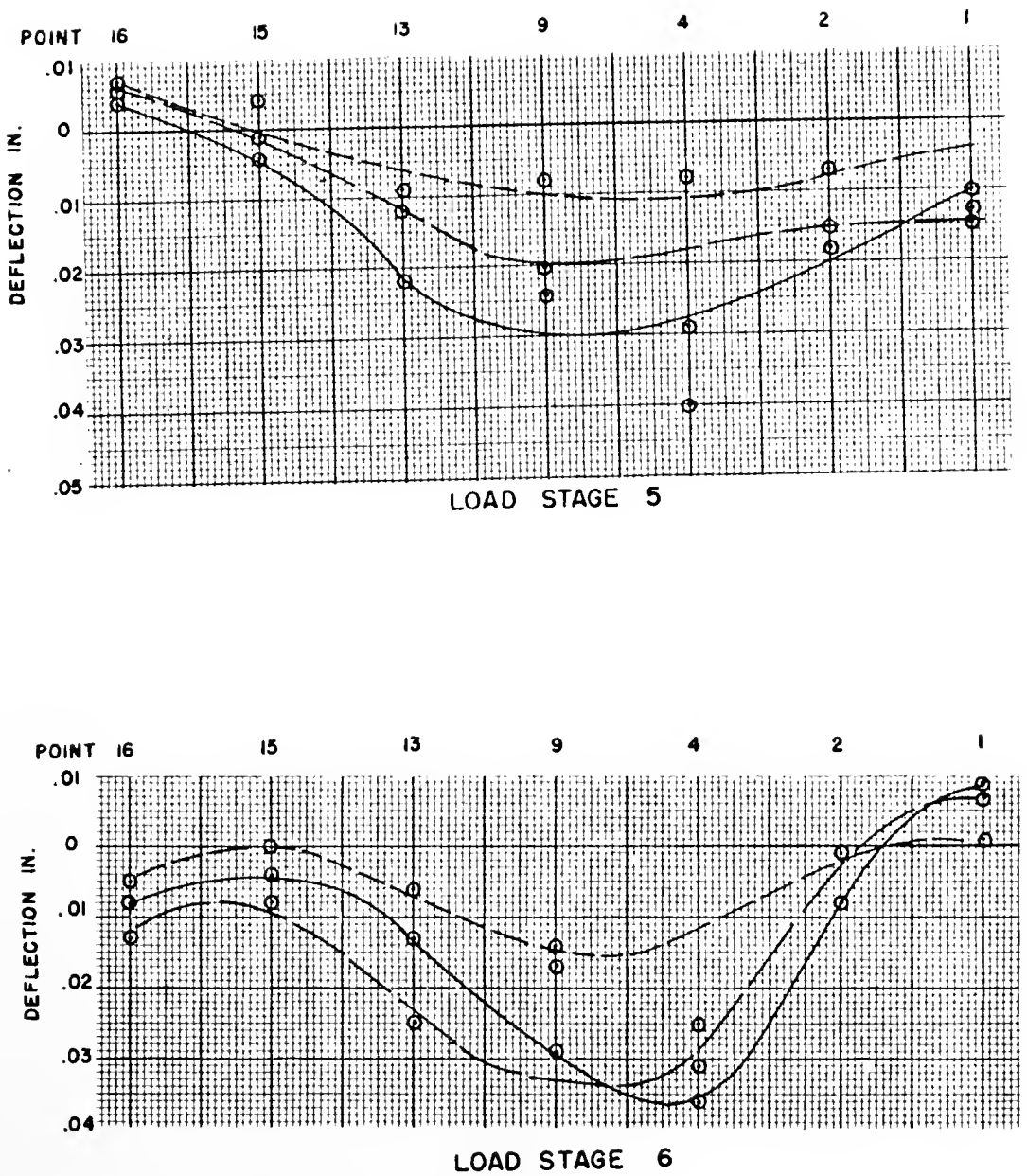

FIGURE 52. LONGITUDINAL CENTER LINE DEFLECTION, 4'-0" BEAM SPACING, LOAD STAGES 5 AND 6

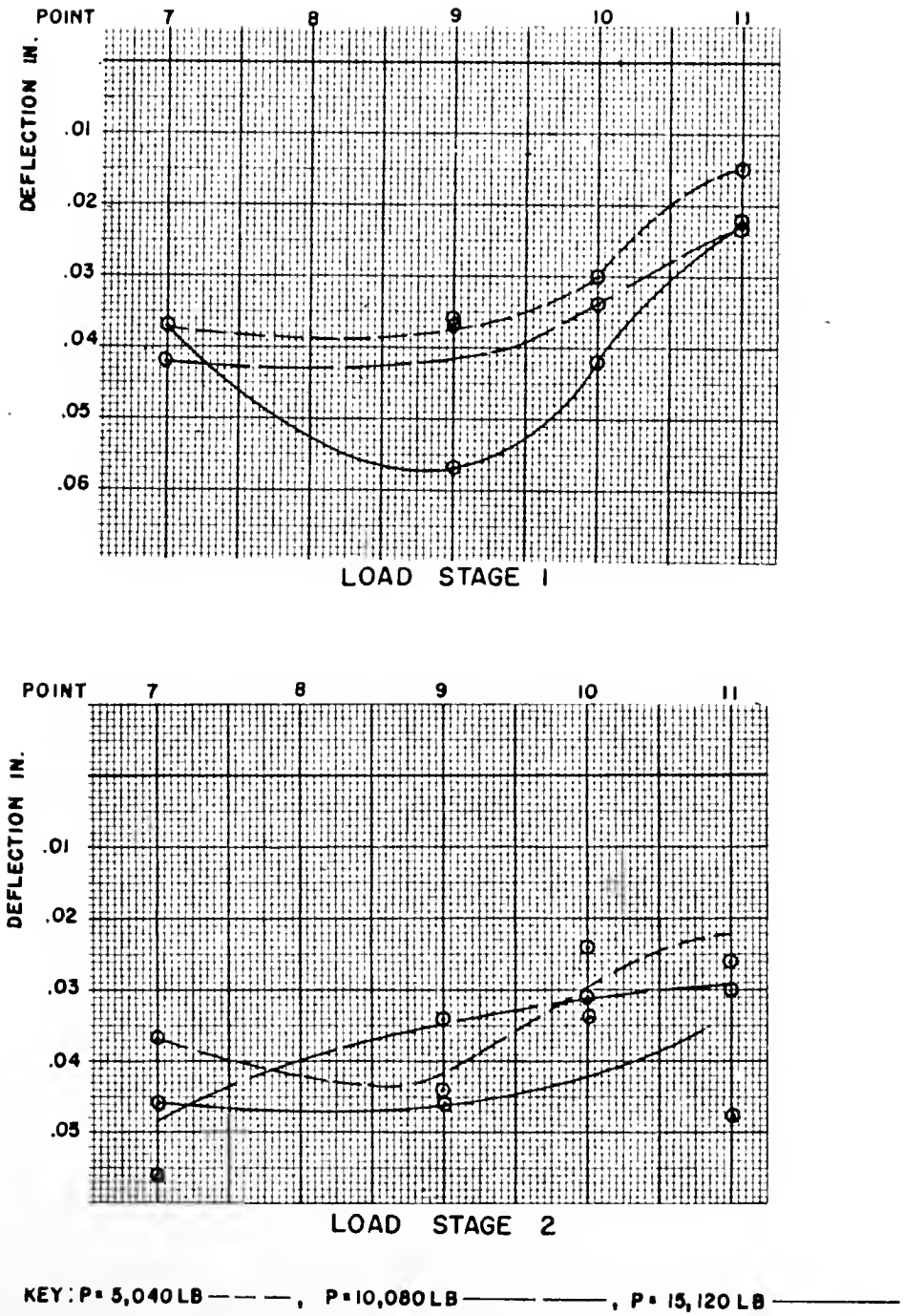

FIGURE 53. TRANSVERSE LINE DEFLECTION NEAR LOAD, 4'-0" BEAM SPACING, LOAD STAGES 1 AND 2

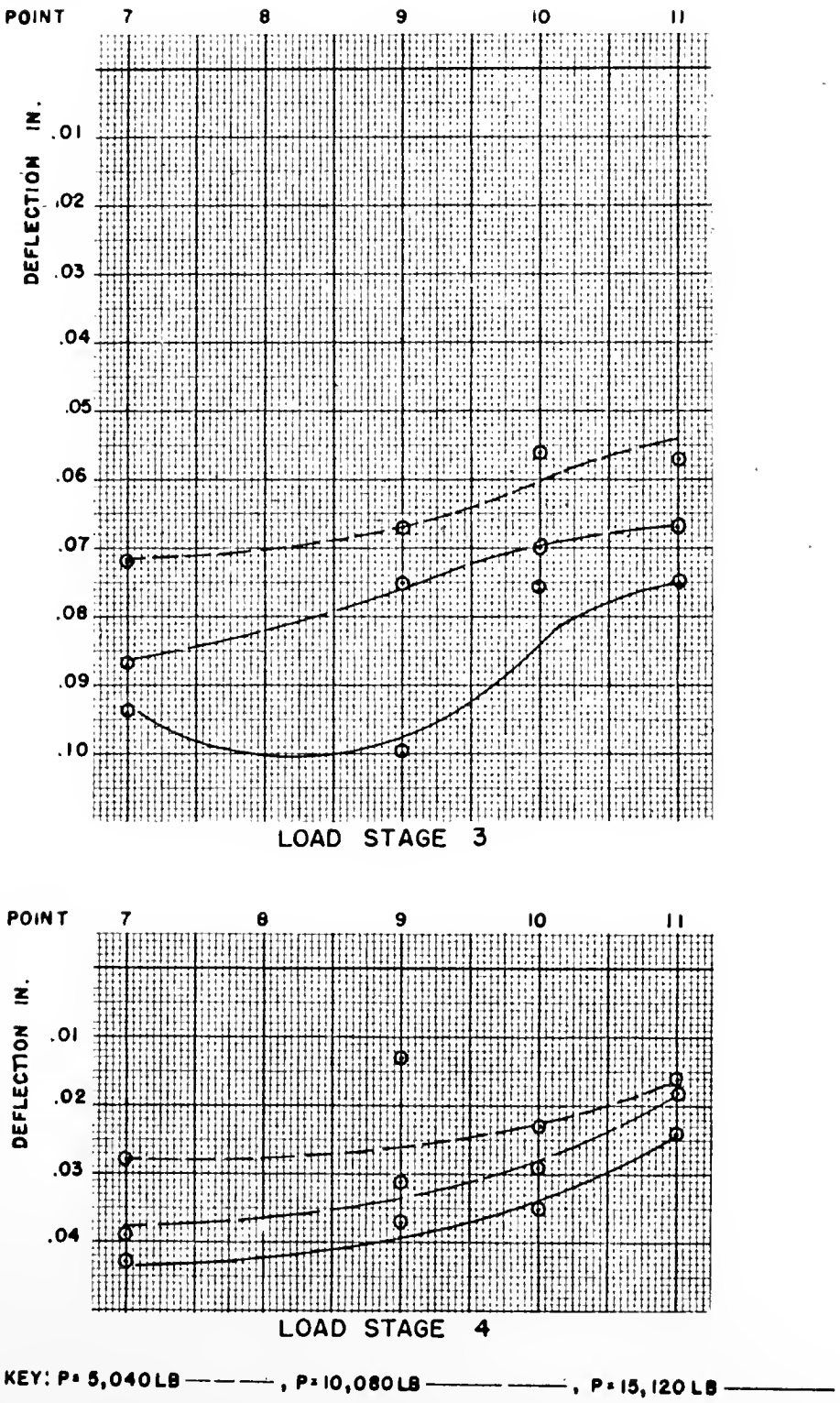

FIGURE 54. TRANSVERSE LINE DEFLECTION NEAR LOAD, 4'-0" BEAM SPACING, LOAD STAGES 3 AND 4

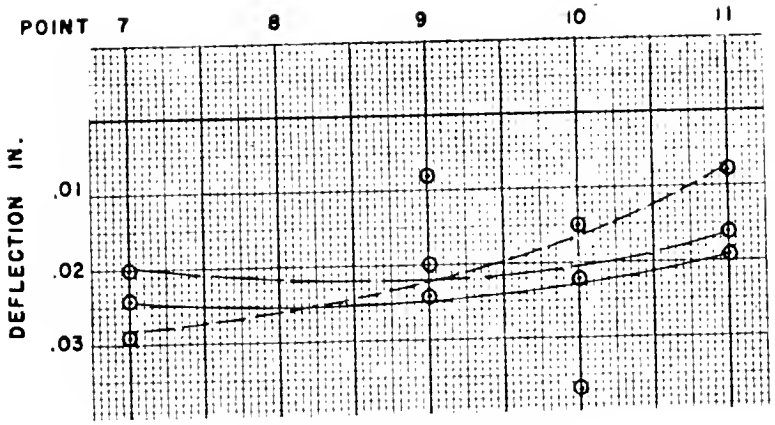

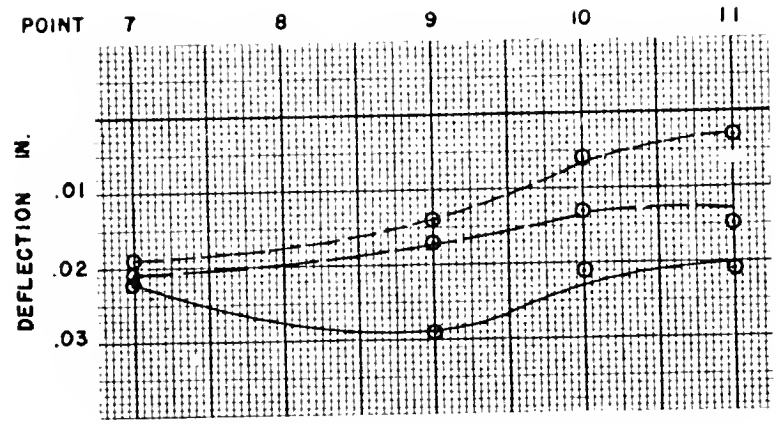

KEY: P = 5,040 LB — — —, P = 10,080 LB ——— ———, P = 15,120 LB ———

FIGURE 55. TRANSVERSE LINE DEFLECTION NEAR LOAD, 4'-0" BEAM SPACING, LOAD STAGES 5 AND 6

ΔR_1 , can be represented as $\frac{\Delta L}{L}$ and is related to the gage factor of the strain gage by the expression $\frac{\Delta L}{L} = \frac{\Delta R_1}{R_1} \times \frac{1}{G.F.}$. Now, entering the applied voltage and equivalent value of $\frac{\Delta R_1}{R_1}$, the expression for the circuit output becomes $E = \frac{\Delta L}{L}(G.F.)$ or, letting ε denote the strain, $\frac{\Delta L}{L}$, $\varepsilon = \frac{E}{G.F.}$ for the circuit used.

Sources of Error arise in not taking into account the length of lead-wires and in voltage supply drift. First, considering the effect of the lead-wires, the resistivity of the wire used was 0.043 ohms per foot measured at 75° F. Assuming a maximum 20 ft. lead, there would be an effective resistance of 1.72 ohms (.043 x 40) due to the length of the lead wires. This would translate to $E = \frac{V}{4.06} \frac{\Delta R_1}{R_1}$ or a discrepancy of 1.5 percent from the assumed value of 4.00 in the denominator of the expression. The second possible source of error would be in voltage supply drift. Maximum drift observed during the test was .005 volts, a 0.125 percent discrepancy from the 4 volts assumed. Neither of the above discrepancies was considered significant enough to necessitate rejection of the method.

For each load stage (see Table 9), a voltage reading was made for each channel prior to load and subsequent readings were taken after changes in applied load. In this way, the voltage change which translates to strain as indicated above, was an indication of the performance of the deck due to flexure.

Strain Gage Application was made using Duco (T.M.) Cement. The concrete surface had first been sanded, cleaned with acetone, and covered with a layer of Duco Cement which was permitted to dry. The

paper gage backing was trimmed to within approximately 1/16 inch of the protective felt pad, the desired location of the gage grid center was marked on the concrete surface, and a new layer of Duco Cement was placed at the desired gage location. The gage was pressed onto the prepared concrete surface and all excess cement and air bubbles were worked to the edges of the gage backing. Gage grid centers were located 3/4 inch in both longitudinal and transverse directions from the points indicated in Figures 56 and 57. Lead wires were then soldered to the strain gage leads and were run to the switch and balance units.

Results

The results of the testing for beam spacings of 4'-0" are presented as Figures 50 thru 55 and Figures 58 thru 63. Table 9 gives the conditions of applied load, bolting, and post-tensioning during the load stages referred to in the figures. p. 72

The load stages which most closely approximate conditions anticipated in a field application are numbered four and five.

Maximum deflections during load stages 4 and 5 were observed to occur when the post-tensioning was at its highest level. This is illustrated in Figures 51 and 52, load stages 4 and 5. The post-tensioning in load stage 5 is approximately 2/3 of the level of post-tensioning in load stage 4; this corresponds to a deflection in load stage 5 of approximately 3/4 of the deflection in load stage 4.

In all cases, deflection was decreased due to bolting. The maximum observed deflections of load stage 3 were decreased by more than half by bolting in load stage 4 (while maintaining the same post-tensioning stress in load stage 4) as shown in Figure 51. This holds

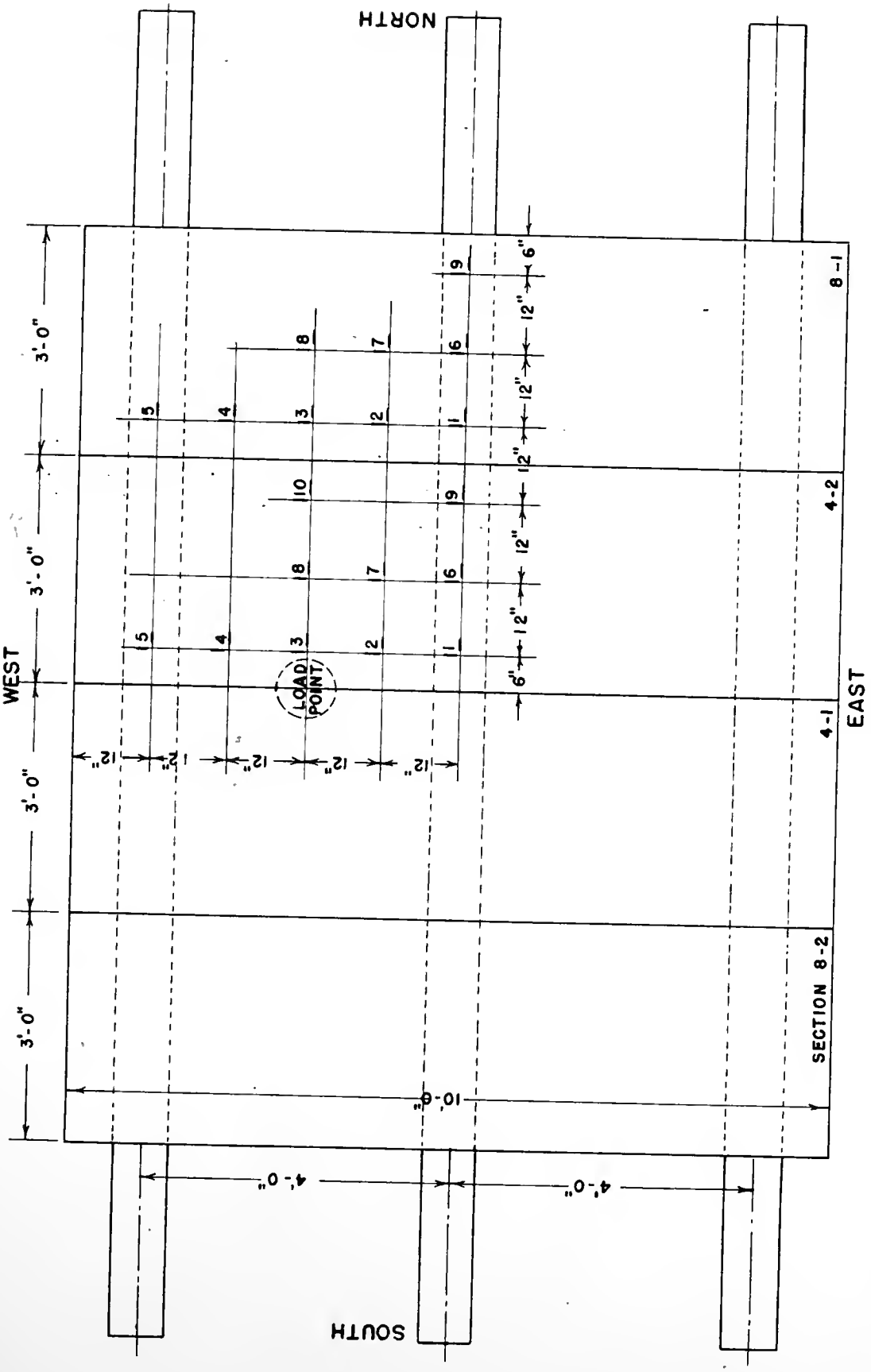

FIGURE 56. STRAIN GAGE LOCATIONS ON TOP SURFACE, STATIC TEST, 4'-0" BEAM SPACING

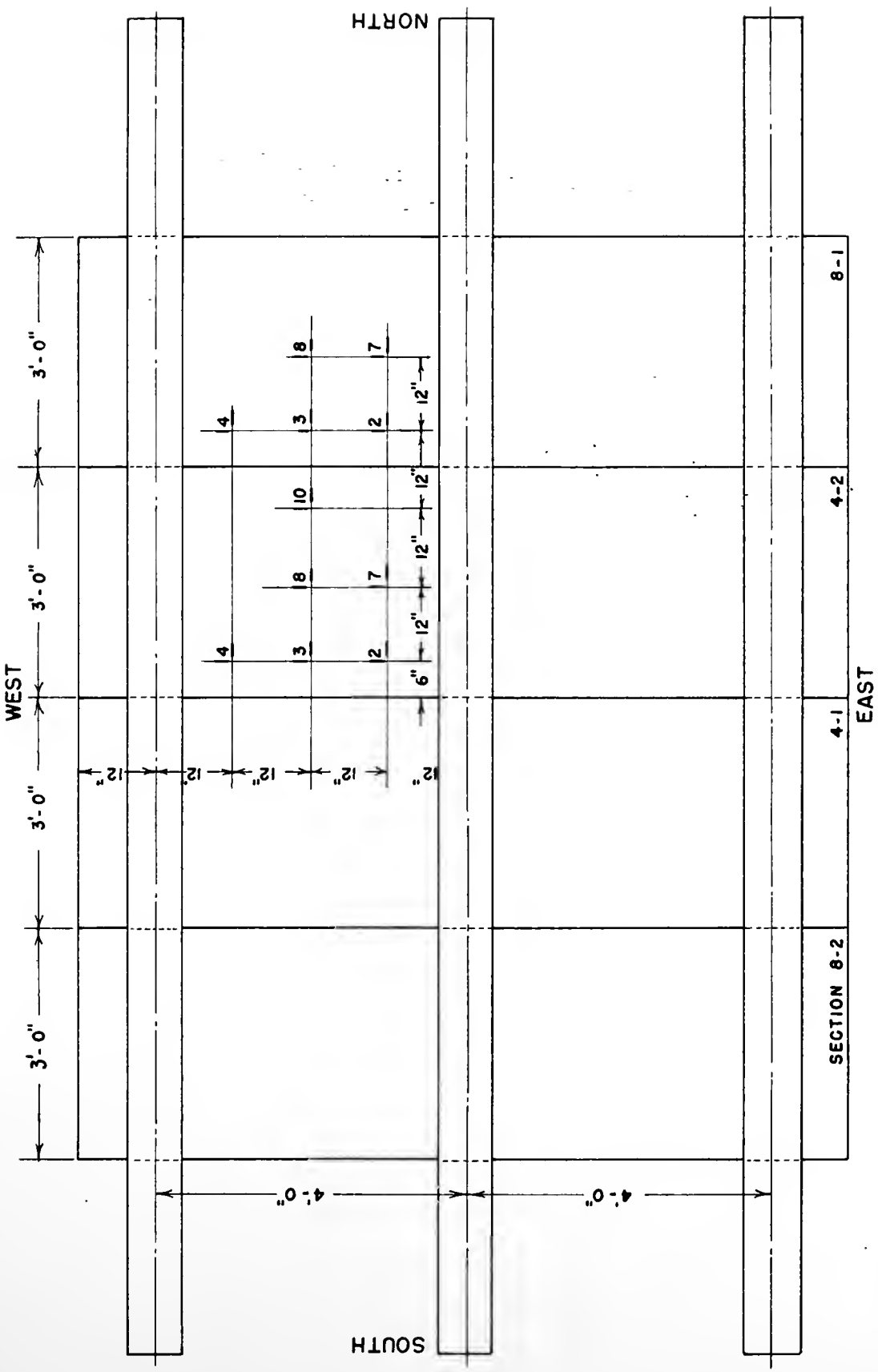

FIGURE 57. STRAIN GAGE LOCATIONS ON BOTTOM SURFACE, STATIC TEST, 4'-0" BEAM SPACING

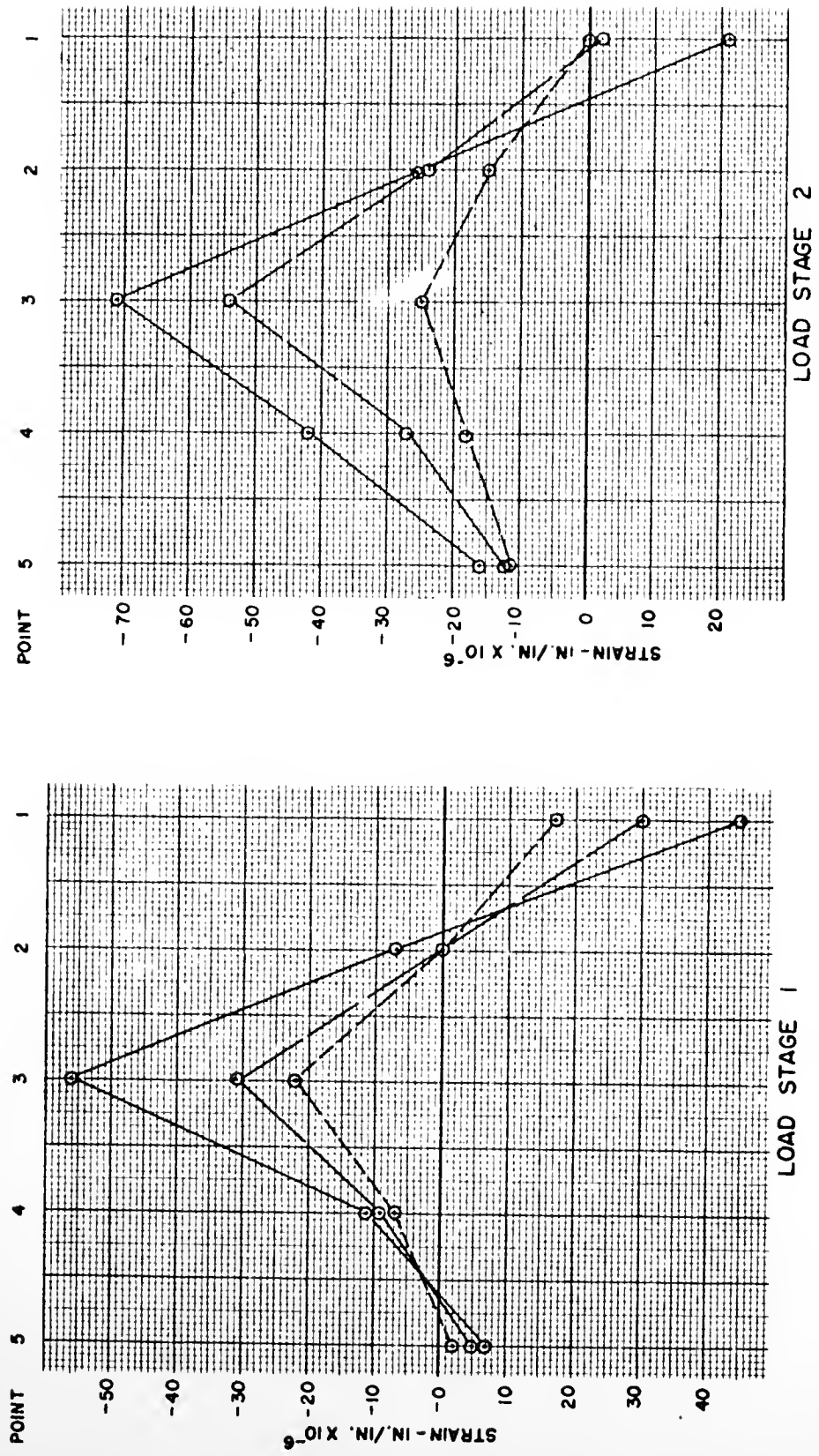

FIGURE 58. TRANSVERSE TOP SURFACE STRAINS, 4'-0" BEAM SPACING, LOAD STAGES 1 AND 2

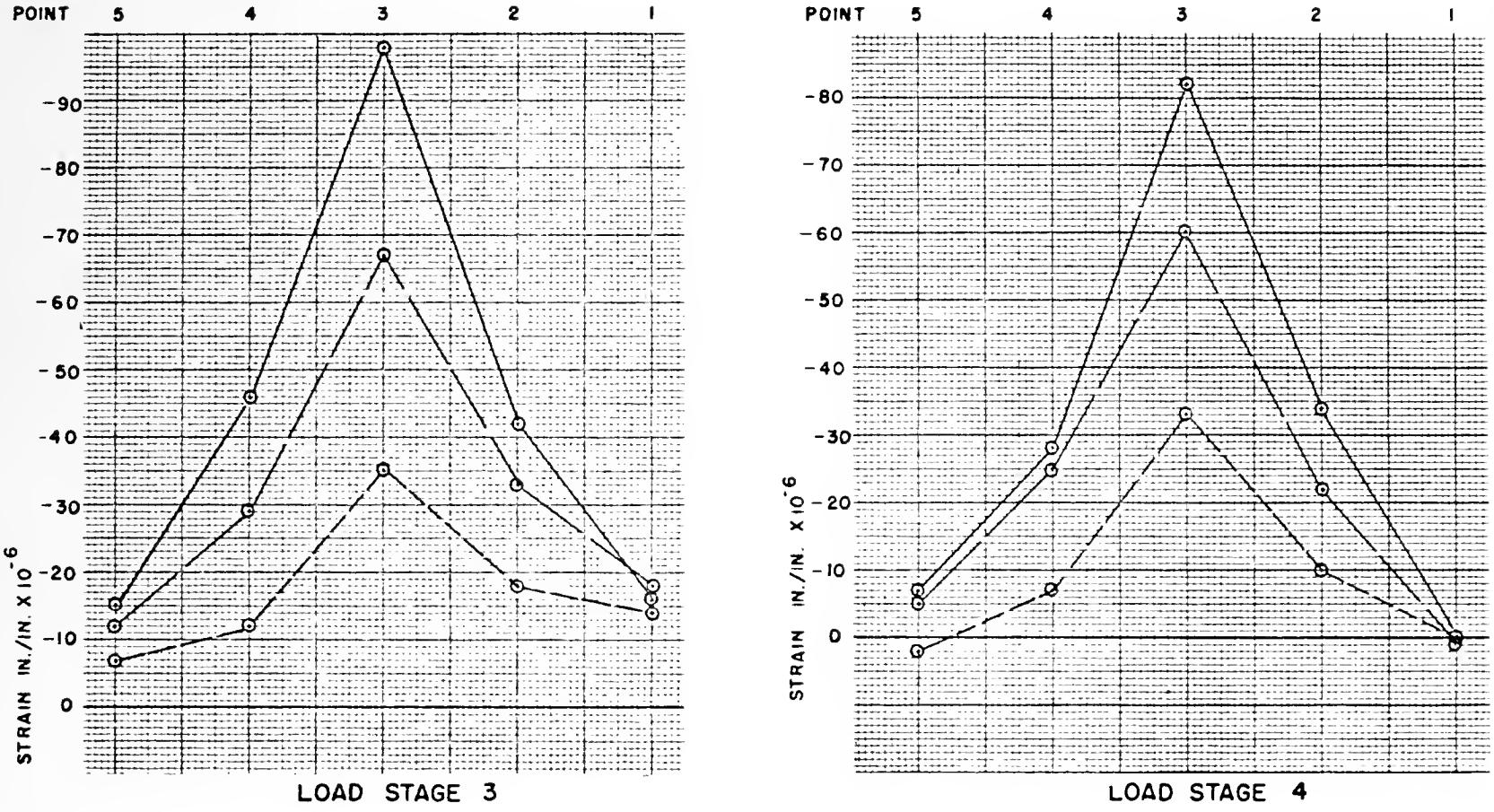

FIGURE 59. TRANSVERSE TOP SURFACE STRAINS, 4'-0" BEAM SPACING, LOAD STAGES 3 AND 4

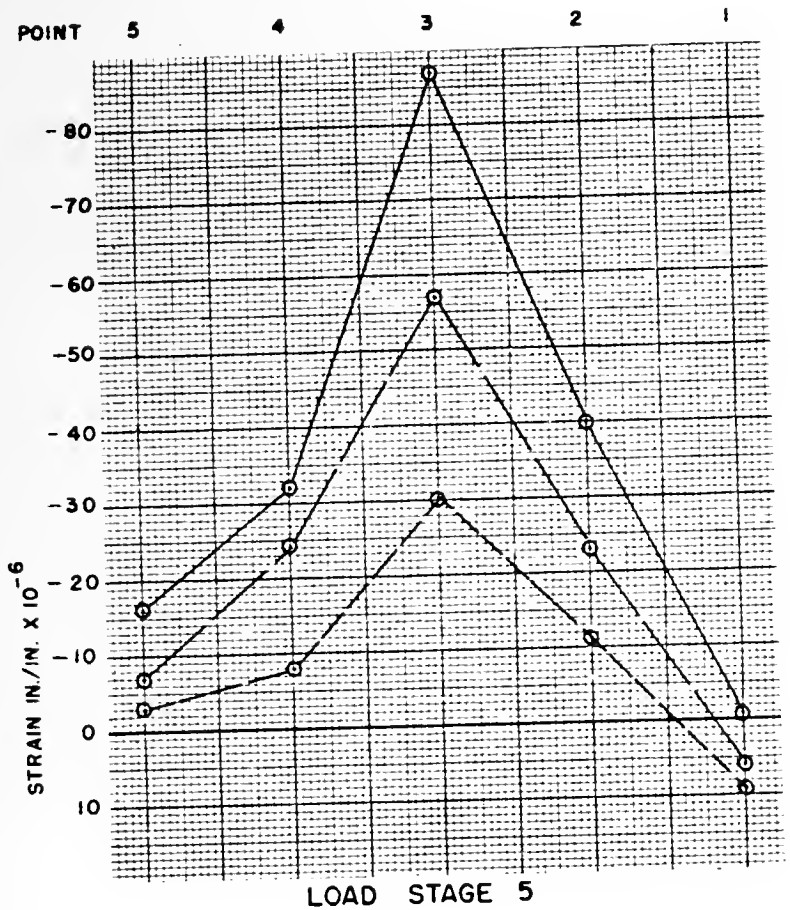

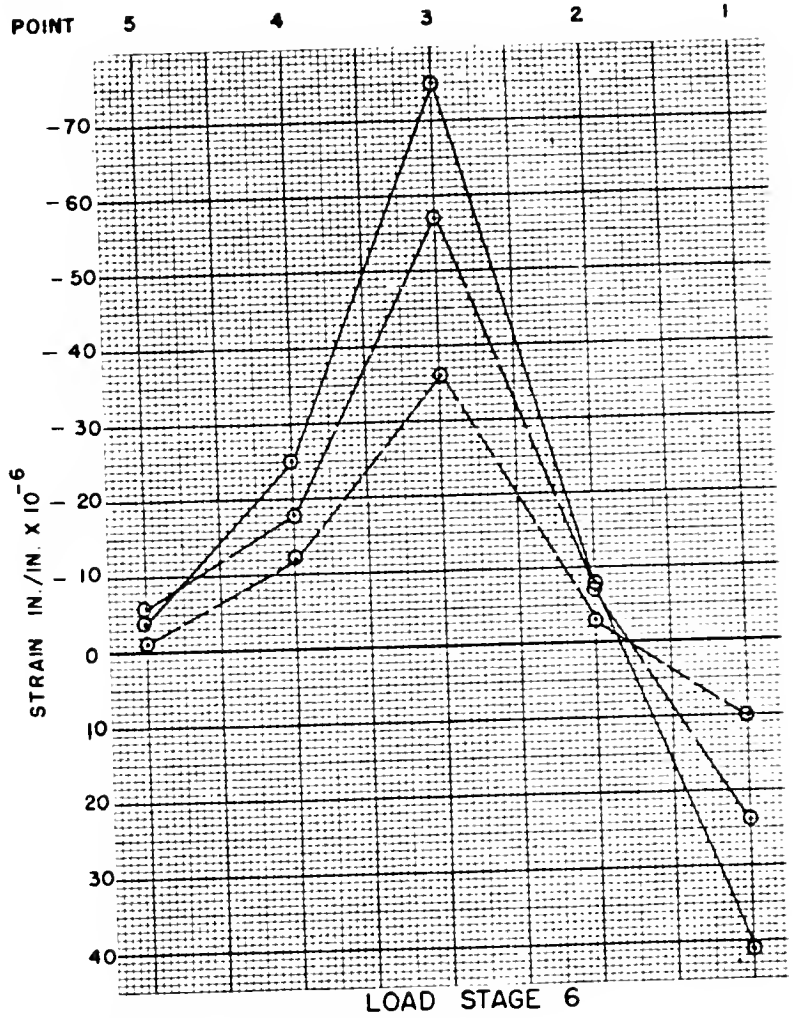

KEY: P= 5,040 LB — — — —, P= 10,080 ——— ———, P= 15,120 LB ———

(-) COMPRESSION (+) TENSION

FIGURE 60. TRANSVERSE TOP SURFACE STRAINS, 4'-0" BEAM SPACING, LOAD STAGES 5 AND 6

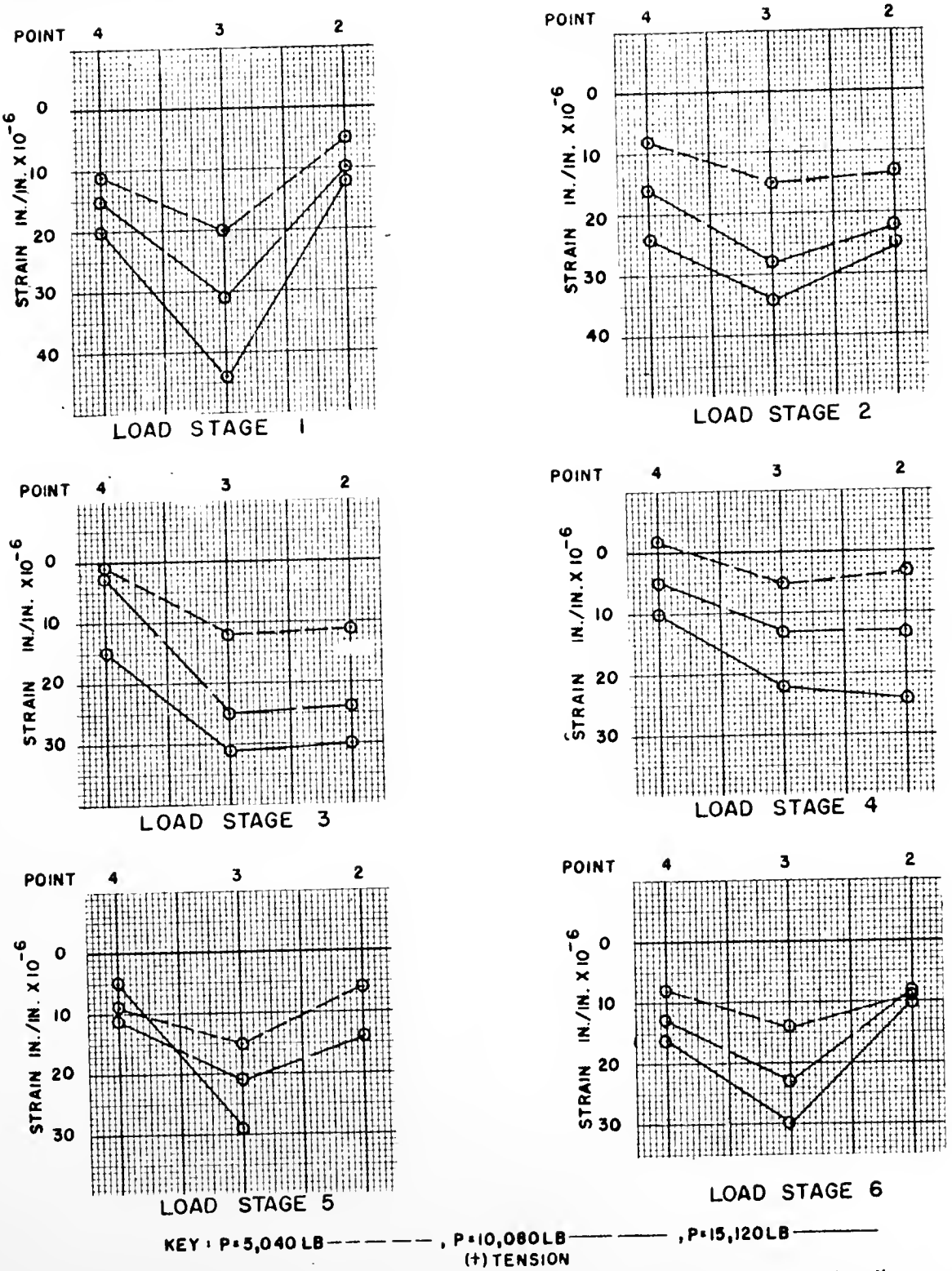

FIGURE 61. TRANSVERSE BOTTOM SURFACE STRAINS, 4'-0" BEAM SPACING, ALL LOAD STAGES

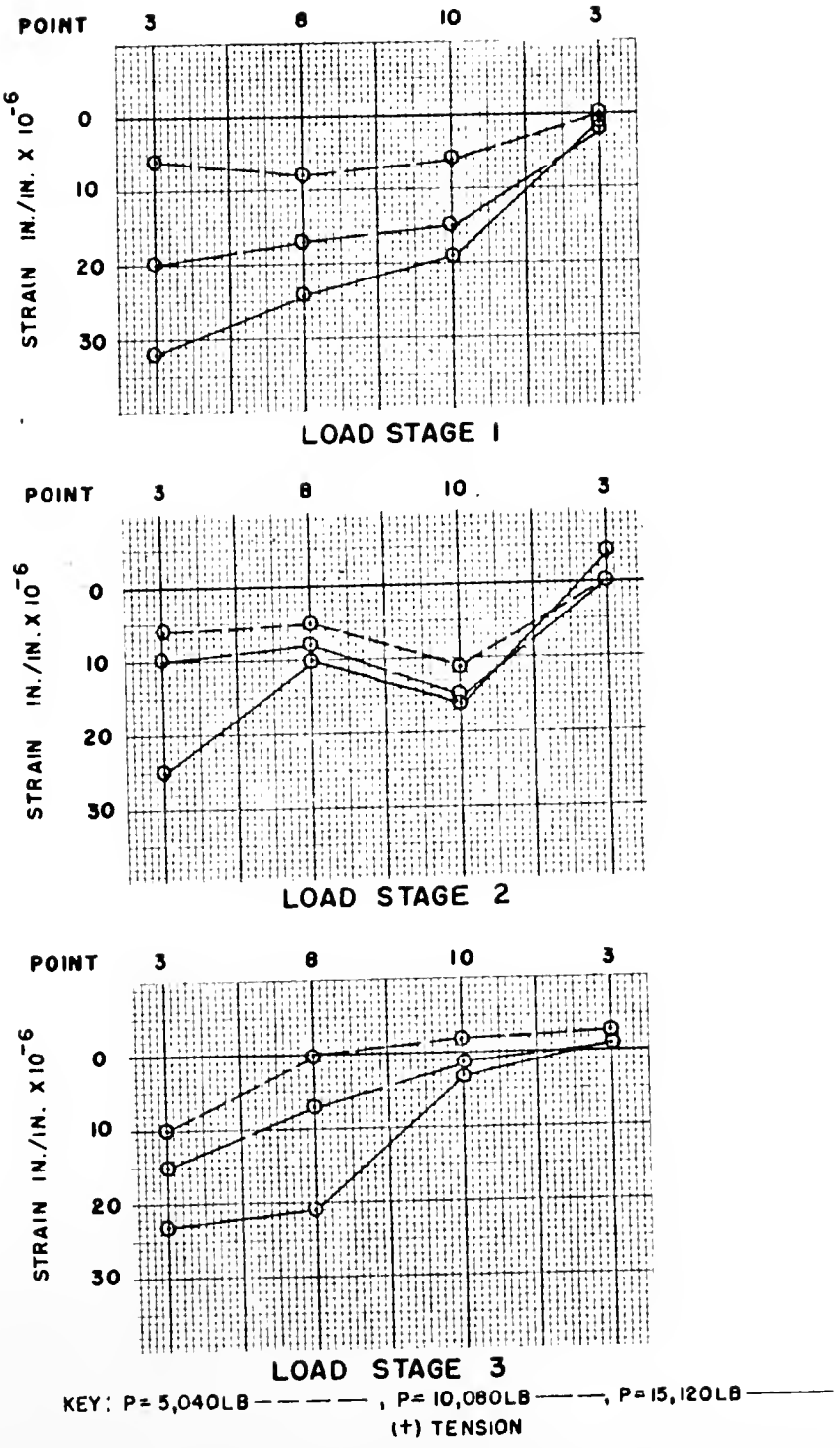

FIGURE 62. LONGITUDINAL STRAIN MEASURED ON LONGITUDINAL CENTER LINE, 4'-0" BEAM SPACING, LOAD STAGES 1,2, AND 3, TOP SURFACE

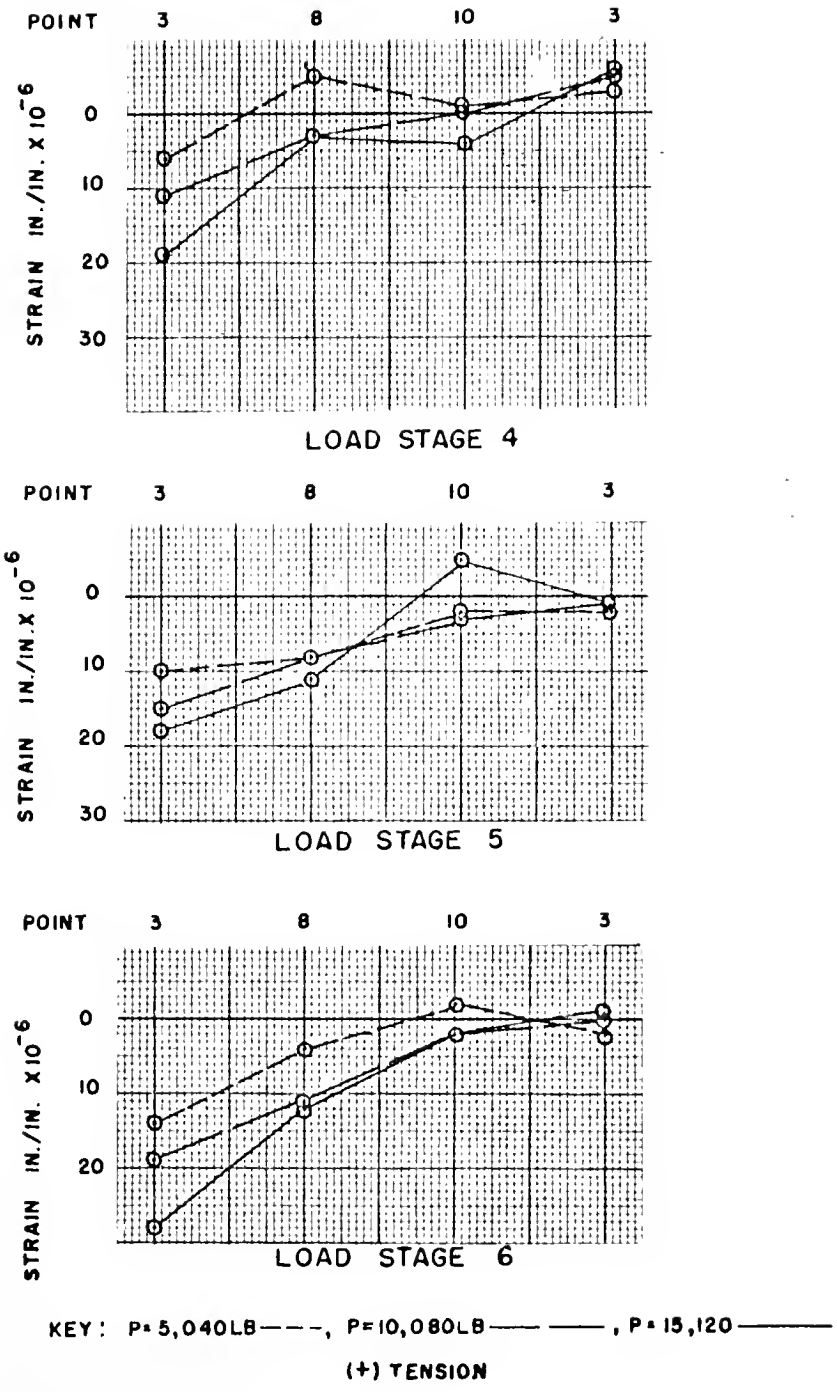

FIGURE 63. LONGITUDINAL STRAIN MEASURED ON LONGITUDINAL CENTER LINE, 4'-0" BEAM SPACING, LOAD STAGES 4,5, AND 6, TOP SURFACE

true for transverse as well as longitudinal line deflections. The decrease is most likely attributed to an increased continuity action caused by pulling the slabs and beams together by bolting.

Strain readings indicated a very small participation in load carrying by deck sections more than one section away from the load point. Near the load point, top and bottom strains varied significantly in that the bottom surface strains were of smaller magnitude. Examination of the top and bottom transverse strains at points 3, 8, and 10 would indicate that the discrepancy is greatest near the loaded joint and that strains somewhat more distant from the joint vary nearly linearly through the slab as would be predicted. One would not necessarily predict agreement between top and bottom strains due to the possibility of eccentricity of the prestressing strand. Owing to the outward appearance of the slabs reinforced for 4'-0" beam spacing upon their delivery, (see Figure 33) it is evident that a loss in bond between the prestressing strand and the concrete might have caused the non-linear strain distribution. The top surface showed signs of distress along the prestressing strand with a definite crack pattern in evidence. The bottom strands were more likely well bonded as no cracking was observed. This is in line with the high top surface strains and the low bottom surface strains which were measured.

Strains shown may be translated to stresses by multiplying the indicated strain by the modulus of elasticity of 3.86×10^6 psi.

Returning to the AASHO equation for bending moment due to live load, $LLM = 0.8 \frac{(S + 2)}{32} P$ where P is the wheel load. If one takes the value of P as the applied load during the test of 15,120 lb, the

LLM becomes 6,390 ft-lb on a 3'-0" section; calculated bending stresses become ± 350 psi. The bending stresses for this load observed in load stages 4 and 5 respectively were 316 psi and 336 psi, measured on the top surface. This would indicate a good predictability of stresses due to live load using the present AASHO equation. The uniform axial prestress of 545 psi (compression) is adequate to maintain the section in compression due to applied load.

Static Testing of Specimens Reinforced for 8'-0" Beam Spacing

Description of Test

The static testing for a beam spacing of 8'-0" was conducted in the same manner as the previous test for the 4'-0" beam spacing. The testing arrangement is shown in Figures 64 and 65. Loads and strains were determined as in the previous test, and deflection measurements were similarly made.

The deflection data are indicated in Figures 66 thru 68. Deflections which were measured may be found in Appendix B, Table 16. An error in the zero reading of the points above the supports on the transverse line was apparently made, as the data would indicate more deflection at the point of support than at points closer to the load and for that reason no figures appear to illustrate transverse line deflections. The load stages for the test are shown in Table 15, with bolting locations shown in Figure 66.

Results

The largest deflections observed occurred under the highest post-tensioning level; this was also true in the case of the 4'-0" beam

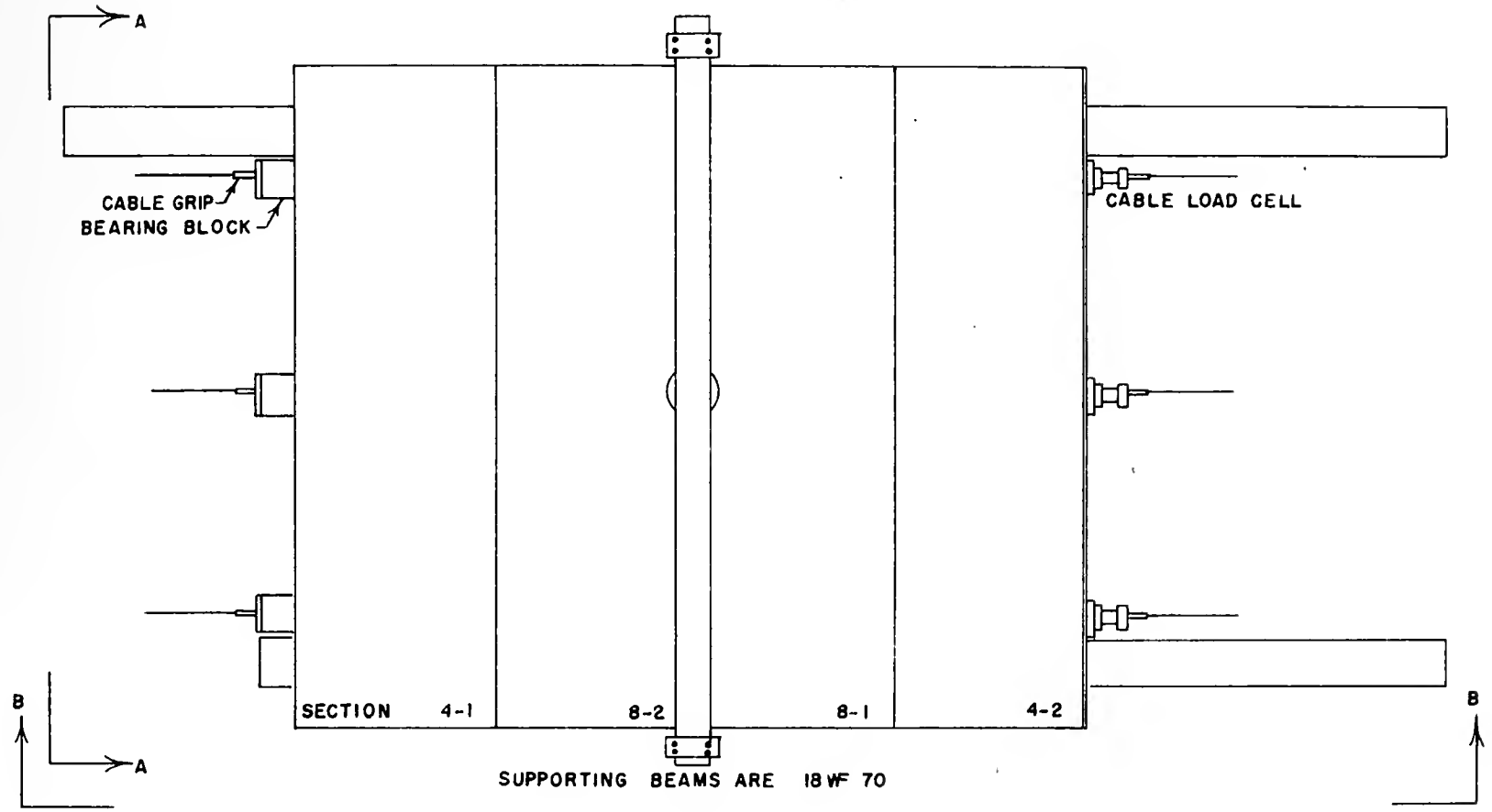

FIGURE 64. PLAN VIEW OF STATIC TEST FOR SECTIONS REINFORCED FOR 8'-0" CENTER-TO-CENTER BEAM SPACING

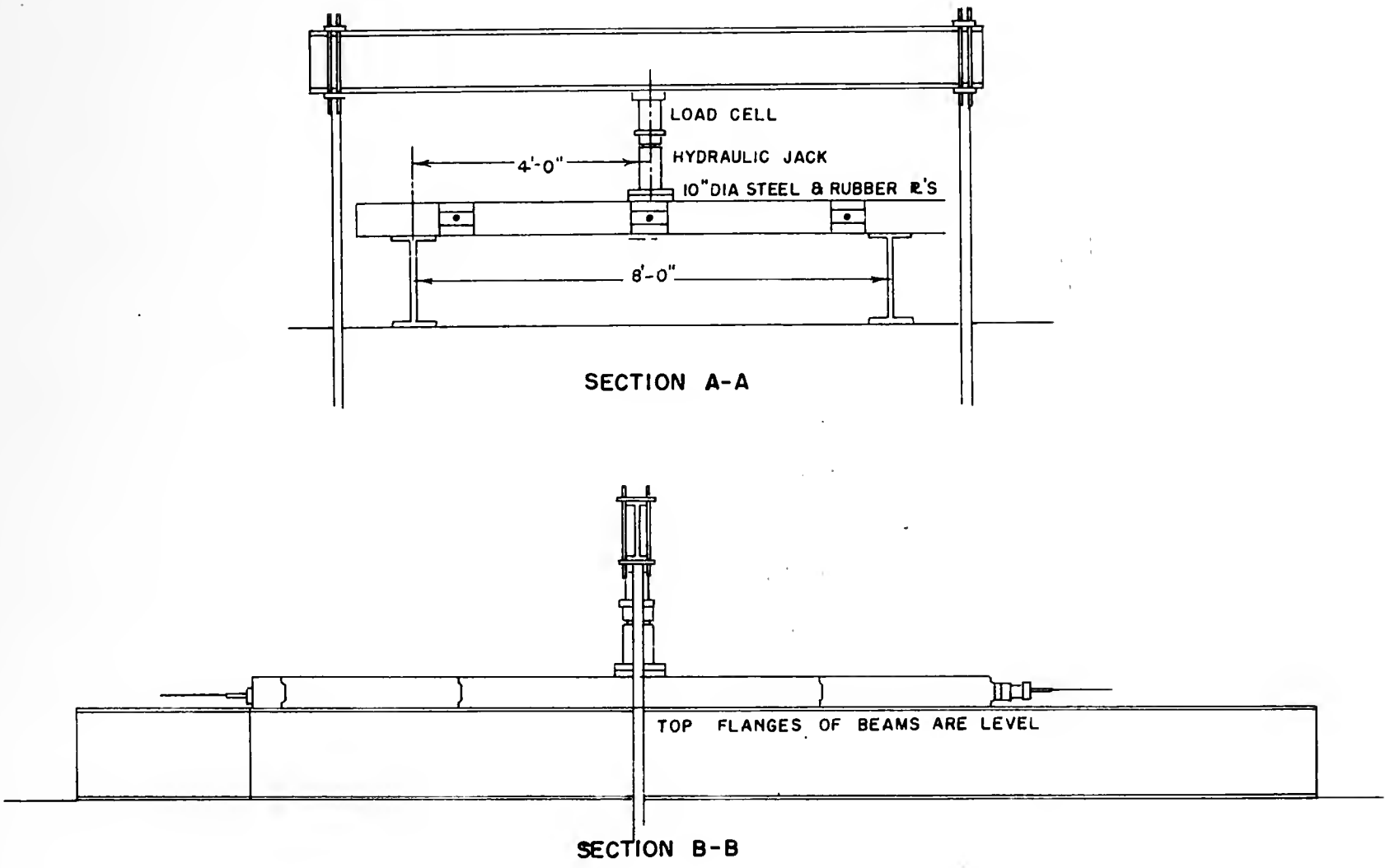

FIGURE 65. SECTIONS A-A AND B-B, STATIC TEST WITH 8'-0" BEAM SPACING

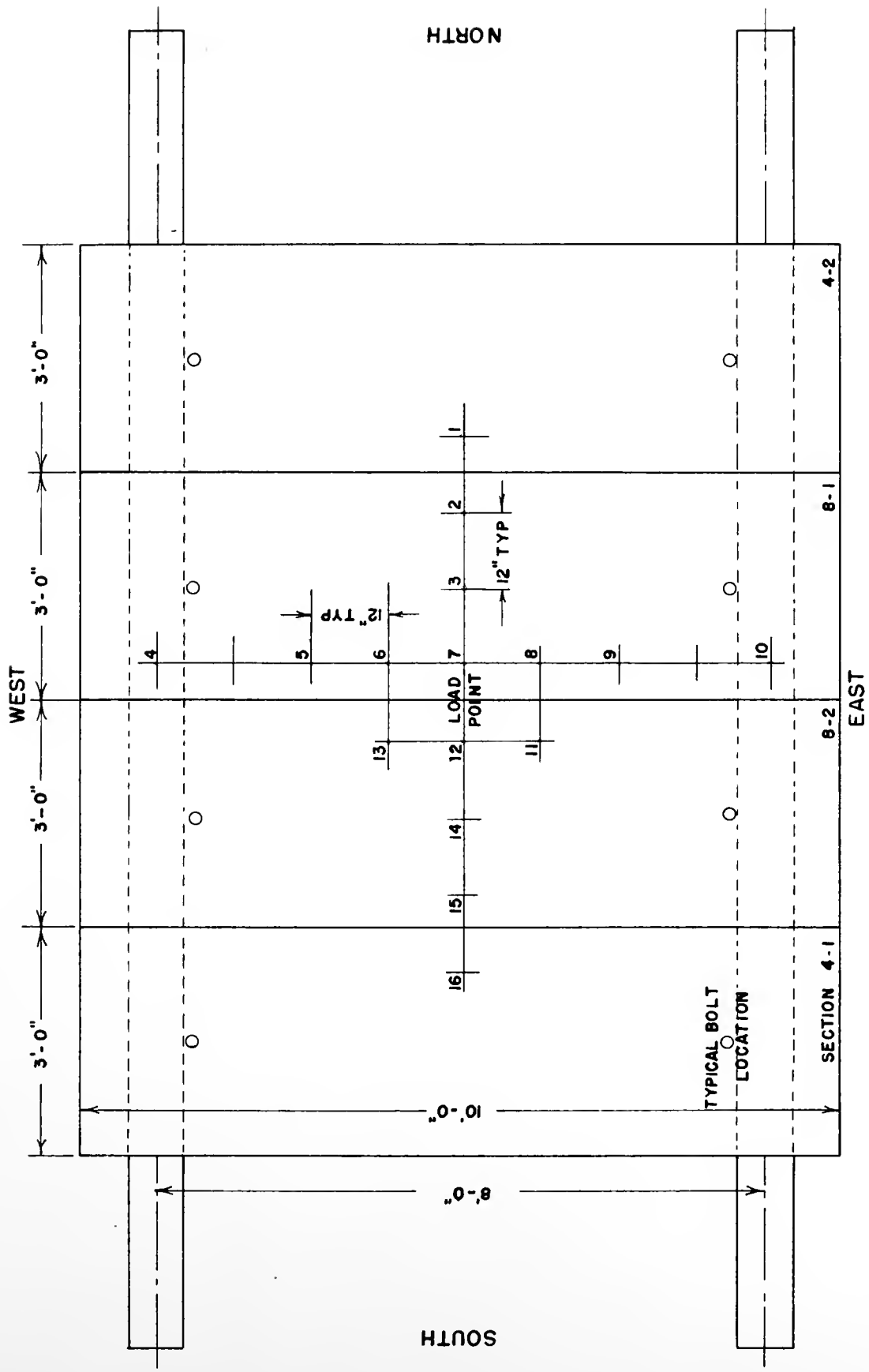

FIGURE 66. LOCATIONS OF DEFLECTION MEASUREMENT, STATIC TEST, 8'-0" BEAM SPACING

Table 10. Load Stages During Testing of Sections Reinforced for 8'-0" Beam Spacing

Load Stage	Post-Tensioning (psi on gross section)	Bolting Force (kips)	Applied Load (pounds)
1	19.0	0	5,040
1	19.0	0	10,080
1	19.0	0	15,120
2	36.9	0	5,040
2	36.9	0	10,080
2	36.9	0	15,120
3	36.8	32	5,040
3	36.8	32	10,080
3	36.8	32	15,120
4	20.1	32	5,040
4	20.1	32	10,080
4	20.1	32	15,120

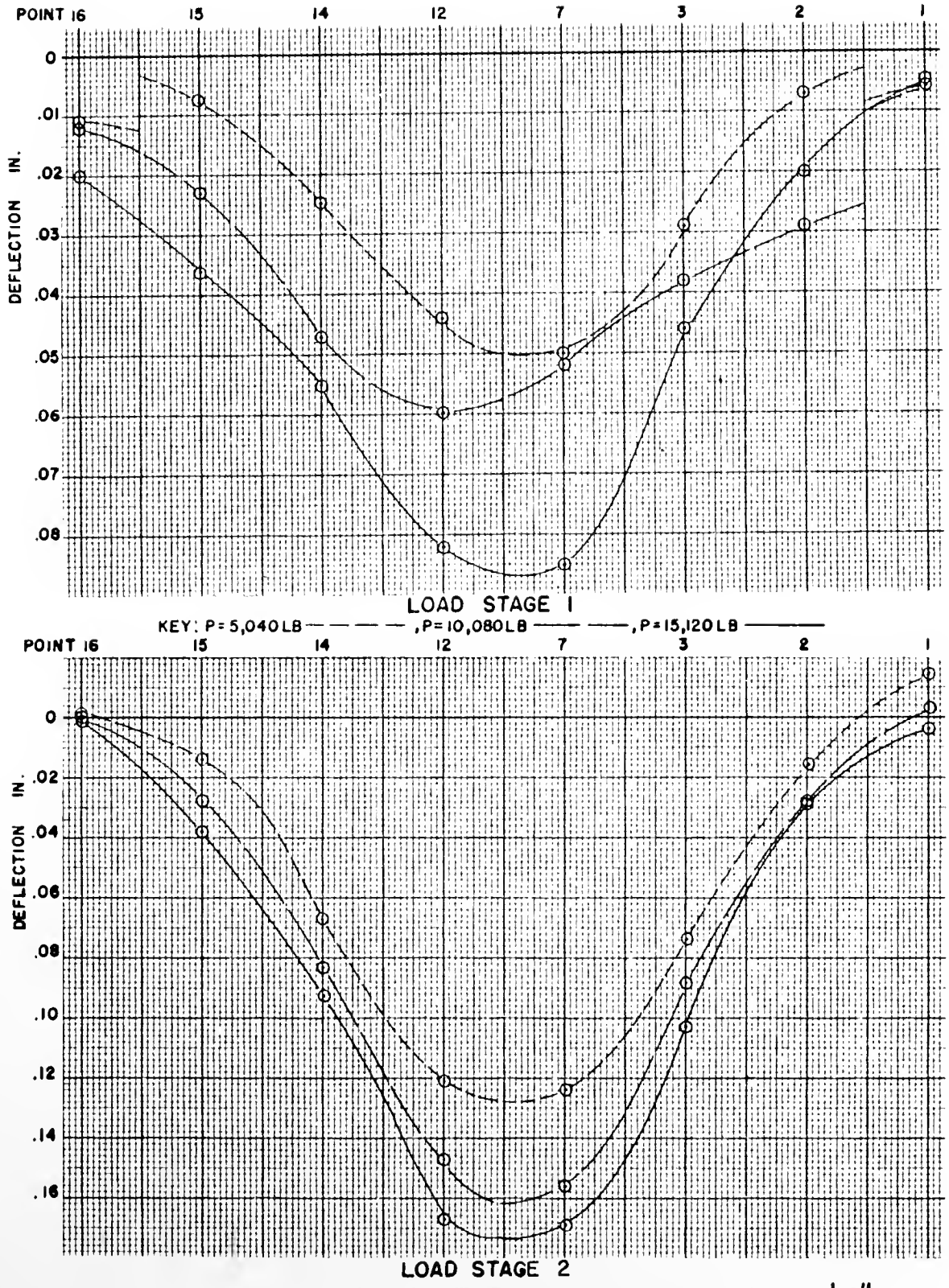

FIGURE 67 .LONGITUDINAL CENTER LINE DEFLECTION, 8'-0" BEAM SPACING, LOAD STAGES 1 AND 2

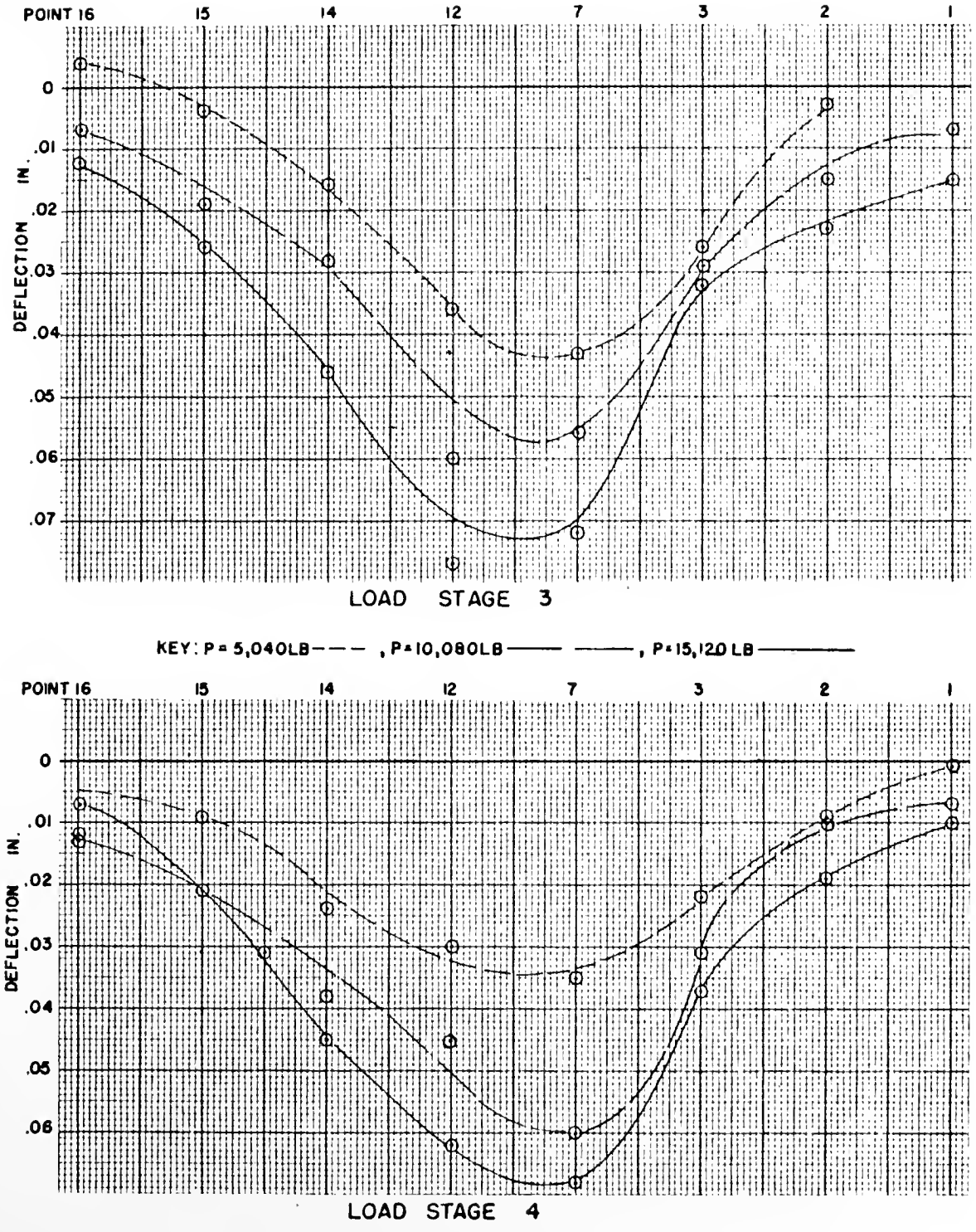

FIGURE 68. LONGITUDINAL CENTER LINE DEFLECTION, 8'-0" BEAM SPACING, LOAD STAGES 3 AND 4

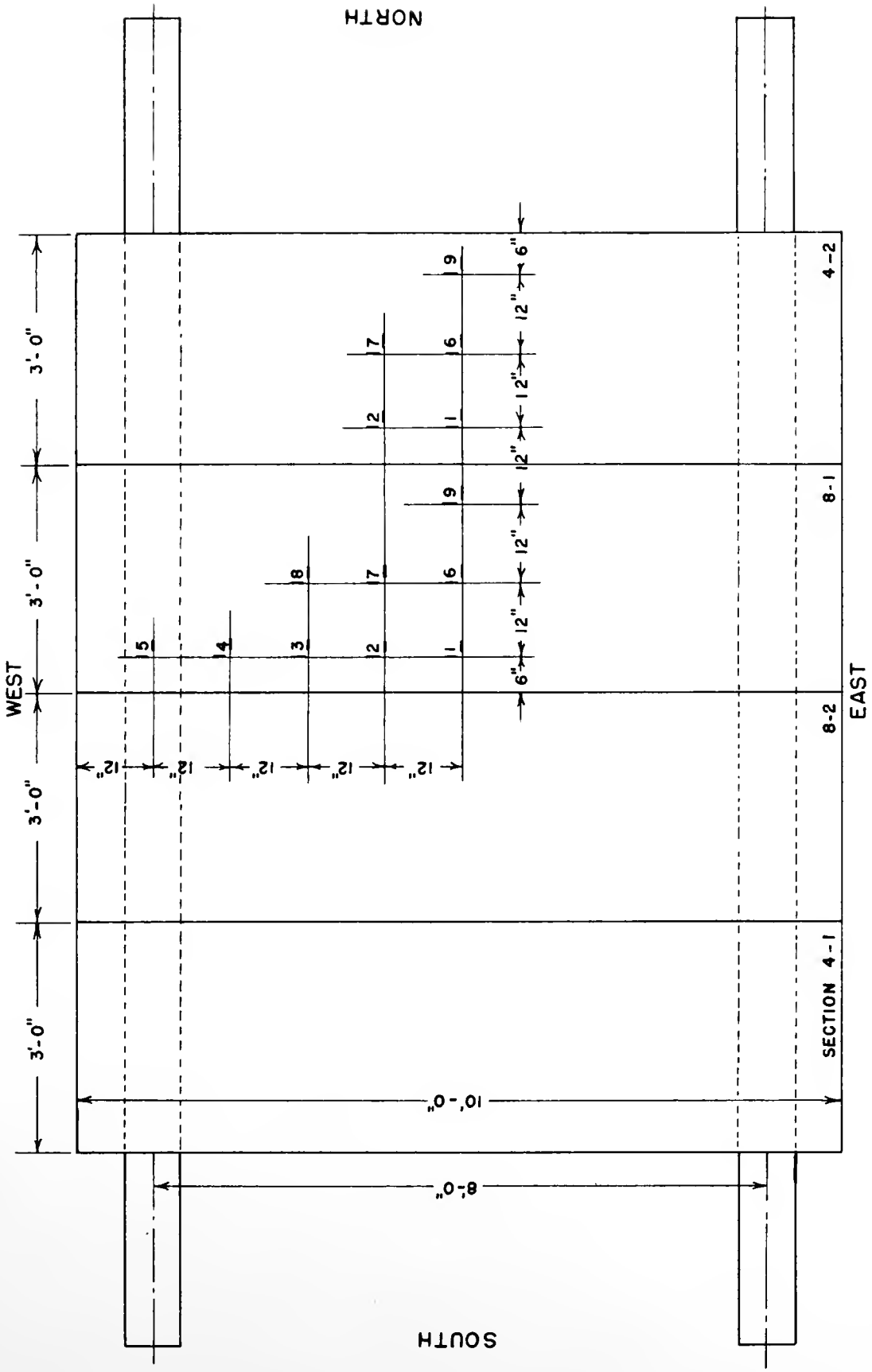

FIGURE 69. STRAIN GAGE LOCATIONS ON TOP SURFACE, STATIC TEST, 8'-0" BEAM SPACING

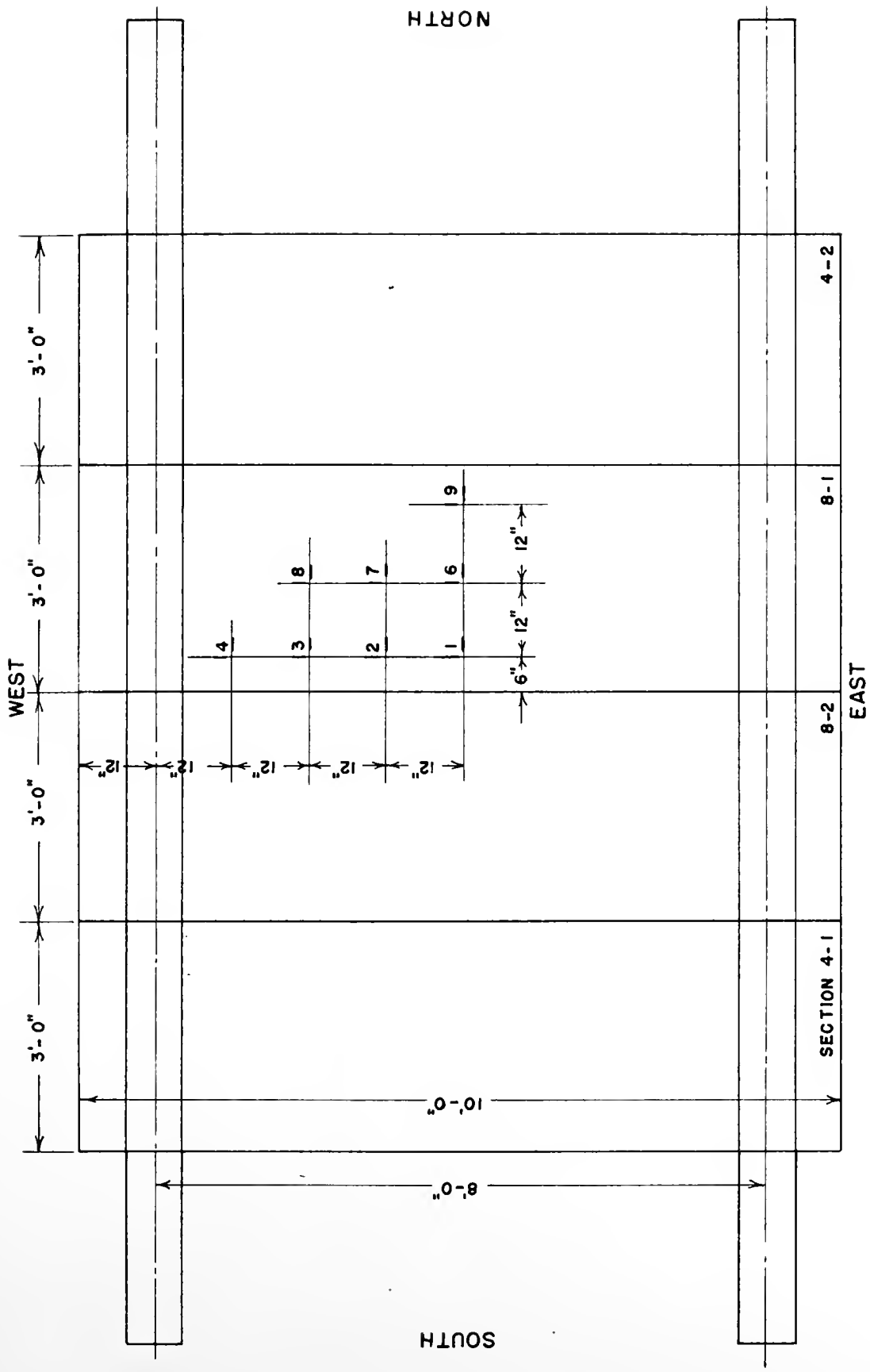

FIGURE 70. STRAIN GAGE LOCATIONS ON BOTTOM SURFACE, STATIC TEST, 8'-0" BEAM SPACING

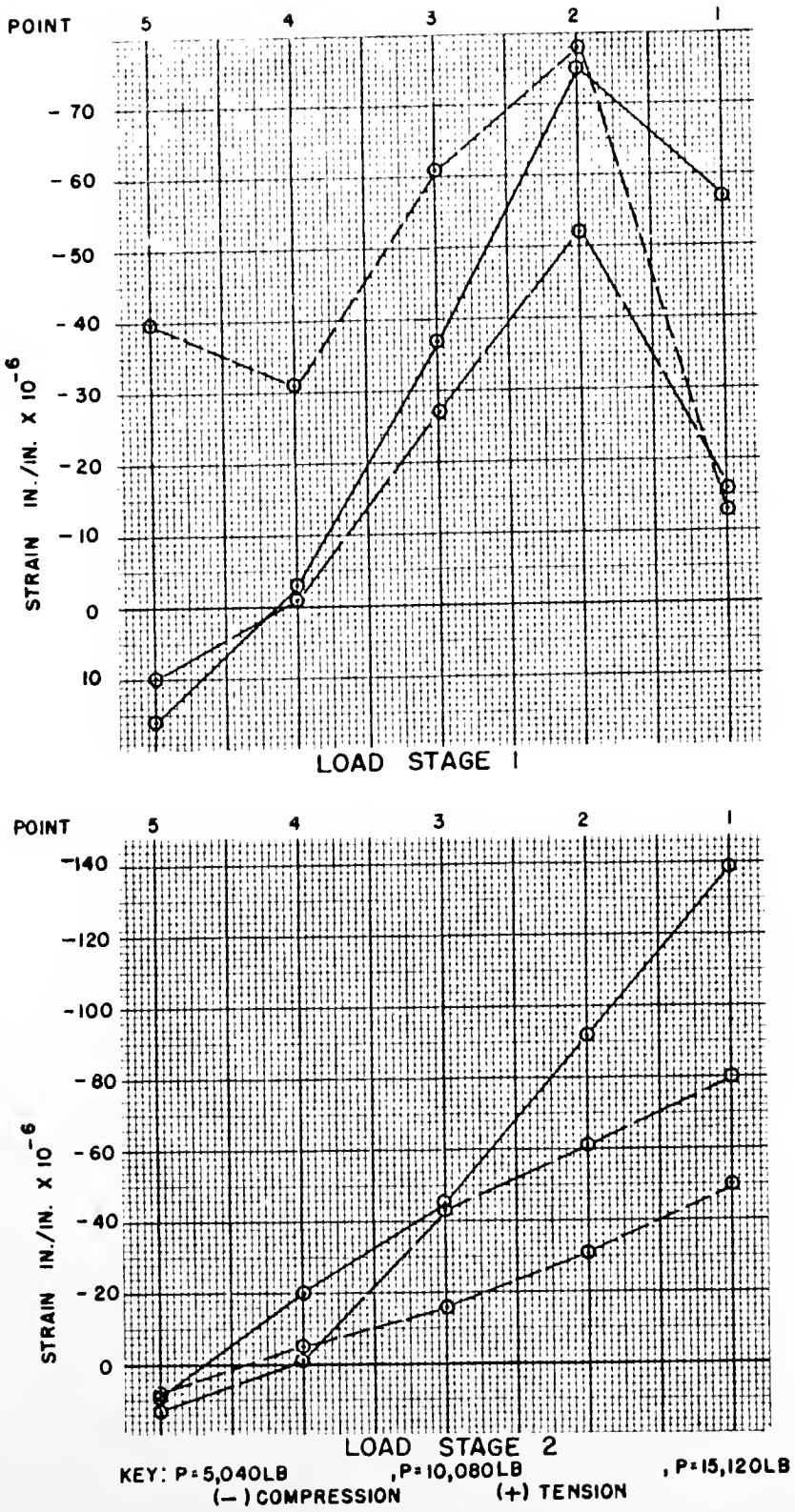

FIGURE 71 . TRANSVERSE TOP SURFACE STRAINS, 8'-0" BEAM SPACING, LOAD STAGES 1 AND 2

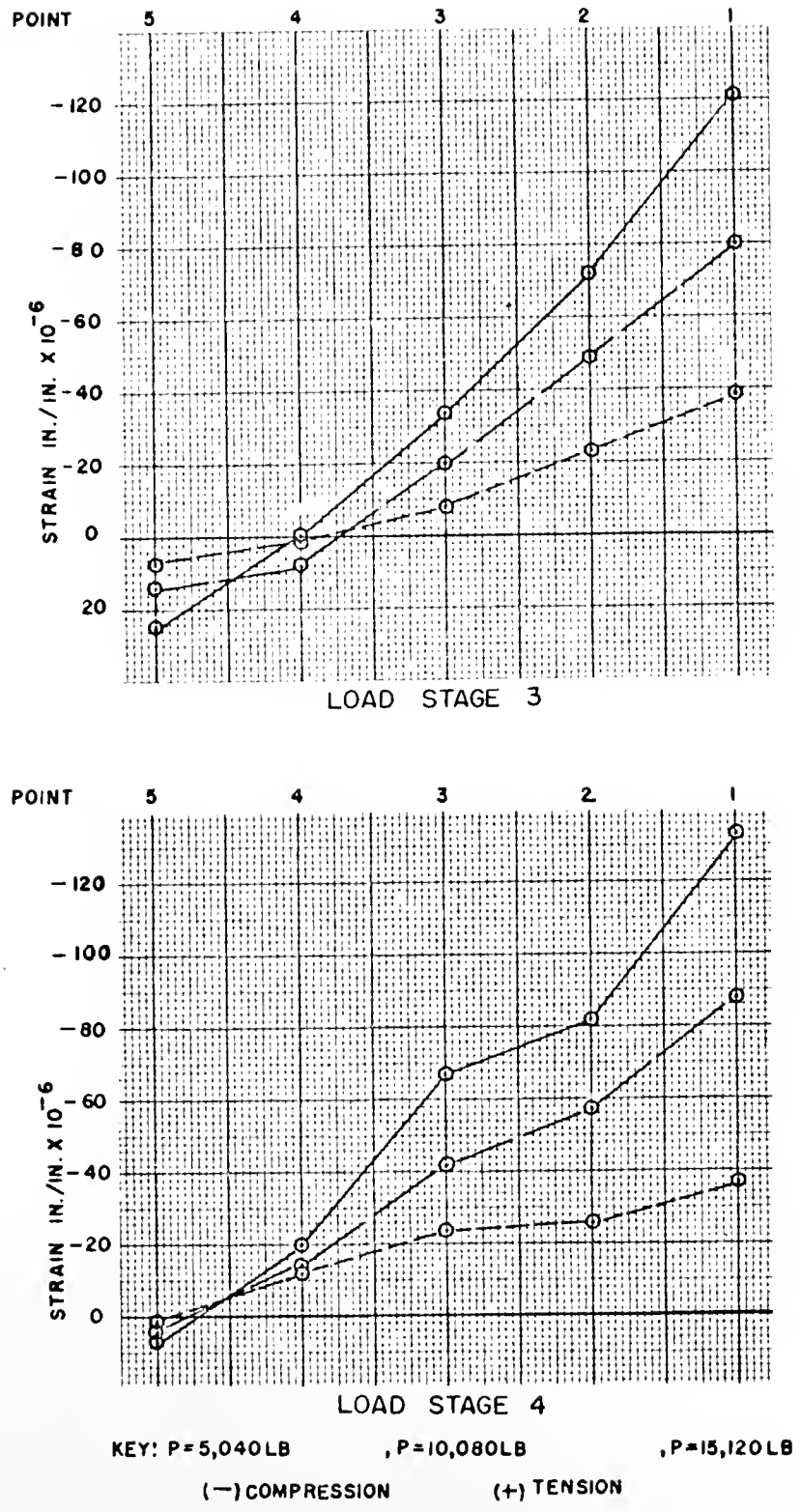

FIGURE 72. TRANSVERSE TOP SURFACE STRAINS, 8'-0" BEAM SPACING, LOAD STAGES 3 AND 4

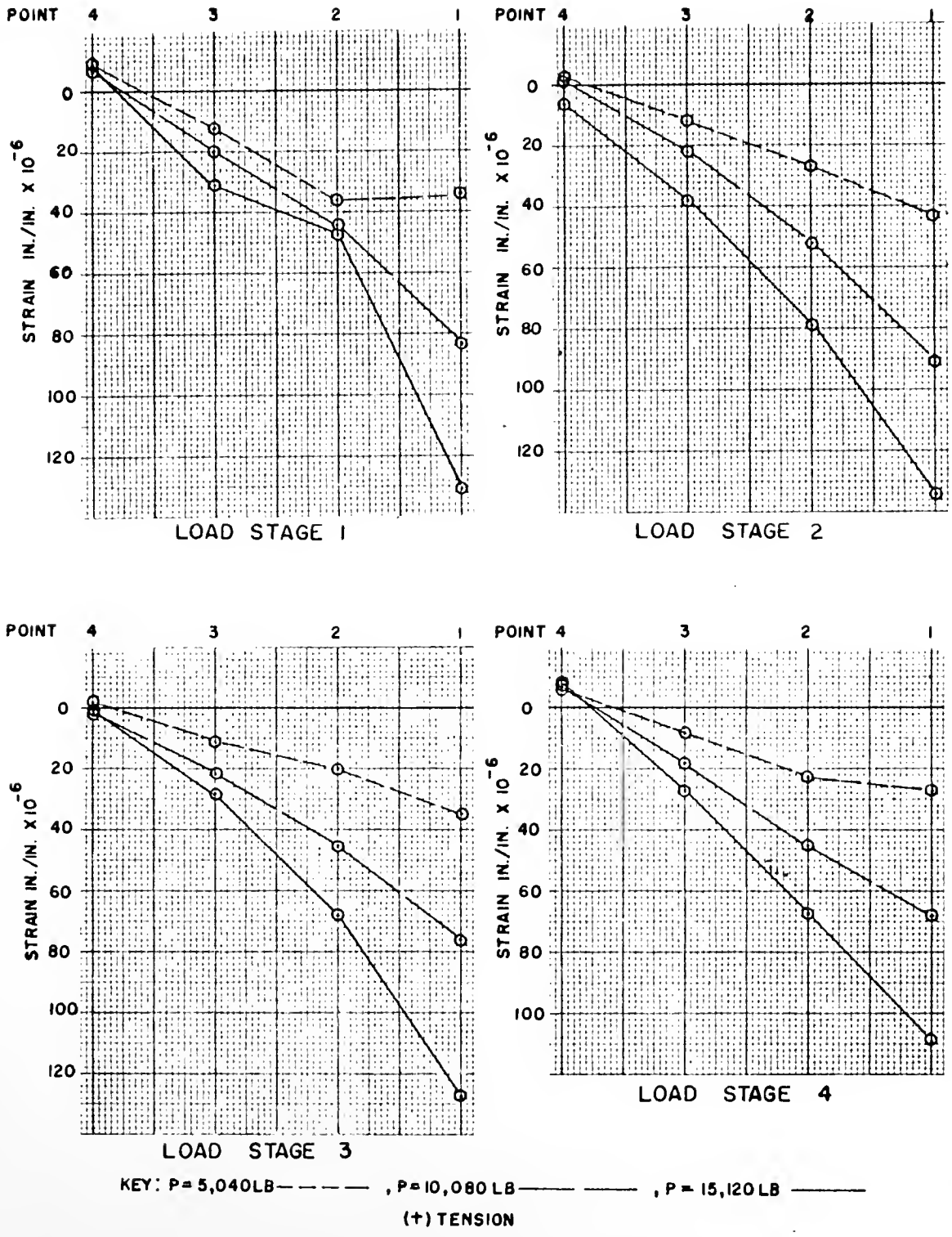

FIGURE 73. TRANSVERSE BOTTOM SURFACE STRAINS, 8'-0" BEAM SPACING, ALL LOAD STAGES

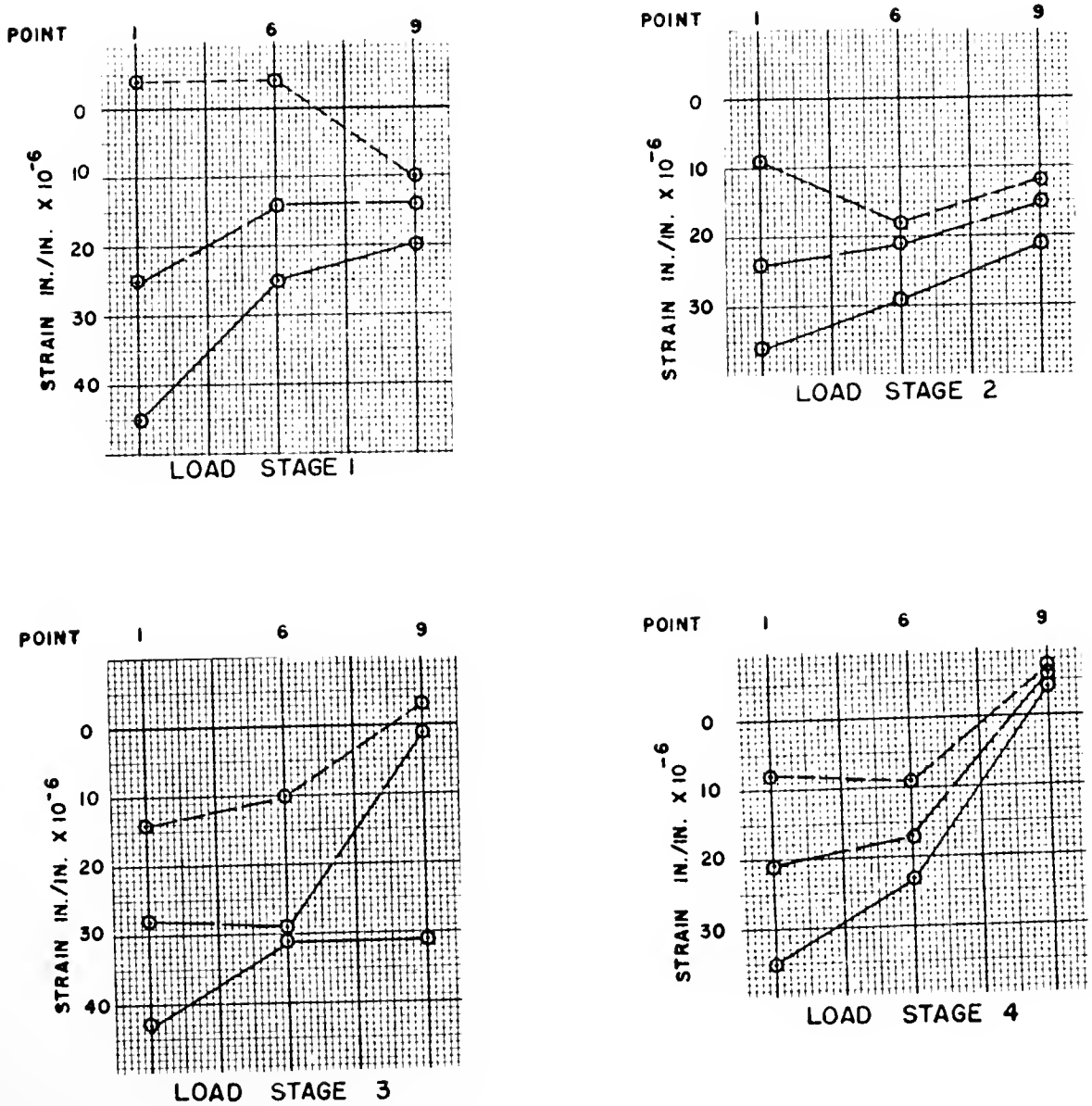

FIGURE 74. LONGITUDINAL STRAIN MEASURED ON LONGITUDINAL CENTER LINE, 8-0 BEAM SPACING, ALL LOAD STAGES, TOP SURFACE

spacing. Continuity over supports does not appear to be responsible for any lessening of this phenomenon, as the specimens on 4'-0" beam spacing were essentially continuous and the beams at 8'-0" nearly approximated a simple support.

Bolting had the effect of lessening deflections by as much as 50% at the same level of post-tensioning stress. In all cases, bolting decreased the deflection due to applied load.

Strain data indicated participation of sections more than one section distant from the load only to a minor degree. Strain magnitudes were very low on the sections thus located and it is possible that the observed strains were due to causes other than bending such as a temperature change.

Good agreement was observed between top and bottom strain gages at the same point in plan and a nearly linear strain distribution through the slab was observed (compare Figures 71 and 72 to Figure 73). This phenomenon would indicate a well manufactured product of uniform or very nearly uniform prestress, unlike the specimens reinforced for 4'-0" beam spacing reported above which definitely showed a non-linearity of strain distribution.

Strains shown may be translated to stresses by multiplying by the modulus of elasticity for the section of 3.65×10^6 psi.

Using the AASHO equation for live load moment $LLM = \frac{S + 2}{32} P$ where P is the wheel load. Again using the maximum applied load of 15,120 pounds for P, LLM = 13,650 ft-lb on the 3 foot section. Stresses become ± 740 psi contrasted to an observed 441 psi and 464 psi observed in load stages 4 and 5. This is probably due to the fact that some

continuity is provided by bolting at the support and due to participation in load carrying by a larger portion of the deck (note the longitudinal center line deflections of Figure 68) than the assumed 3'-0" section, indicating a plate action as opposed to a shallow beam action. The applied uniform prestress of 935 psi (compression) is sufficient to maintain the section in compression under applied load.

TESTING OF PRESTRESSED SPECIMENS UNDER REPEATED LOAD

Repeated Load Test With 8'-0" Beam Spacing

Testing Procedure

The testing arrangement for the repeated load test is shown in Figures 75, 76, and 77. The supporting beams were spaced at 8'-0" center-to-center of web and were simply supported with a 20'-0" span on the laboratory floor. The two interior slab sections were reinforced for an 8'-0" beam spacing and the two outside sections were reinforced for a 4'-0" beam spacing. Centers of the load points were spaced at 18 inches, nine inches on either side of the center joint.

Load Application. Load was applied on alternating sides of the center joint at a rate of 250 cycles per minute to approximate the passing of a wheel over the joint. The system of jacks used to supply the load is illustrated in Figures 76 and 77. In Figure 76, Jack 1 was connected to an Amsler Dynamometer with which a constant load was maintained. Jacks 2 and 3 were connected to another machine, an Amsler pulsator, which supplied a sinusoidally varying load. The pulsator was set with a maximum of 9 kips and a minimum of 1 kip while the dynamometer was set with a constant load of 10 kips.

Jacks 1 and 2 were connected with a system of two beams and two rods, as shown in Figures 76 and 77, in order that the load supplied at the load point under jack 1 would be the same as the load supplied under

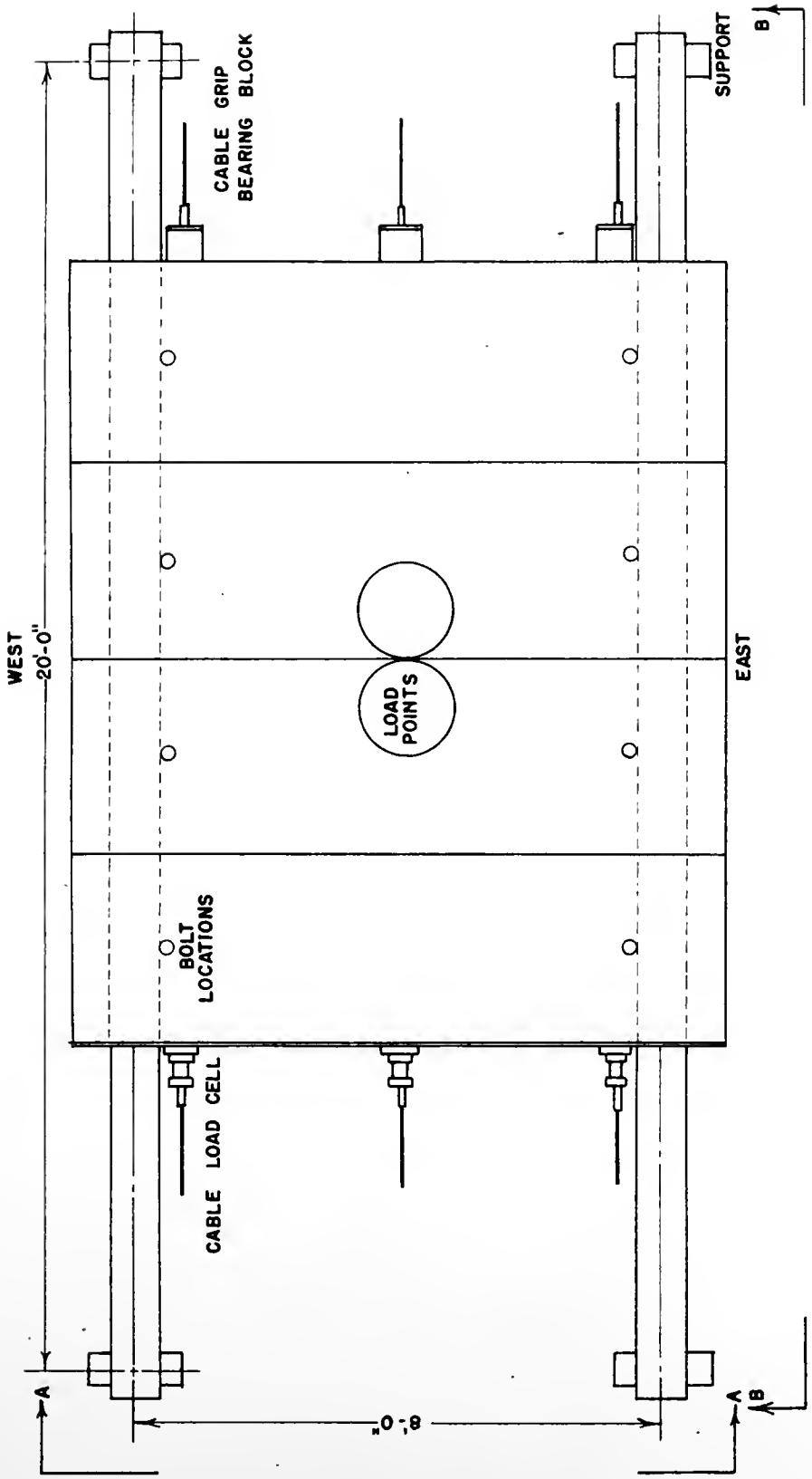

FIGURE 75. TESTING ARRANGEMENT FOR REPEATED LOAD TEST WITH 8'-0" BEAM SPACING

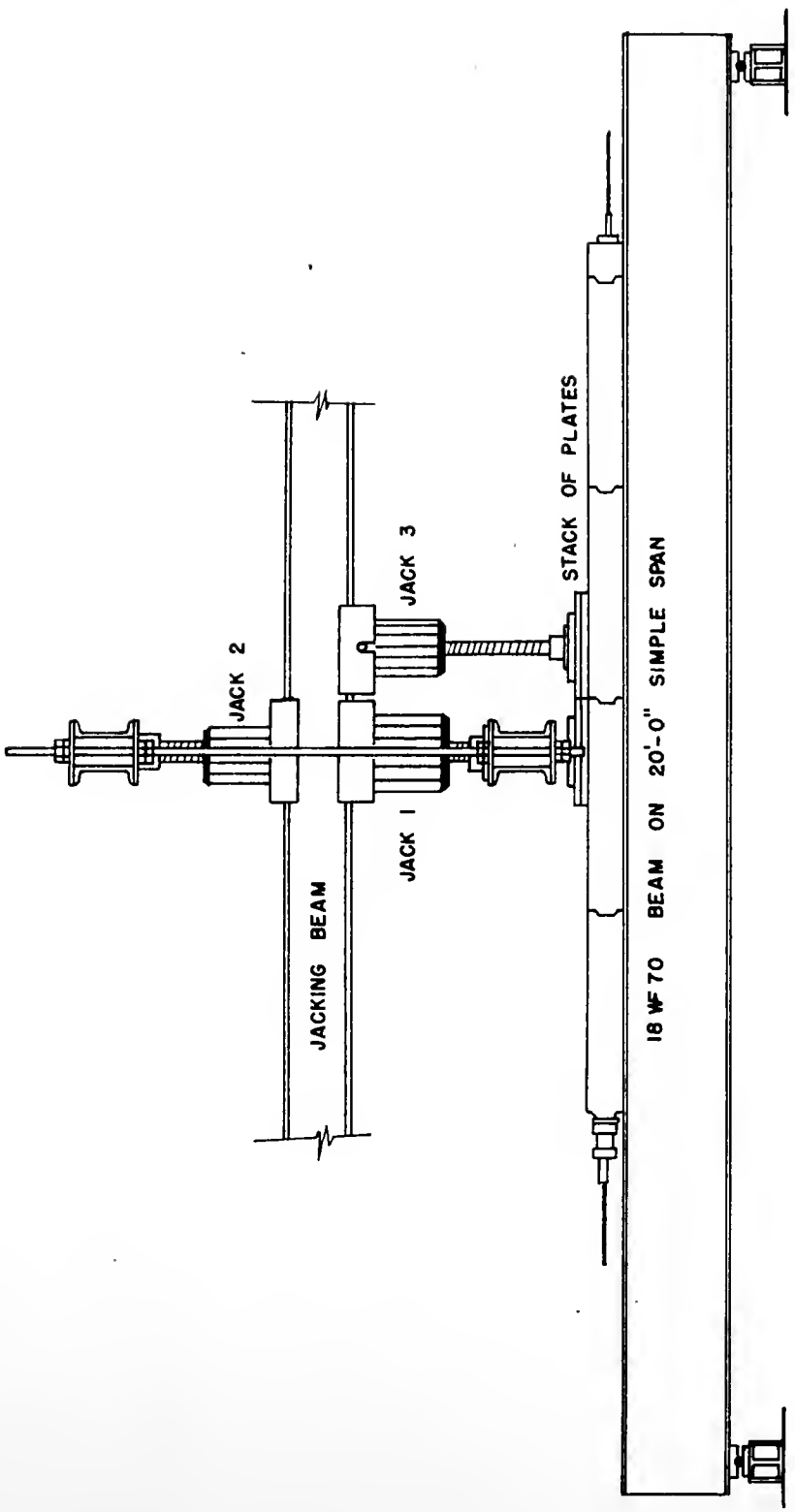

FIGURE 76. SECTION B-B , REPEATED LOAD TEST

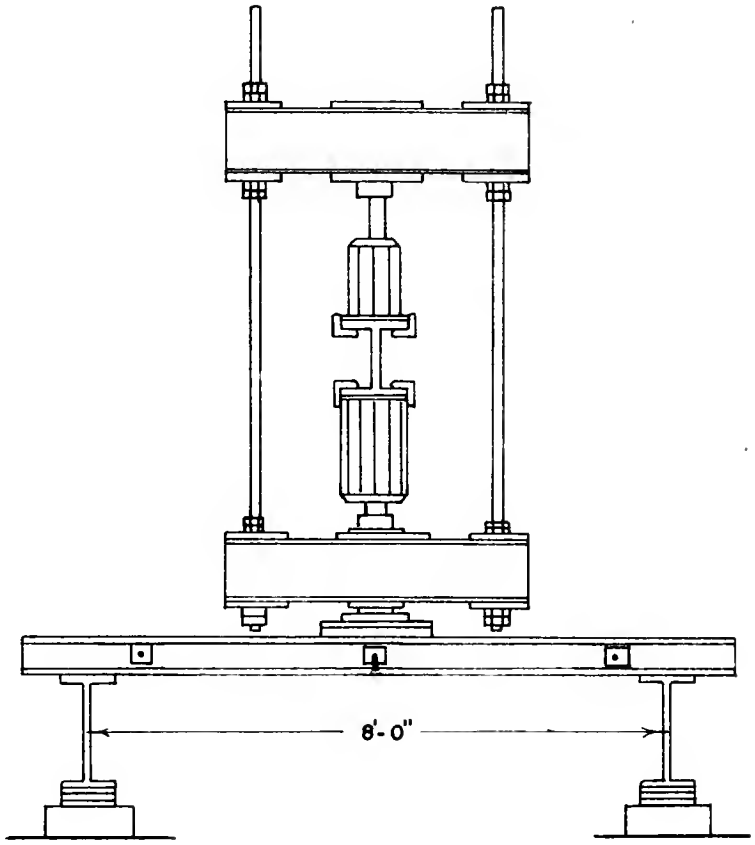

FIGURE 77 . SECTION A-A , REPEATED LOAD TEST , 8'-0" BEAM SPACING

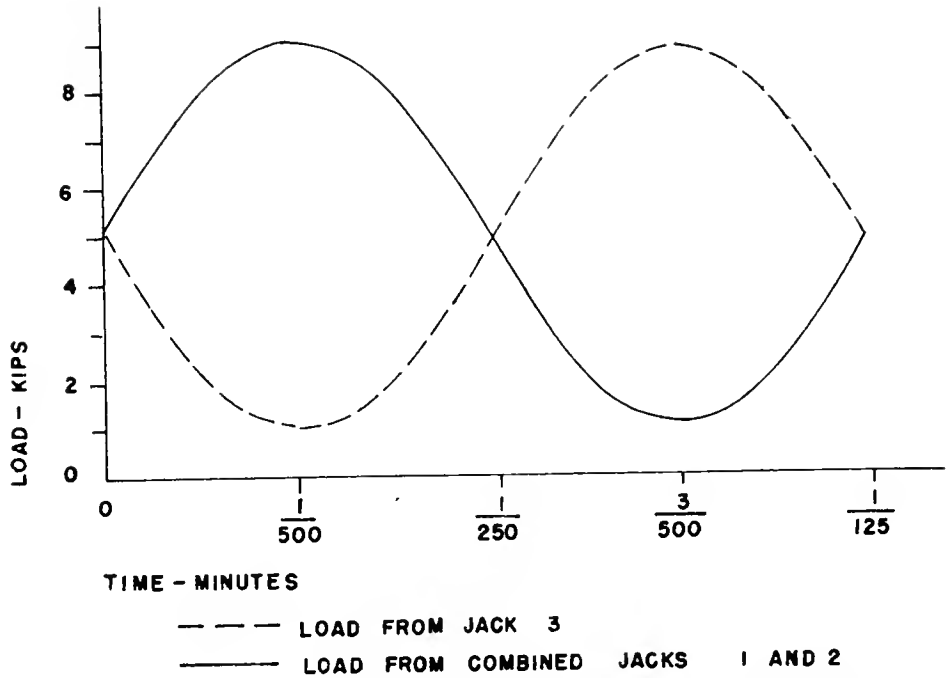

FIGURE 78. LOAD-TIME RELATIONSHIP DURING REPEATED LOAD TEST

jack 3. At the peak of the sinusoidal load supplied by the pulsator to jacks 2 and 3 (9 kips), the effective loads applied on the slab under jacks 1 and 3 were 1 kip and 9 kips respectively (the 10 kip constant load in jack 1 was reduced by the 9 kip load in jack 2 acting in the opposite direction). When the minimum load of 1 kip was supplied to jacks 2 and 3, the loads applied to the slab under jacks 1 and 3 were 9 kips and 1 kip respectively.

Loads were measured by gages which were a part of each machine and were continuously monitored.

The load point consisted of a stack of steel plates of increasing diameter, the largest diameter being 18 inches. The stack of plates rested on an 18 inch diameter 1 inch thick rubber pad.

Loads applied to the post-tensioning cables were measured by the

cable-tension load cells coupled to a strain indicator.

Strain Measurement. Strain gages were used in a one-active-arm Wheatstone bridge circuit, with one adjacent arm of the bridge consisting of a similar strain gage mounted on an unstrained concrete cylinder for compensation.

Strain gages were connected to a switch-and-balance unit and the switch-and-balance unit was connected to a portable strain indicator which supplied power to the bridge circuit. The strain indicator was connected to a strip recorder where the dynamic strain was recorded. The strain indicator, in addition to serving as a power source for the bridge circuit, served as an amplifier for the strain gage signal, and as a calibration instrument for the strip recorder. To make strain readings, the strain indicator was set to zero and activated, and the strip recorder was started. Individual channel outputs were then recorded on the strip recorder by switching to the desired channel on the switch-and-balance unit.

Strain gage application was similar to that described in the static testing and the locations of the strain gages used are shown in Figure 79. Table 22 contains the strain gage results.

Results

The test had been in progress for 32,000 cycles of loading when a large spall occurred at the center joint near the west supporting beam. The spall, shown in Figure 80, was observed to grow along the joint adjacent to the original cracking on the concave side of the joint. The cause of the cracking was a combination of several factors, the foremost being a misfit between the joint faces at the point of failure.

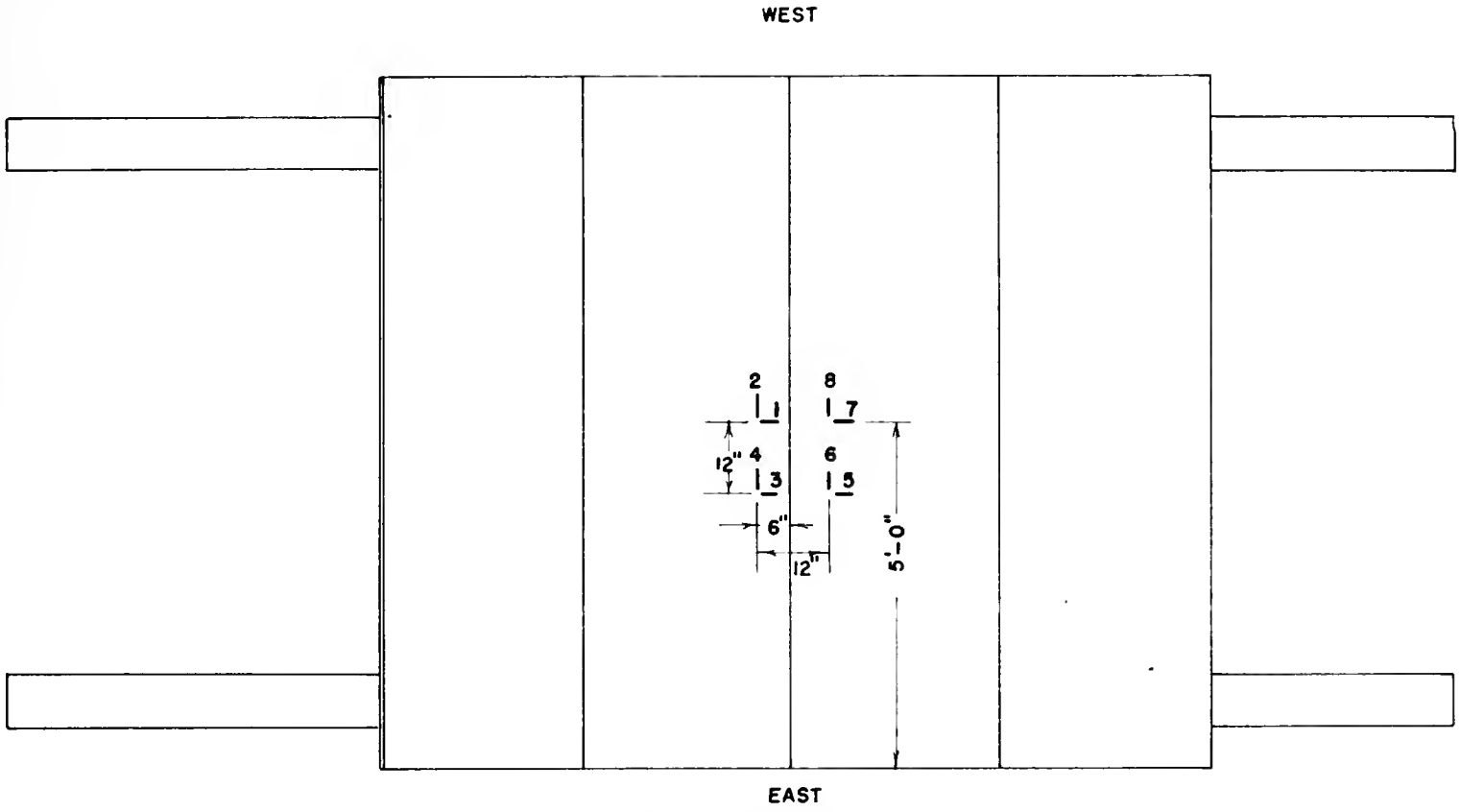

FIGURE 79. STRAIN GAGE LOCATIONS FOR REPEATED LOAD TEST WITH 8'-0" BEAM SPACING

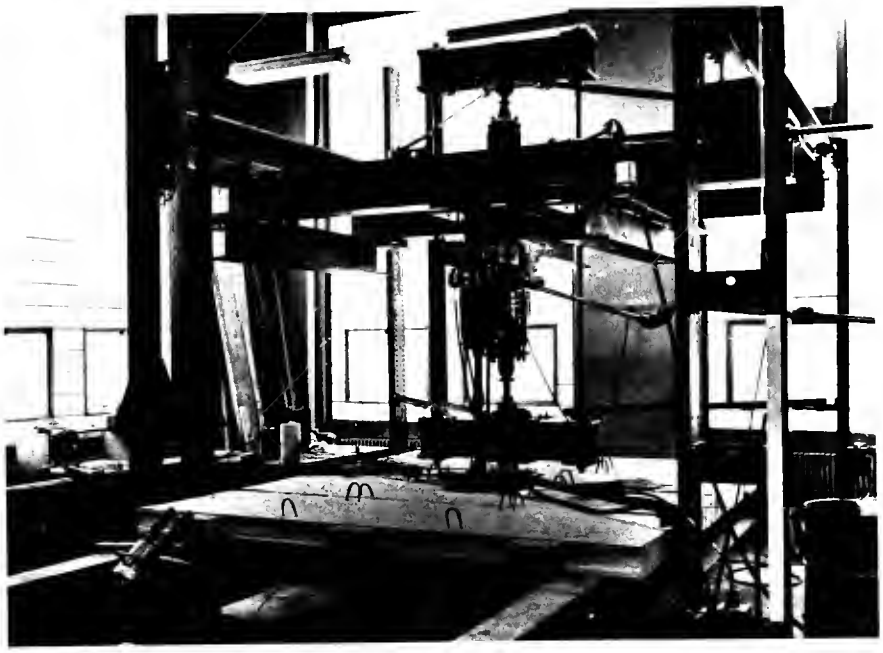

TESTING ARRANGEMENT

SPALL AT CENTER JOINT

FIGURE 80. REPEATED LOAD TEST WITH 8'-0" BEAM SPACING

(A complete discussion of the spall appears in the recommendations which follow.) After the spall occurred, the load in the post-tensioning cable which passed nearly under the spalled area was observed to decrease by 900 pounds, indicating that after the spall, the adjacent concrete sections moved together and the post-tensioning cable shortened. The average post-tensioning stress on the gross concrete section after the spall was found to be 3 psi less than the stress before the spall. The stress before the spall was 33.3 psi and the stress after the spall was 30.1 psi.

The test was discontinued at 715,000 cycles of loading; no further cracking was observed after the cracking at the spall stopped.

Strains remained nearly constant throughout the test and no pattern of increase or decrease in strain due to fatigue was noted.

Testing was begun again with the supporting beams spaced at 4'-6" with the sections reinforced for 8'-0" beam spacing again in the center but interchanged with regard to location. This served to remove the spalled area (from the first test) from the location of the center critical joint and permitted a re-examination of the joint.

Repeated Load Test With 4'-6" Beam Spacing

This test was identical to the previous test with the exception of supporting beam spacing (4'-6" v.s. 8'-0"), strain gage locations (see Figure 81), and an interchange of location of the center two deck sections.

Strain gage readings, loading, and load measurement were accomplished as in the previous test. The strain gage locations are illustrated in Figure 81 and strain readings appear as Table 23.

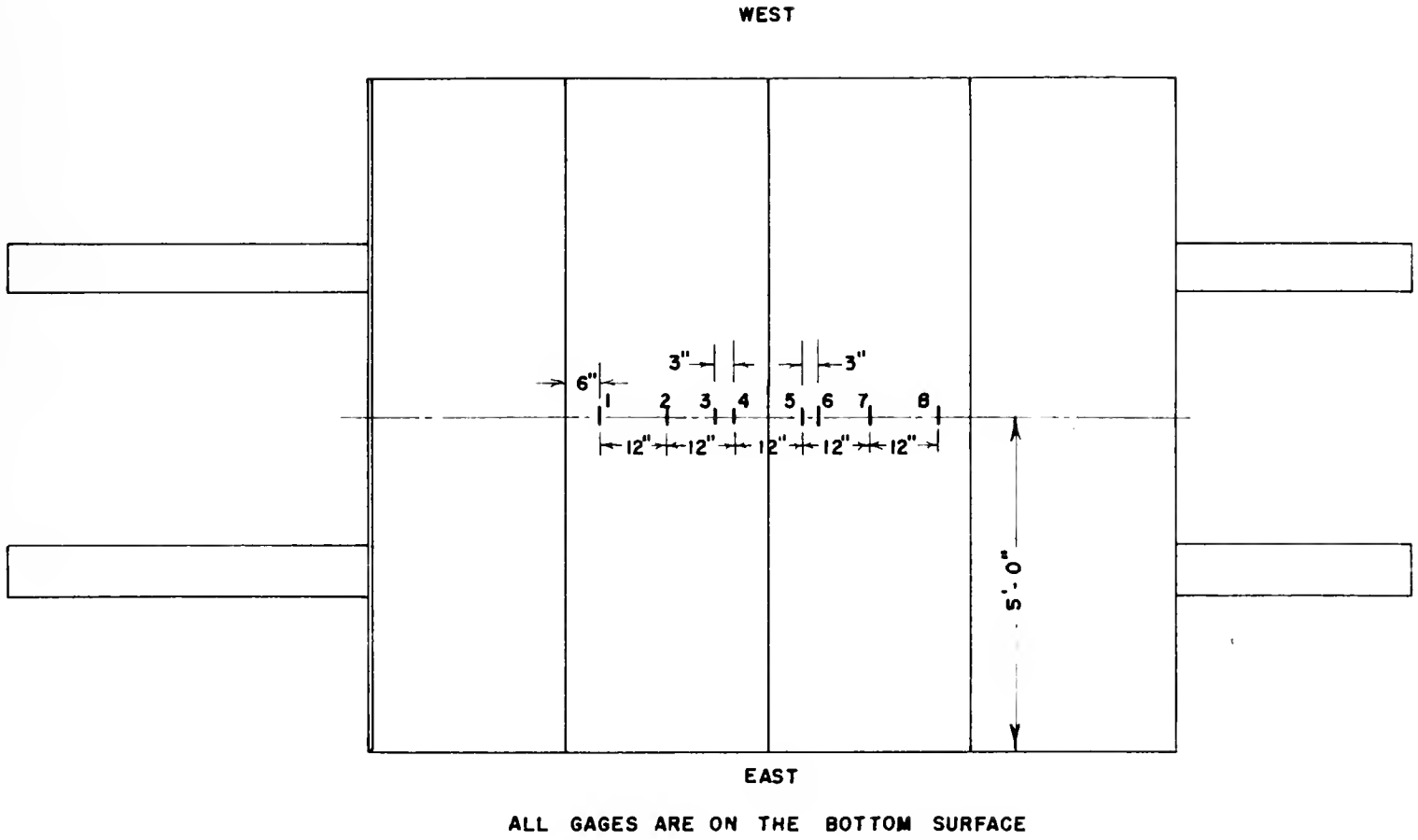

FIGURE 81 . STRAIN GAGE LOCATIONS FOR REPEATED LOAD TEST WITH 4'-6" BEAM SPACING

In this test, no cracking or other failure pattern was observed through nearly two million cycles of repeated load. Therefore, since the post-tensioning stress level on the gross concrete section was maintained at 32 psi, nearly the same stress as in the previous test, it would confirm that the spall of the previous test occurred due to a disconformity at the location of the spall. Although there was not as much deflection between adjacent sections due to a smaller beam spacing, it should be noted that the spall of the previous test occurred under one of the post-tensioning cables very near one of the supporting beams where there was very little deflection between adjacent sections.

Strain magnitudes did not increase or decrease appreciably over the two million cycles of loading and the post-tensioning stress level remained constant throughout the test.

Although the test confirmed that full-face bearing with a well-fitting joint could perform satisfactorily, it is strongly felt that an improved overall performance can be realized by modification of the joint shape. The proposed modification is presented in the recommendations which follow.

COST ANALYSIS

Precast, Prestressed System

The cost of a typical bridge deck has been estimated by Construction Products Corporation of Lafayette, Indiana. The cost estimate was based on a 4'-0" x 6" x 32'-0" section reinforced for a beam spacing of 8'-0", erected in place. The sum of $3.76 per square foot of deck surface does not include field labor for bolting or other operations performed in the field.

Estimates for the associated materials are made as follows: post-tensioning, 2.5 cents per square foot; tie-downs, 8 cents per square foot; joint material, 8 cents per square foot. The total cost of the deck is estimated at approximately $3.95 per square foot of deck.

Reinforced Concrete System

A cost estimate for a conventionally reinforced concrete deck was made using construction estimates and itemized proposals supplied by the Indiana State Highway Commission. An estimate for the concrete cost was made using an 8" deep deck, and a unit cost of $140.70 per cubic yard of concrete. Reinforcing steel was estimated at 275 pounds per cubic yard and 18 cents per pound. Total estimated cost is $3.52 per square foot of deck surface.

Cost Comparison

The cost estimates made above are not assumed to be the actual cost at which either system could be constructed as neither cost estimate is based on a completed structure. However, it is believed that the costs represent a reasonable estimate. Neither cost estimate allows for construction of any item other than the concrete deck within the span of the bridge. The cost of approach pavement and other items would vary depending upon the particular application.

The cost of the precast, prestressed deck appears to be the most expensive method when one considers only the cost of construction. The cost estimate for construction of the prestressed system is approximately 12 percent higher than the estimate for the conventionally reinforced system. This may be misleading since the producer of the prestressed deck is not experienced in manufacturing the product on a large scale. Experience on the part of the producer could reduce the cost of construction as the majority of the construction cost is reflected in his estimate for precasting.

The short down-time of a bridge for deck replacement using the precast system may easily make the precast system the most economically feasible. At least one month could be saved with each application of the precast system since reinforced concrete would require curing of nearly a month after it was in place on the bridge.

The cost of the precast deck system is not only competitive with a reinforced concrete deck but is possibly the most attractive when one considers the element of time. Included in any cost analysis must also be the projected life of the structure. The planned superior durability

of the precast deck should provide a longer service life with resulting economy than a cast-in-place deck.

Additional economy may result in replacement of the precast deck. Worn or deteriorated sections may be replaced individually and quickly, with no time lag for forming or curing of concrete.

CONCLUSIONS

A prestressed concrete deck system which was designed according to the 1965 standards set by the American Association of State Highway Officials has been examined under a static load and under a repeated load in the laboratory. The testing indicated that the design procedure using the limiting parameters established by the 1965 AASHO specifications are adequate and conservative. Bending stresses under static loading approached but did not in any case exceed the stresses which would be predicted using the guidelines enumerated in the specifications when the deck system was arranged in the planned prototype configuration.

The results of the testing indicated that precasting can produce a deck of sufficient smoothness if proper care is exercised during casting. Dimensional control, especially at the joint face, was the largest single problem that was encountered. The laboratory investigation indicated that even very slight dimensional irregularities at the joint face would cause spalling upon post-tensioning; this led to recommending a slight modification in joint shape to alleviate the problem. Whereas full-face bearing was attempted at the joint, it is now believed that bearing on the flat center half of the joint would be sufficient. Examination of a photoelastic model confirmed that this would be acceptable and would not cause problems due to stress concentrations.

The hardware used to mechanically tie the precast deck to the supporting steel beams performed satisfactorily. Ultimate capacities

of the bolting system were examined by others[4] and found to be substantially above the working load level anticipated in this application.

The design of the prestressed sections was made under the assumption that a wheel load would be carried by one section. This assumption was found to be basically accurate. Simulated wheel loads were carried by the loaded section with little interaction or load carrying from adjacent sections. Some insignificant interaction between adjacent sections, a plate action, was observed for the largest beam spacing.

The precast deck is competitive on a cost basis with a cast-in-place deck. Although construction costs may be slightly higher for the precast deck, the short down time for implementing the system as well as possible cold weather construction should make the precast deck economically attractive.

This constitutes the initial work in a continuing study of the precast, prestressed concrete bridge deck concept which will culminate in the construction of a monitored prototype.

RECOMMENDATIONS

Some difficulty was encountered in the laboratory with joint surfaces which did not fit properly on the prestressed specimens. Close inspection and careful casting cannot relieve all of the dimensional irregularities but should minimize them. The problem lies in joint performance due to improper fit.

In several cases, corners of the concave face of the joints were broken off, due to both post-tensioning and bolting. In the case of post-tensioning induced failure, the larger convex surface could not be accommodated by the smaller concave surface and the post-tensioning force caused the convex surface to act as a wedge, forcing the corners of the concave face to spall off. The bolting caused the same type failure but always on the top surface of the concave joint face. Here, the concrete cracked due to a relative movement between two adjacent pieces as the bolts were tightened. Here, again, the problem is attributed to misfit.

The spall in Figure 80 was observed to occur under repeated load when the supporting beams were at 8'-0" centers. Upon examination of the spalled area, it was evident that several conditions contributed to the spall. First, and foremost, there was evidence of improper fit. The neoprene joint material had apparently been under high pressure at the point and left a distinct color impression on the high points on the spalled joint face. Secondly, the neoprene material had slipped

approximately one inch at this location and may have contributed to the cracking by causing an uneven bearing. The spall occurred directly above one post-tensioning cable, a factor which coupled with the unevenness at that point would hasten trouble. Under the action of the repeated load, the relative motion between the slabs cannot be overlooked as a contributor to the spalling.

Failures of the aforementioned type cannot be tolerated. It is apparent that full-face bearing at the joint is practical but not the most desired configuration. Rather, if bearing at the joint was limited to the flat, center portion of the joint, stresses at the joint would be approximately doubled (a tolerable circumstance) and the contributors to corner break-off, the only type failure that was observed, would be eliminated. The portions above and below the flat, center part of the joint could be cut back on both sides of the joint with closure of the joint provided by a joint material of sufficient (probably varying) thickness.

The flat joint photoelastic study was conducted with a joint shape of nearly this configuration (see Figures 17, 18, and 19) and only minor tension stresses were encountered.

It is further recommended that the top edge of the joint be tooled to a small-radius corner after casting. Without this shape, traffic would probably irregularly break off the square corner.

It is recommended that the modified joint shape be subjected to a test similar to the repeated load test reported herein. The modified joint shape is shown in Figure 82. The strand and insert patterns are illustrated in Figures 29 and 26. The same strand pattern could be

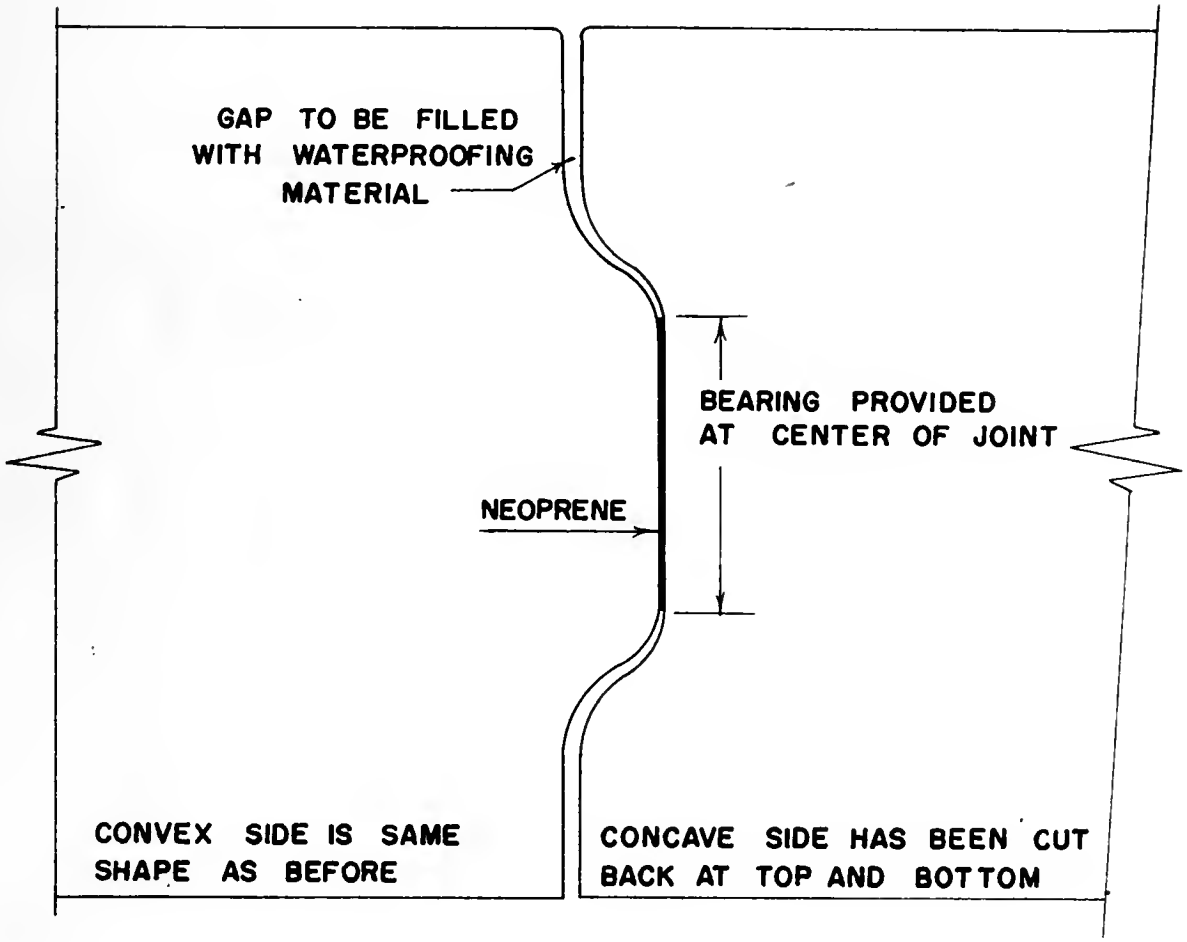

FIGURE 82. RECOMMENDED MODIFICATION OF JOINT DETAIL

used in all sections (12 - 7/16 in. diameter - 270k strands) for economy.

A test of some or all of the prestressed sections to failure in flexure is recommended to examine the ultimate flexural capacity of the designed sections. Comparison to the theoretically determined ultimate flexural capacity reported herein would be of value.

BIBLIOGRAPHY

1. Dally, James W. and William F. Riley. Experimental Stress Analysis. New York: McGraw-Hill Book Company, 1965.

2. Faupel, Joseph H. Engineering Design. New York: John Wiley and Sons, Inc., 1964, pp. 953-954.

3. Harvard, David G. "Photographic Display of Stress Directions in Plane Photoelasticity," Experimental Mechanics, September 1967, pp. 407-408.

4. Hsu, T. T. C. and Norman W. Hanson. "An Investigation of Rail-to-Concrete Fasteners," Journal of the PCA Research and Development Laboratories, Portland Cement Association Vol. 10, No. 3, September 1968, pp. 14-35.

5. Perry, C. C. and H. R. Lissner. The Strain Gage Primer. New York: McGraw-Hill Book Company, Inc. 1962.

6. Specifications for Design, Materials, Construction of Prestressed Concrete Ties Revised October 27, 1967. (Obtained in personal correspondence with E. J. Ruble, Executive Research Engineer, Association of American Railroads).

7. Standard Specifications for Highway Bridges. Washington, D. C.: American Association of State Highway Officials, Ninth Edition 1965.

8. Whitney, C. S. "Design of Reinforced Concrete Members Under Flexure or Combined Flexure and Compression," Proceedings, American Concrete Institute, Vol. 33, 1937, pp. 483-498.

9. Craig, Robert John. "Bridge Slab Joint Connection Study," Unpublished Report.

APPENDIX A

Table 11. Static Bending Test, 4'-0" Beam Spacing, Deflections

Point	1	2	3	4	5	6	7	8	9	10	11	12	13	14	15	16
Load Stage	Deflections (inches), (-) indicates uplift															
1 i	.007	.011	.018	.051	.036	.046	.037		.037	.030	.015	.023	.005	.027	.000	.001
1 ii	-.011	.007	.023	.035	.043	.053	.042		.036	.034	.023	.016	.019	.015	.002	-.011
1 iii	-.021	.011	.028	.035	.045	.056	.037		.057	.042	.022	.035	.011	.026	-.003	-.007
2 i	.001	-.009	.010	.020	.026	.031	.037		.044	.024	.026	.031	.019	.024	-.002	-.002
2 ii	.006	-.008	.018	.021	.042	.039	.056		.034	.031	.030	.029	.023	.038	-.004	-.006
2 iii	.004	-.009	.030	.036	.047	.051	.046		.046	.034	.048	.035	.034	.040	-.005	-.009
3 i	-.001	.023	.059	.065	.025	.068	.072		.067	.056	.057	.039	.044	.044	.022	.004
3 ii	.001	.037	.073	.077	.081	.069	.087		.075	.070	.067	.045	.047	.036	.020	.004
3 iii	.003	.038	.078	.086	.104	.077	.094		.100	.076	.075	.046	.051	.046	.014	.004
4 i	.001	.005	.022	.022	.023	.027	.028		.013	.023	.016	.006	.010	.005	-.004	-.009
4 ii	.014	.013	.039	.027	.039	.033	.039		.031	.029	.018	.005	.011	.016	-.008	-.011
4 iii	.007	.025	.057	.038	.039	.056	.043		.037	.035	.024	.009	.015	.006	-.010	-.012
5 i	.010	.007	.022	.008	.021	.004	.029		.008	.015	.008	.001	.009	.001	-.004	-.005
5 ii	.015	.015	.030	.040	.032	.011	.020		.020	.022	.016	.010	.012	.008	.001	-.007
5 iii	.013	.018	.032	.029	.038	.024	.024		.024	.037	.019	.013	.022	.016	.004	-.004
6 i	-.001	.001	.022	.025	.019	.026	.019		.014	.006	.003	.005	.006	.013	.000	.005
6 ii	-.007	.002	.043	.031	.036	.048	.021		.017	.013	.015	.014	.024	.008	.008	.013
6 iii	-.009	.008	.030	.036	.053	.043	.022		.029	.021	.021	.014	.011	.016	.004	.008

Table 12. Strain Data, 4'-0" Beam Spacing Static Test, Top North-South Gages on Section 4-2

Gage	1	2	3	4	5	6	7	8	9	10
Load Stage	Strain $\left(\frac{in}{in} \times 10^{-6}\right)$ (-) compression, (+) tension									
1 i	5	2	6	2	0	10	7	8	-13	6
1 ii	16	11	20	12	-5	10	11	17	-10	15
1 iii	23	18	32	22	-12	14	3	24	5	19
2 i	3	0	6	-15	-8	11	1	8	5	11
2 ii	3	7	10	-10	-8	27	11	5	16	15
2 iii	6	10	25	-9	-11	25	15	10	4	16
3 i	-1	3	10	-36	-14	0	6	0	3	-2
3 ii	-3	5	15	-34	-23	7	9	7	0	1
3 iii	-2	5	23	-35	-25	19	18	21	6	3
4 i	5	6	6	-10	-7	12	5	-5	2	-1
4 ii	0	5	11	-20	-15	14	8	3	-5	0
4 iii	6	12	19	-19	-20	25	15	3	8	4
5 i	0	3	10	-5	-2	14	8	8	10	2
5 ii	-4	3	15	-12	-10	21	12	8	4	3
5 iii	-11	3	18	-12	-14	18	15	11	-2	-5
6 i	5	7	14	3	-4	4	-1	4	-2	-2
6 ii	2	7	19	3	-6	5	1	11	-3	2
6 iii	9	6	28	5	-1	1	4	12	-1	2

Table 13. Strain Data, 4'-0" Beam Spacing Static Test, Bottom North-South Gages on Section 4-2

Gage	2	3	4	7	8	10
Load Stage	Strain $\left(\frac{in}{in} \times 10^{-6}\right)$ (-) compression, (+) tension					
1 i	2	1	0	0	-5	0
1 ii	-1	-11	-1	3	-10	-1
1 iii	-2	-16	-4	-2	-16	1
2 i	-2	-7	1	-6	-7	-5
2 ii	-5	-16	1	-11	-12	-5
2 iii	-9	-25	0	-18	-19	-7
3 i	-15	-6	6	-8	-19	-22
3 ii	-7	-19	3	-16	-29	-16
3 iii	-10	-28	2	-24	-32	-21
4 i	-9	-18	-4	-12	-10	-6
4 ii	-14	-27	-5	-21	-22	-8
4 iii	-19	-33	-6	-28	-32	-12
5 i	-1	-6	0	-5	-4	-3
5 ii	-11	-19	-2	-16	-16	-5
5 iii	-	-35	112	-21	-23	-11
6 i	-5	-6	1	-5	-6	-1
6 ii	-8	-18	-1	-4	-9	0
6 iii	-13	-26	-4	-9	-16	-8

Table 14. Strain Data, 4'-0" Beam Spacing Static Test, Top East-West Gages on Section 4-2

Gage	1	2	3	4	5	6	7	8	9	10
Load Stage	Strain $\left(\frac{in}{in} \times 10^{-6}\right)$ (-) compression, (+) tension									
1 i	17	0	-22	-7	2	12	5	-5	8	0
1 ii	30	0	-31	-9	5	18	-3	-5	9	-4
1 iii	45	-7	-56	-11	7	15	11	-22	10	-6
2 i	0	-15	-25	-18	-11	2	-6	-8	5	1
2 ii	2	-24	-54	-27	-12	6	-17	-32	17	-5
2 iii	21	-25	-71	-42	-16	17	-17	-41	5	-9
3 i	-14	-18	-35	-12	-7	-10	-14	-16	-2	0
3 ii	-18	-33	-67	-29	-12	-9	-29	-40	-3	-24
3 iii	-16	-42	-98	-46	-15	-6	-29	-61	-2	-18
4 i	0	-10	-33	-7	2	2	-11	-20	1	-2
4 ii	1	-22	-60	-25	-5	0	-17	-40	1	-11
4 iii	0	-34	-82	-28	-7	1	-27	-52	-4	-21
5 i	9	-11	-30	-8	-3	5	-6	-19	-2	-1
5 ii	6	-23	-57	-24	-7	7	-17	-38	-6	-21
5 iii	-1	-40	-87	-32	-16	10	-29	-55	-12	-36
6 i	10	-3	-36	-12	-1	7	-8	-12	-11	-21
6 ii	24	-7	-57	-18	-6	20	-7	-25	2	-16
6 iii	41	-8	-75	-25	-4	25	-8	-33	6	-23

Table 15. Strain Data, 4'-0" Beam Spacing Static Test, Bottom East-West Gages on Section 4-2

Gage	2	3	4	7	8	10
Load Stage	Strain $\left(\frac{in}{in} \times 10^{-6}\right)$ (-) compression, (+) tension					
1 i	5	20	11	9	8	3
1 ii	10	31	15	11	17	8
1 iii	22	44	20	18	26	17
2 i	13	15	8	11	11	4
2 ii	22	28	16	19	25	10
2 iii	25	34	24	22	29	14
3 i	11	12	1	11	11	7
3 ii	24	25	3	19	18	18
3 iii	30	31	15	29	32	24
4 i	3	5	-2	6	7	6
4 ii	13	13	5	12	18	13
4 iii	24	22	10	23	27	22
5 i	6	15	9	-	11	6
5 ii	14	21	11	13	17	13
5 iii	-49	29	5	19	27	17
6 i	9	14	8	6	8	6
6 ii	8	23	13	7	15	8
6 iii	10	30	16	7	20	10

APPENDIX B

Table 16. Deflections During Testing of Sections Reinforced for 8'-0" Beam Spacing

Point	1	2	3	4	5	6	7	8	9	10	11	12	13	14	15	16
Load Stage	(Deflections in inches) (-) indicated uplift															
1 i	.006	.007	.029	.023	.046	.037	.050	.065	.035	.050	.046	.044	.041	.025	.008	.011
1 ii	.006	.029	.038	.032	.051	.056	.052	.061	.048	.069	.068	.000	.053	.047	.023	.012
1 iii	.005	.020	.046	.044	.067	.067	.085	.076	.063	.074	.085	.082	.077	.056	.036	.020
2 i	-.015	.016	.074	.091	.073	.124	.124	.133	.132	.142	.121	.121	.111	.067	.014	-.001
2 ii	-.003	.029	.088	.101	.101	.144	.156	.160	.154	.165	.148	.147	.135	.083	.028	.000
2 iii	.004	.028	.103	.121	.107	.162	.169	.179	.176	.171	.157	.167	.156	.093	.038	.001
3 i	.007	.003	.026	.024	.039	.036	.043	.033	.044	.052	.039	.036	.027	.016	.004	-.004
3 ii	.015	.015	.029	.030	.051	.050	.056	.061	.064	.067	.059	.060	.047	.028	.019	.007
3 iii	.015	.023	.032	.038	.078	.065	.072	.071	.081	.076	.071	.077	.063	.046	.026	.012
4 i	.009	.009	.022	.008	.021	.024	.035	.027	.034	.033	.030	.030	.024	.024	.009	.012
4 ii	.010	.010	.031	.032	.049	.040	.060	.054	.063	.042	.040	.045	.041	.038	.022	.013
4 iii	.019	.019	.037	.036	.053	.062	.068	.063	.070	.054	.058	.062	.052	.045	.031	.007

Table 17. Strain Data, 8'-0" Beam Spacing Static Test, Top East-West Gages on Section 8-1

Gage	1	2	3	4	5	6	7	8	9
Load Stage	Strain $\left(\frac{in}{in} \times 10^{-6} \right)$								
1 i	-13	-78	-61	-31	-40	-82	-82	-53	-28
1 ii	-16	-52	-27	-1	10	-55	-58	-25	-49
1 iii	-57	-75	-37	-3	16	-82	-81	-30	-65
2 i	-50	-31	-16	-5	8	-28	-30	-28	-31
2 ii	-96	-16	-43	-1	13	-62	-47	-28	-57
2 iii	-;39	-92	-45	-20	9	-92	-79	-63	-79
3 i	-39	-23	-8	1	7	-23	-21	0	-16
3 ii	-80	-49	-20	8	14	-50	-45	-12	-42
3 iii	-121	-72	-34	0	25	-77	-59	-25	-60
4 i	-37	-26	-24	-12	1	-26	-29	-15	-20
4 ii	-88	-57	-42	-14	4	-54	-49	-25	-45
4 iii	-133	-82	-57	-20	7	-83	-74	-42	-64

Table 18. Strain Data, 8'-0" Beam Spacing Static Test, Bottom East-West Gages on Section 8-1

Gage	1	2	3	4	6	7	8	9
Load Stage	Strain $\left(\frac{in}{in} \times 10^{-6}\right)$							
1 i	34	36	12	-9	3	-25	3	7
1 ii	83	44	20	-7	20	-20	11	14
1 iii	131	47	31	-9	47	6	20	31
2 i	43	27	12	-3	25	27	17	24
2 ii	91	52	22	-2	51	54	27	47
2 iii	134	79	38	6	74	81	46	59
3 i	35	20	11	-2	21	21	13	17
3 ii	76	45	22	2	45	47	23	35
3 iii	127	68	28	1	66	71	31	52
4 i	27	23	8	-6	-8	25	9	14
4 ii	68	45	18	-7	13	50	21	32
4 iii	109	67	27	-8	38	73	35	51

Table 19. Strain Data, 8'-0" Beam Spacing Static Test, Top North-South Gages on Section 8-1

Gage	1	2	3	4	5	6	7	8	9
Load Stage	Strain $\left(\frac{in}{in} \times 10^{-6}\right)$								
1 i	-4	-10	-17	-13	-13	-4	-7	1	10
1 ii	25	9	3	-2	-7	14	24	6	14
1 iii	45	17	8	-3	-4	25	22	14	20
2 i	9	5	4	-9	-14	18	11	-5	12
2 ii	24	10	7	-7	-21	21	22	-2	15
2 iii	36	13	13	-7	-21	29	25	2	21
3 i	14	5	5	-5	-15	10	9	14	-3
3 ii	28	11	9	0	-17	31	14	13	1
3 iii	43	20	15	2	-12	29	28	17	31
4 i	8	5	-1	0	-13	9	16	6	-7
4 ii	21	7	1	-2	-23	17	22	2	-6
4 iii	35	10	4	0	-19	23	22	5	-4

Table 20. Strain Data, 8'-0" Beam Spacing Static Test, Bottom North-South Gages on Section 8-1

Gage	1	2	3	4	6	7	8	9
Load Stage	Strain $\left(\frac{in}{in} \times 10^{-6}\right)$							
1 i	-19	-4	-3	21	22	6	-8	-4
1 ii	-26	-10	-8	12	10	23	13	10
1 iii	-37	-18	-13	16	0	16	6	5
2 i	-10	-7	-9	-5	-15	-14	-16	-20
2 ii	-26	-10	-13	-7	-25	-20	-22	-26
2 iii	-36	-17	-19	-12	-36	-29	-35	-30
3 i	-13	-4	-5	-5	-12	-11	-9	-14
3 ii	-10	-6	-7	-4	-20	-13	-12	-16
3 iii	-29	-11	-12	-8	-30	-20	-21	-24
4 i	-11	36	37	74	50	38	-11	-10
4 ii	-25	33	30	66	36	32	-18	-15
4 iii	-39	27	26	63	29	27	-25	-17

Table 21. Strain Data, 8'-0" Beam Spacing Static Test, Gages on Top Surface of Section 4-2

Gage	1 E-W	1 N-S	2 E-W	2 N-S	6 E-W	6 N-S	7 E-W	7 N-S	9 E-W	9 N-S
Load Stage	Strain $\left(\frac{in}{in} \times 10^{-6}\right)$									
1 i	75	-21	54	-14	43	-12	49	-16	39	-12
1 ii	95	-14	69	-13	59	-4	64	-9	54	-5
1 iii	97	-27	68	-15	61	-14	63	-19	55	-13
2 i	9	5	2	0	8	8	6	7	6	7
2 ii	6	-9	1	-4	6	-4	2	-4	4	-4
2 iii	18	-14	3	-4	10	-5	4	-5	7	-4
3 i	4	-5	3	-3	3	-4	2	-3	3	-2
3 ii	9	-16	1	-5	3	-11	1	-12	1	-12
3 iii	16	-18	9	-7	9	-15	7	-7	15	-5
4 i	5	-4	2	-1	5	-1	3	-2	4	-2
4 ii	15	-8	7	-3	11	-3	8	-4	10	-3
4 iii	22	-11	13	-4	19	-6	14	-6	18	-5

APPENDIX C

Table 22. Strain Gage Readings, Repeated Load Test With 8'-0" Beam Spacing

Load Cycles	Gage 1	2	3	4	5	6	7	8
0	-7 ± 4	81 ± 34	6 ± 2	-45 ± 20	11 ± 4	-75 ± 31	-10 ± 1	78 ± 45
2,000	-7 ± 5	83 ± 37	6 ± 2	-48 ± 22	11 ± 4	-70 ± 40	-10 ± 1	84 ± 51
20,800	-26 ± 5	81 ± 36	9 ± 2	-57 ± 24	11 ± 5	-66 ± 40	-11 ± 1	61 ± 39
32,400*	-26 ± 4	67 ± 32	33 ± 2	-63 ± 19	11 ± 4	-71 ± 37	-15 ± 2	65 ± 35
59,000	-25 ± 3	58 ± 27	10 ± 2	-56 ± 16	11 ± 4	-62 ± 32	-13 ± 2	69 ± 47
88,000	-7 ± 2	81 ± 20	10 ± 2	-55 ± 15	14 ± 3	-60 ± 30	-7 ± 2	76 ± 39
138,000	-12 ± 2	74 ± 22	10 ± 2	-56 ± 16	12 ± 3	-60 ± 29	-7 ± 2	76 ± 37
157,000	-12 ± 2	67 ± 18	10 ± 2	-56 ± 15	13 ± 3	-62 ± 30	-7 ± 2	74 ± 41
294,000	-36 ± 2	43 ± 21	10 ± 2	-61 ± 17	16 ± 3	-63 ± 28	-7 ± 2	76 ± 36
378,000	+7 ± 2	86 ± 21	21 ± 2	-61 ± 16	21 ± 4	-60 ± 29	-3 ± 2	85 ± 37
425,000	+5 ± 3	84 ± 22	10 ± 2	-61 ± 15	22 ± 4	-61 ± 30	-3 ± 2	87 ± 37
675,800	-12 ± 2	65 ± 22	11 ± 2	-35 ± 15	19 ± 4	-63 ± 29	-10 ± 3	88 ± 25
715,000	-21 ± 3	59 ± 27	12 ± 1	-62 ± 15	22 ± 3	-60 ± 28	-5 ± 2	78 ± 36

* Large spall occurred just prior to this reading.

Table 23. Strain Gage Readings, Repeated Load Test With 4'-6" Beam Spacing

Cycles of Loading	Gage 1	2	3	4	5	6	7	8
0	17 ± 13	53 ± 10	50 ± 10	61 ± 11	35 ± 20	36 ± 18	24 ± 14	15 ± 15
84,400	26 ± 8	54 ± 11	51 ± 11	63 ± 13	34 ± 21	37 ± 20	25 ± 15	16 ± 14
327,500	22 ± 5	52 ± 12	41 ± 8	61 ± 9	27 ± 17	28 ± 13	14 ± 11	11 ± 11
555,000	36 ± 4	67 ± 7	51 ± 9	76 ± 10	46 ± 18	28 ± 12	29 ± 13	20 ± 12
794,000	38 ± 6	71 ± 8	55 ± 9	84 ± 10	40 ± 18	47 ± 17	32 ± 13	22 ± 12
896,000	34 ± 5	70 ± 8	51 ± 9	81 ± 10	37 ± 17	47 ± 18	32 ± 12	20 ± 11
1,035,000	30 ± 5	62 ± 7	45 ± 7	75 ± 9	33 ± 18	41 ± 16	16 ± 11	5 ± 5
1,163,000	30 ± 5	39 ± 8	45 ± 6	77 ± 9	34 ± 17	43 ± 16	21 ± 11	13 ± 10
1,270,000	37 ± 6	69 ± 5	55 ± 10	88 ± 10	43 ± 19	52 ± 17	34 ± 12	21 ± 11
1,400,000	22 ± 5	55 ± 7	38 ± 8	72 ± 8	27 ± 17	62 ± 16	14 ± 12	4 ± 10
1,865,000	28 ± 5	62 ± 8	46 ± 8	82 ± 9	57 ± 17	42 ± 16	49 ± 11	9 ± 13
1,927,800	43 ± 5	52 ± 7	60 ± 9	97 ± 9	47 ± 18	59 ± 17	42 ± 9	21 ± 11